SYNTHESIS AND EVALUATION OF N-AND S-HETEROCYCLES AS ANTI-PARKINSON AGENTS

Thesis submitted to the Delhi Technological University

for the award of the Degree of

DOCTOR OF PHILOSOPHY

by

POONAM

(2k16/PhD/AC/02)

DEPARTMENT OF APPLIED CHEMISTRY

DELHI TECHNOLOGICAL UNIVERSITY

DELHI – 110042

INDIA

March 2023

Dedicated

To

My Parents

DECLARATION

I hereby declare that this Ph.D. thesis entitled "**Synthesis and Evaluation of N-and S-Heterocycles as Anti-Parkinson Agents**" was carried out by me for the degree of Doctor of Philosophy under the supervision of **Prof. Ram Singh**, Department of Applied Chemistry, Delhi Technological University, Delhi, India.

This thesis is a presentation of my original research work. Wherever contributions of others are involved, every effort has been made to indicate this clearly with proper citation.

For the present thesis, which I am submitting to the University, no degree or diploma has been conferred on me before, either in this or in any other University.

Place: Delhi

Date: 21-03-2023 (Poonam)

DELHI TECHNOLOGICAL UNIVERSITY

DEPARTMENT OF APPLIED CHEMISTRY
Bawana Road, Delhi-110042, India

CERTIFICATE

This is to certify that the thesis entitled "**Synthesis and Evaluation of N- and S-Heterocycles as Anti-Parkinson Agents**" submitted to the Delhi Technological University, Delhi-110042, in fulfilment of the requirement for the award of the degree of **Doctor of Philosophy** by the candidate **Ms. Poonam** [2K16/PhD/AC/02] under the supervision of **Prof. Ram Singh**, Department of Applied Chemistry, Delhi Technological University, Delhi - 110042, India.

It is further certified that the work embodied in this thesis has been neither partially nor fully submitted to any other university or institution for the award for any degree or diploma.

(**Prof. Ram Singh**)
Supervisor
Department of Applied Chemistry
Delhi Technological University,
Delhi – 110042, India

(**Prof. Anil Kumar**)
Head of the Department
Department of Applied Chemistry
Delhi Technological University,
Delhi – 110042, India

ACKNOWLEDGEMENTS

I express my deep sense of gratitude and reverence to my supervisor Prof. Ram Singh for his constant support, timely advice, meticulous scrutiny, and invaluable suggestions for carrying out this work. He not only gave me the freedom to do things in my own order but also offered innumerable opportunities beyond the domain of my Ph.D. work which enriched me both professionally and personally.

I would like to express my profound gratitude to the present and previous Head of Department and faculty members of the Department of Applied Chemistry, DTU for their kind guidance and criticism on several occasions during this research work.

My sincere thanks to the previous and present Vice Chancellor of Delhi Technological University for allowing me to carry out this research work and providing the necessary facilities.

I wish to convey my sincere thanks to Dr. Amulya K. Panda (National Institute of Immunology), Prof. Rina Chakrabarti (Dept. of Zoology, University of Delhi), Prof. Jai Gopal Sharma (Dept. of Biotechnology, DTU), and Mr. Nilesh (Dept. of Biotechnology, DTU) for helping me in carrying out the in-vitro studies. I would like to mention the name of Dr. Mamta Singh specially to express my gratitude to her for her constant support in my work and for being present there as a friend whenever needed.

I acknowledge my deep appreciation and thanks to Prof. Geetanjali (Kirori Mal College, University of Delhi), for her constant help in every possible way to carry forward my research work. I am also thankful to Dr. M.S. Mehata for helping in catalyst preparation.

I am fortunate to have an excellent work environment in the laboratory which facilitated my work to a great deal till its completion. I express my special thanks to my lab-mates Dr. Atiya Fatima, Dr. Deepshikha, Dr. Geetika, Dr. Deepak, Dr. Priyanka, Dr. Sankar Suman, Dr. Babita Veer, Dr. Ashwini, Dr. Prateek, Mr. Yogesh, Mr. Chandra Prakash, Ms. Nidhi, Ms. Aman, Ms. Tanushee, Ms. Anvita, Ms. Parul, Ms. Aanchal and Ms. Charu for their motivation and constant help in every possible manner.

My sincere thanks are also due to Mr. Himansh and Mr. Surya who have provided their valuable suggestions and time to time help needed during the research work.

I greatly appreciate and acknowledge the support received from laboratories at DTU, and Non-teaching staffs of the department.

I acknowledge the University for awarding me the DTU fellowship to carry out research work.

I feel great pleasure in expressing my reverence to my parents, brothers for their blessings, help, trust and appreciations all along this journey. Finally, I feel humble to bow my head to the Almighty who led me to fulfil my goal.

Poonam

CONTENTS

ABSTRACT

The thesis entitled '**Synthesis and Evaluation of N- and S-Heterocycles as Anti-Parkinson Agents**' has been carried out to design and synthesize the MAO-B inhibitors for Parkinson's Disease (PD). The work has been divided into four chapters excluding reference section.

Chapter 1 covers the description of PD and possible pathways for treatments. The literature given in this chapter covers the role of MAO-B inhibitors for the treatment of PD.

Chapter 2 is the experimental section which explains the procedures for the synthesis of different N- and S-containing heterocyclic molecules. The methods for the synthesis of pyrazole derivatives, thiazole derivatives, 2-(4-nitrophenyl)-1H-benzimidazole, 2-(4-aminophenyl)-1H-benzimidazole, pyrazole-thiazole conjugates through amide bond and amine bond and benzimidazole-pyrazole/thiazole conjugates through amide bond and amine bond have been given in this chapter. Method for *in-silico* studies, *in-vitro* studies, and anti-oxidant studies have also been covered in this chapter.

Chapter 3 is the results and discussion chapter which covers detailed explanation about the design of molecules through their *in-silico* studies. The *in-silico* studies have been carried out for individual compounds and their conjugates. A total of 309 compounds have been docked, which included pyrazole-thiazole derivatives (amide linkage), benzimidazole-pyrazole/thiazole derivatives (amide linkage), pyrazole-thiazole derivatives (amine linkage), and benzimidazole-pyrazole/thiazole derivatives (amine linkage). A novel, facile, one-pot, multicomponent protocol for the synthesis of 5-amino-1H-pyrazole-4-carbonitrile derivatives (**4**) has been developed using alumina–silica supported MnO_2 as recyclable catalyst in water and sodium dodecyl benzene sulphonate at room temperature. A sustainable, one-pot, multicomponent protocol for the synthesis of 4-phenylthiazole-2-amine derivatives catalyzed by MoS_2 QDs in aqueous medium has been developed. The cyclo-condensation of phenacyl bromide and thiourea gave the thiazole derivatives in 89–96% yields. Apart from this, their amide and amine conjugates have also been synthesized. The synthesized derivatives were evaluated for MAO-B inhibition. The *in-vitro* study of fifteen compounds was done using Amplex™ Red Monoamine Oxidase Assay Kit. The two compounds **P11** and **P10** with IC_{50} values of 80.17 and 86.03 μM have been identified as potential molecules. The antioxidant evaluation of the compounds has also been done. The results showed 13 to 83 % antioxidant activities of the compounds. Interestingly, the compounds that shows better in-vitro results also showed good antioxidant activities.

Chapter 4 is the conclusion chapter where all the work carried out has been summarized. This chapter is followed by references and publications.

*****

List of Figures and Schemes

List of Tables

List of important abbreviations and notations

S. No.	Abbreviations	Full Name
1	PD	Parkinson's disease
2	SN	Substantia nigra
3	LB	Lewy body
4	α-syn	α-synuclein
5	ROS	Reactive oxygen species
6	RNS	Reactive nitrogen species
7	RSS	Reactive sulphur species
8	MRI	Magnetic resonance imaging
9	US	Ultrasonography
10	SPECT	Single-photon emission computed tomography
11	PET	Positron emission tomography
12	MPTP	Methyl phenyl tertrahydropyridine
13	EOPD	Early-onset Parkinson's disease
14	DA	Dopamine
15	DA	Dopamine agonists
16	NEDA	Non-ergot derivatives
17	*LEAP*	*Levodopa* in Early Parkinson's Disease
18	CNS	Central nervous system
19	SPNs	Spiny projection neurons
20	MAO-B	Monoamine oxidase-B
21	hMAO	Human monoamine oxidase
22	AD	Alzheimer’s Disease
23	MPTP	1-Methyl-4-phenyl-1,2,3,6-tetrahydropyridine

24	DMF	Dimethyl Formide
25	THF	Tetrahydrofuran
26	FTIR	Fourier transform infrared
27	NMR	Nuclear magnetic resonance
28	UV-Vis	Ultraviolet-Visible
29	DPPH	2,2-Diphenyl-1-picrylhydrazyl
30	AA	Antioxidant activity
31	SEM	Standard error of means

CHAPTER 1

Parkinson’s Disease: An overview

1.1. Introduction

Parkinson's disease (PD) is a neurological disorder developed usually between the ages of 55 and 65 years which affects the movement coordination (Qu et al., 2023; Bohnen and Albin, 2011). PD is the second-most prevalent neurodegenerative condition. This is characterized primarily by the functional impairment of dopaminergic neurons within the substantia nigra (SN) of the midbrain (Kordower et al., 2013; Kalia and Lang, 2015; Bohnen and Albin, 2011). Despite significant efforts over the past few decades, PD continues to be difficult to cure (Poewe et al., 2017). This has been observed that there is continuous increase in the number of PD cases due to increase in average population age and life expectancy (De Lau and Breteler, 2006; Vos et al., 2016). This has also been observed that men are more likely than women to be impacted. Some of the typical symptoms of PD includes bradykinesia, tremors, loss of coordination, stiffness, postural instability, and impaired gait. These symptoms are employed in early diagnostic tests in the clinic (Jankovic, 2008; Moustafa, 2016). Olfactory function, autonomic and the cerebral cortex, and the nigrostriatal dopaminergic system are also impacted by the PD (Bohnen and Albin, 2011). In around 83% of PD patients, non-motor symptoms and dementia coexist.

In recent times, identifying the causes of or elements involved in the development of PD have been the focus of research globally. This is vital to understand the precise aetiology of PD. This is principally brought on by the development of proteinaceous intraneuronal Lewy body (LB) inclusions, Lewy neuritis, and the gradual death of dopaminergic neurons and their axons in the SN (Horrocks et al., 2015; Hely et al.; 2008), α-synuclein (α-syn) abnormal accumulation (Aliyan et al. 2019; Ilie and Caflisch, 2019; Stefanis, 2012), metal ion dyshomeostasis (Barnham and Bush, 2008; Cruces-Sande et al., 2019), oxidative stress (Tipton, 2018), aberrant activity of reactive species (e.g., reactive oxygen species (ROS), reactive nitrogen species (RNS), and reactive sulphur species (RSS) (Onyango, 2008; Wu et al., 2019), mitochondrial dysfunction, and neurotransmitter deficiencies are the other possible reasons for the development of PD (Figure 1.1). In brief, the numerous features and related biomarkers implicated in PD highlight the complexity of its pathogenesis. Therefore, it is challenging to research PD and comprehend its underlying processes.

Significant diagnostic criteria for PD include the presence of Lewy pathology and the preferential degradation of dopaminergic neurons in the SN pars compacta (Wegrzynowicz et al., 2019; Armstrong and Okun, 2020; Mahul-Mellier et al. 2020). The magnetic resonance imaging (MRI) (Arribarat and Péran, 2020), ultrasonography (US, (Lin et al., 2020), single-photon emission computed tomography (SPECT) (Lu and Yuan, 2015), and positron emission tomography (PET) are clinically accessible imaging methods that are used to diagnose the progression of PD (Gharibkandi and Hosseinimehr, 2019). The diagnosis and treatment of PD is still an evolving field of research. The work presented in this thesis is a step toward the search for possible MAO-B inhibitors for the treatment of PD.

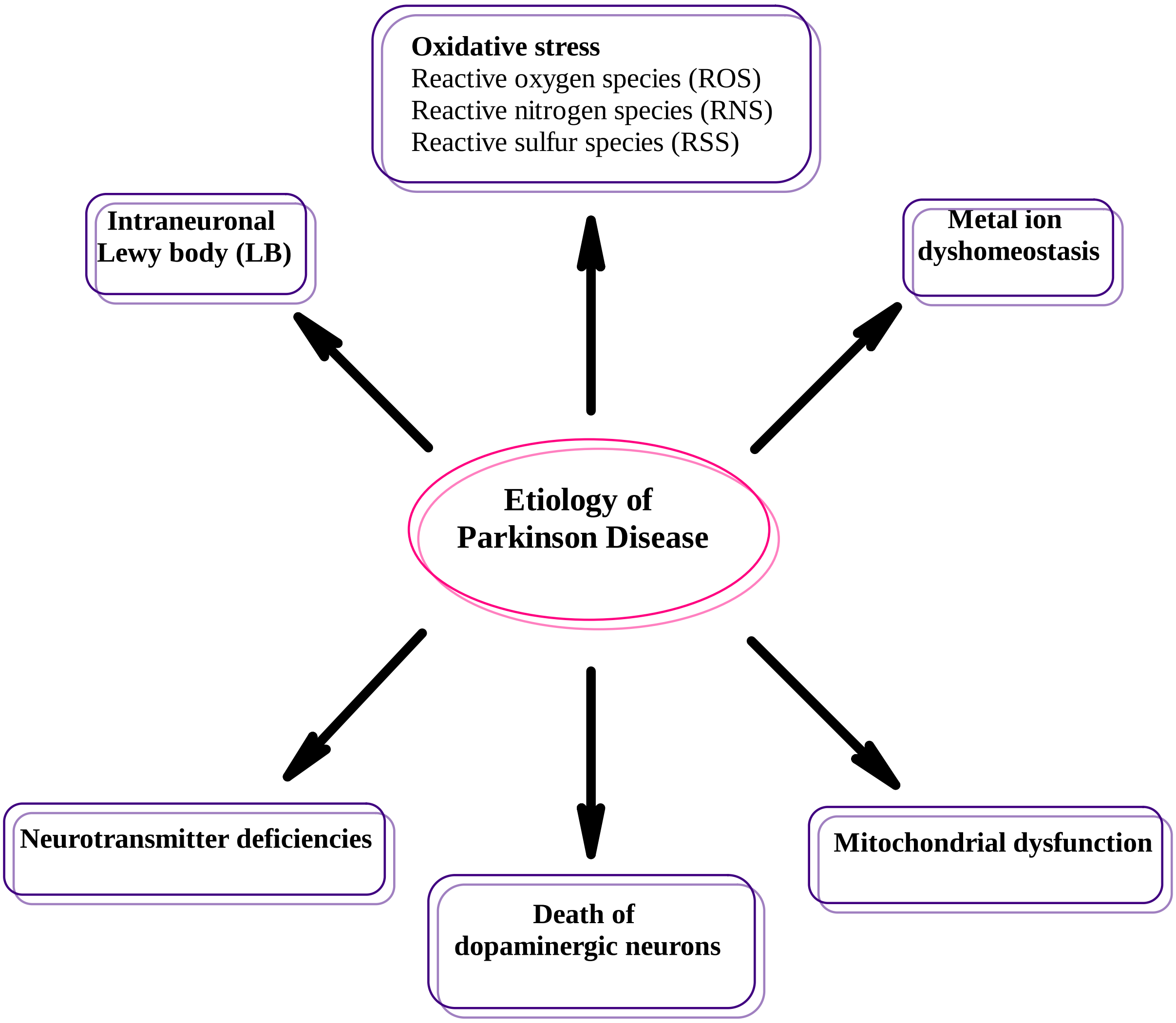

Figure 1.1. Aetiology of PD

1.2. Parkinson's Disease (PD): A brief overview

Traditional Indian scriptures from thousands of years ago, about 1000 BC, and ancient Chinese sources contain descriptions that seem to point to PD (Manyam, 1990). In 1817, James Parkinson for the first time concluded that PD is a neurological syndrome and coined the name

Parkinson's Disease (PD). The description of PD was there earlier also with related symptoms (De Sauvages, 1768; Tyler, 1992; Hoehn and Yahr, 1998). In 1912, the concept of 'Lewy bodies' came into the PD etiopathogenesis given by Frederick Lewy. This was followed by the dopamine deficiency concept in PD (Jankovic and Tan, 2020). Working on PD, Carlsson and Hornykiemiz in 1957 gave a relationship between dopamine deficiency and PD which was further supported by various studies done between 1961 and 1967 (Fahn, 2018). Later, Langston in 1982, gave the concept of drug-induced parkinsonism (Langston et al., 1983; Langston, 2017). According to him, the patients taking synthetic heroin developed symptoms of PD. The compound MPTP (methyl phenyl tertrahydropyridine) came out as a neurotoxin that affected SN dopaminergic neurons (Langston, 2017). Further investigations on PD also gave information about its genetic aetiology (Golbe et al., 1996; Polymeropoulos et al., 1997). The lifestyle of a person and environmental factors also contribute to PD (Ascherio and Schwarzschild, 2016; Simon et al., 2020). These developments helped not completely but yes up to some extent in the identification of therapeutic targets (Chan and Tan, 2017; Montaut et al. 2018).

According to the website 'parkinson.org' (retrieved on 4th February, 2023), only in U.S., about one million people are suffering from this disease and the number is expected to increase to 1.2 million by the year 2030. Global estimate is more than 10 million cases of PD where men are more prone to get affected than women. Women's sex hormones are believed to have a protective effect towards PD (Baldereschi et al., 2000, Eeden et al., 2003). The occurrence of gender-related genetic processes or/and gender-specific differences in exposure to environmental risk factors may help to explain why PD predominate in males (Baldereschi et al., 2000, Eeden et al., 2003; Haaxma et al., 2007). PD is an adult neurodegenerative disease affecting approximately 1% of the population over 65 and 4-5% over 80 years of age, which has an increasing incidence and prevalence with age (Lang and Lozano, 1998). The beginning of parkinsonian symptoms before the age of 40 is referred to as early-onset Parkinson's disease (EOPD). It makes up 3–5% of all instances of PD. It is divided into the "juvenile" and "young-onset" PDs, which develop before the age of 21 years, occurring in the age range of 21- 40 years (Schrag and Schott, 2006). All the statistical studies confirms that PD is a rapidly spreading disease globally increasing the economic and social burden (Lampropoulos et al., 2022; Dorsey et al., 2018; Li et al., 2019).

1.3. Parkinson's Disease (PD): Treatments Approach

Biochemical studies show a decrease of dopamine (DA) in the caudate nucleus and putamen; PD is therefore considered to be a disease of the neuronal system, which largely involves the nigrostriatal dopaminergic system (Kasper et al.; 2015). Various approaches have been adopted by the medicinal chemists to treat PD (Figure 1.2) (Ellis and Fell, 2017; Sun and Armstrong, 2021; Bologna et al., 2022). This disease is identified on the premise of two considerable pathological processes: early selective loss of dopamine neurons, and the build-up of LBs made up of α-synuclein that become misfolded and accumulate in a number of body systems of Parkinson's patients (Rizek et al., 2016). The dopamine is a neurotransmitter that helps towards the communication with neurons which further supports the movements coordination in the body. The lowering down of the dopamine levels leads to decline in movement coordination, an important symptom of PD (Triarhou, 2013). Resting tremor, rigidity, declining balance and motor coordination, and bradykinesia, which is characterized by a creeping slowness of voluntary movement, are all movement-related symptoms of PD (Robertson et al., 1990; Triarhou, 2013).

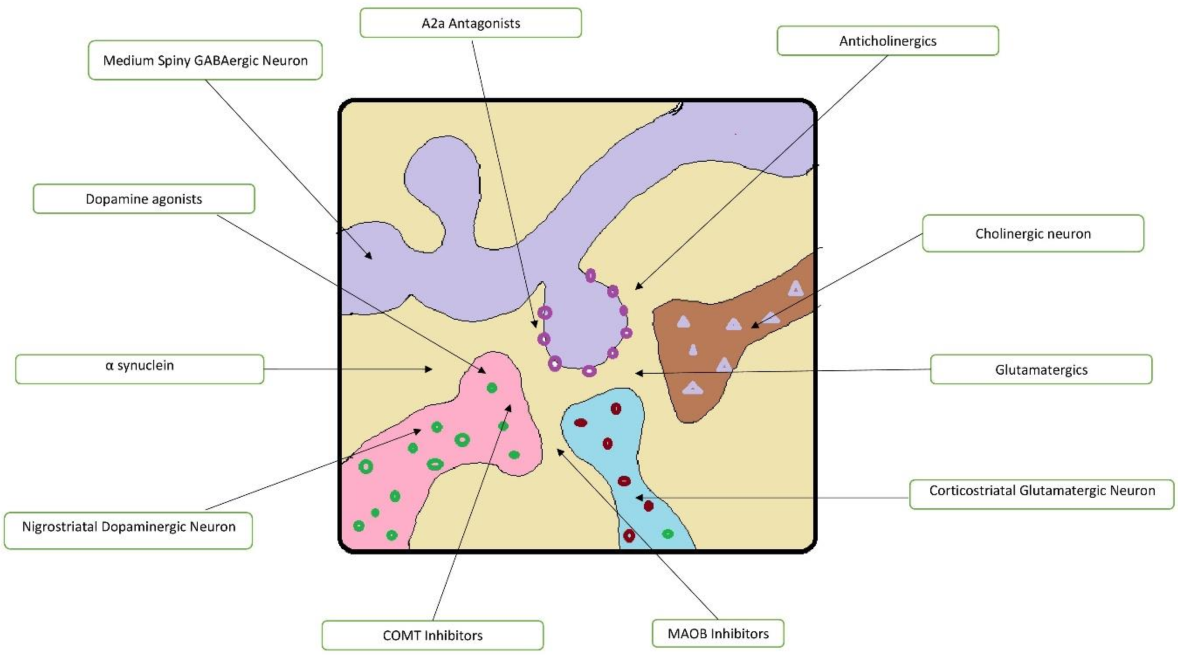

Figure 1.2. Different approaches for the treatment of PD

LBs are fibrillar aggregates whose major constituents include α-synuclein (Wakabayashi et al., 2007; Inskip et al., 2016). LBs and Lewy neurites are pathologically important to PD as they serve to be a prominent indication of the disease, being actively associated with PD pathogenesis (Mehra et al., 2019). Six genetic PD-associated mutations of α-synuclein have been discovered (Sahay et al.; 2017). The acceleration of α-synuclein aggregation showed in three mutations, while an additional three show delay of aggregation kinetics. It is therefore troublesome to provide a unifying mechanism describing how familial PD-associated mutations affect the structure of α-synuclein, and how their accumulation and function link with PD, as there have been several suggestions pointing in this direction (Sahay et al.; 2017).

LBs have been found in the neurons of the nucleus basalis of Meynert, the source of cholinergic innervation of the cerebral cortex (Bohnen and Albin, 2011). The basal forebrain complex, which provides the principal cholinergic input of the entire cortical mantle, degenerates in PD and can lead to symptoms such as dementia, depression, or apathy (Bohnen and Albin, 2011). Anosmia and hyposmia are common side effects of PD. While the pathophysiology is not fully understood, it could be related to α-synuclein deposits in the olfactory bulb, medulla oblongata, anterior olfactory nucleus, and limbic rhinencephalon (Braak et al., 2002; Bohnen and Albin, 2011). Progressive, non-linear loss also occurs in serotonergic terminals, although slower than the progressive loss seen in dopaminergic terminals. It can lead to both motor and non-motor symptoms such as depression, tremors, weight loss, and visual hallucinations (Politis and Niccolini, 2015). Reduced levels of serotonin and its metabolite are found in the caudate nucleus, hippocampus, brainstem, and frontal cortex (Scatton et al., 1983; Halliday et al. 1990). Additionally, adrenergic neurons are impacted. One study has shown an increase in α_1 and β_1 receptors, especially in demented PD patients, and a decrease in α_2 receptors within the pre-frontal cortex (Cash et al., 1984). Disruptions in adrenergic pathways may lead to or worsen dementia and depression (Cash et al., 1984). One of the effective ways to alleviate PD is to block the α-synuclein receptors. Some of other most studied treatment approaches have been discussed in the following sections:

1.3.1 Dopamine Agonists

Dopamine agonists (DA) are powerful drugs in the management of PD and have shown equal evidence of being clinically useful both as monotherapy and as adjunct to levodopa in early and mid-stage/advanced PD patients (Aradi and Hauser, 2020). DA have also demonstrated efficacy in delaying the introduction of levodopa therapy and the risk of motor complications (Nutt et al., 2000; Stocchi, 2011), becoming preferable drugs for the treatment of younger patients (Fox et al., 2011). They are commonly classified in two groups: ergot derivatives (e.g. bromocriptine, pergolide, lisuride and cabergoline) and non-ergot derivatives (e.g. pramipexole, ropinirole, piribedil and rotigotine (Cerri and Blandini, 2020). The DA mostly used today belong to the class of non-ergot derivatives (NEDA) (Stocchi et al., 2020). There are several indications of gender differences in PD: incidence and prevalence of the disease is higher in men than in women who show a more benign progression and lower striatal degeneration at the time of diagnosis (Kotagal et al., 2013). According to some studies, both levodopa and DA agonists significantly improve motor symptoms when used as monotherapy in early/stable PD. However, the Levodopa in Early Parkinson's Disease (LEAP) study demonstrated a more rapid disease progression in patients receiving early levodopa treatment (Verschuur et al., 2019). The use of DA agonists is also recommended for mitigating levodopa-associated motor complications in older PD patients without a history or risk of psychosis or impulse control disorders (Latt et al., 2019).

1.3.2 Anticholinergic approach

The first medications used to treat PD patients were anticholinergic medicine. Currently, they are either utilised as an earlier start monotherapy or as an adjuvant therapy with Levodopa. In young PD patients, these medications are frequently used to treat tremor, delay the need for L-dopa treatment, and also to lower the dose of L-dopa in individuals with severe disease stages (Katzenschlager et al., 1996). Anticholinergics' primary adverse effects are bladder dysfunction, gastrointestinal distress, diminished focus, disorientation, attention deficit disorder, memory impairment, and psychological issues (Wawruch et al., 2012). Patients' short-term memory and frontal lobe function are impaired by anticholinergic activities at extrastriatal locations, and gait and postural impairments may get worse (Perez et al., 2018). Tremor and bradykinesia, two parkinsonian symptoms, were exacerbated by acetylcholinesterase inhibitors (Duvoisin, 1967). Although the exact mechanism has not been fully elucidated, it is thought that inhibiting muscarinic acetylcholine receptors corrects the imbalance between dopamine and acetylcholine in the striatum. Trihexyphenidyl (Artane®) and biperiden (Akineton®) (Figure 1.3) are two examples of anticholinergic medications that are still in use today (Kawabata and Katsuno, 2021). Drugs having anticholinergic action that cross the blood-brain barrier and fight with acetylcholine for the same binding sites on muscarinic receptors in the central nervous system provide central anticholinergic effects (Kersten and Wyller, 2014).

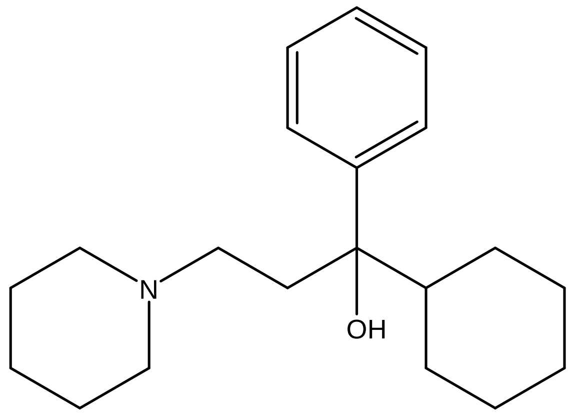

Trihexyphenidyl

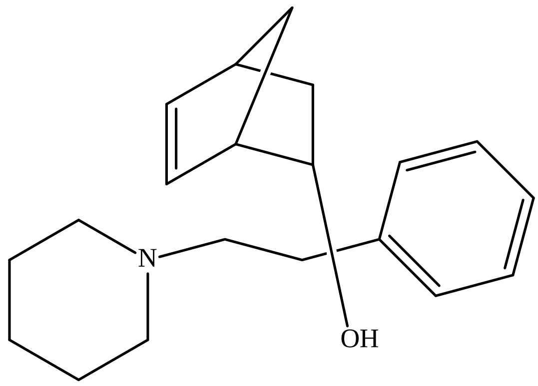

Biperiden

Figure 1.3. Chemical structures of Artane® and biperiden Akineton®

1.3.3 Glutamatergic approach

The neurotransmitter glutamate predominates in the excitatory synapses of the central nervous system (CNS). It is essential for basic brain processes like synaptic plasticity and the evolution of neural networks (Reiner and Levitz, 2018). Excitatory amino acid transporters transfer glutamine, the precursor of glutamate, into the presynaptic terminals of glutamatergic neurons where it is converted into glutamate. Glutaminase turns glutamine into glutamate in this instance. Glutamate is released into the synaptic cleft upon activation of the neuron and binds to pre- and post-synaptic receptors (Niciu et al., 2012; Tozzi et al., 2021). Due to the degradation of dopaminergic afferents, the striatal dopamine (DA) release is reduced in PD (Natale et al., 2021; Babinski et al., 1921). This results in numerous modifications to the synaptic physiology, mostly impacting the striatal glutamatergic transmission, with modest changes to the spiny projection neurons (SPNs), which in turn cause the striatal microcircuitry to activate compensatory mechanisms (Tozzi et al., 2011, Tozzi et al., 2016). With a novel method of action that comprises inhibiting excessive glutamate release when nerve terminals are hyperactive, safinamide (Figure 1.4) is a recognised treatment for PD. In most of the studies only animal models have been used to show the direct effects of safinamide on glutamate release (Caccia et al., 2006; Morari et al., 2018; Gardoni et al., 2018; Pisanò et al., 2020).

1.3.4 Role of monoamine oxidase-B (MAO-B) in PD treatment

Mammal CNS and peripheral tissues have cells that contain the flavoenzyme MAO in their outer mitochondrial membranes (Cohen et al., 1997; Edmondson et al., 2009; Blazevic et al., 2017). It catalyzes the conversion of dietary and biogenic amines to their corresponding aldehydes (Figure 1.5), subsequently, hydrogen peroxide and ammonia are produced. The two isoforms of MAO, MAO-A, and MAO-B, are distinguished by their unique properties, substrates, and inhibitors (Bach et al., 1988; Vindis et al., 2001; Li et al., 2014, 2015; Binda et al., 2005). The hydroxylated amines and serotonin (5-HT) are preferred substrates for the MAO-A isoform, which is specifically inhibited by clorgyline. While MAO-B is selectively inhibited by rasagiline, pargyline, and low quantities of selegiline (Figure 1.4). It metabolises non-hydroxylated amines as benzylamine and β-phenylethylamine (Youdim et al., 2006a; Finberg and Rabey, 2016). Drugs with amines moieties such as DA, tyramine, tryptamine and epinephrine works to inhibit both the isoforms of MAO (Youdim et al., 2006b). In this regard, MAO inhibitors (Figure 1.6) have a long history of usage as anti-parkinsonian and anti-depressant medications that enhance patients' quality of life (Marti et al., 1990).

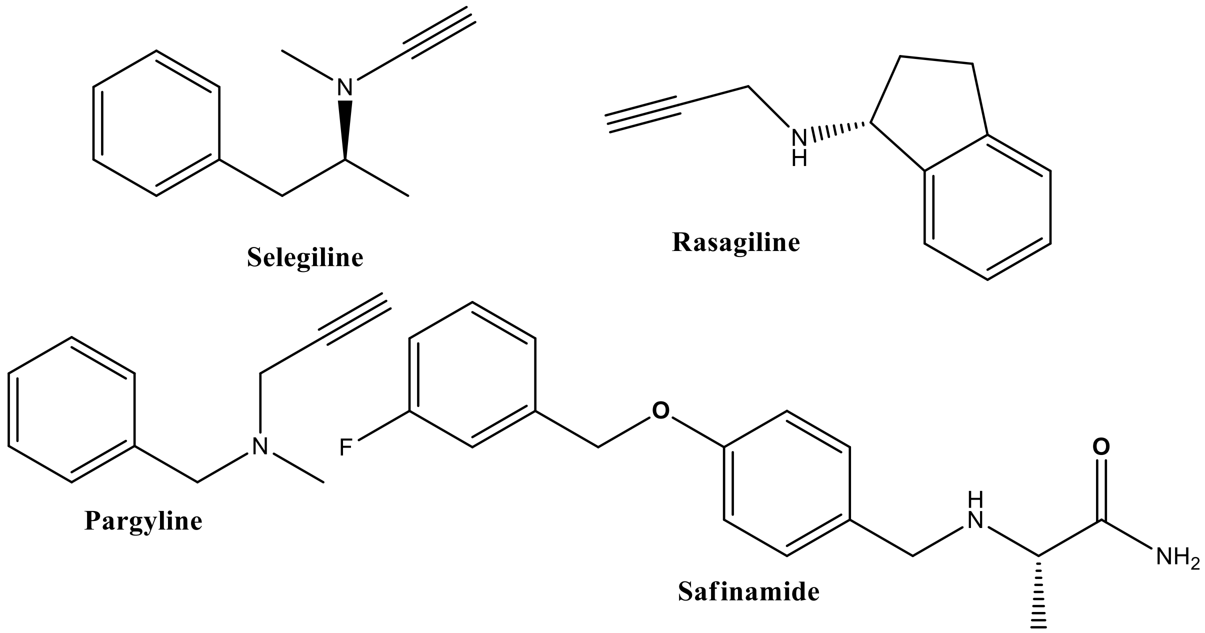

Figure 1.4. Chemical structures of approved drugs for PD

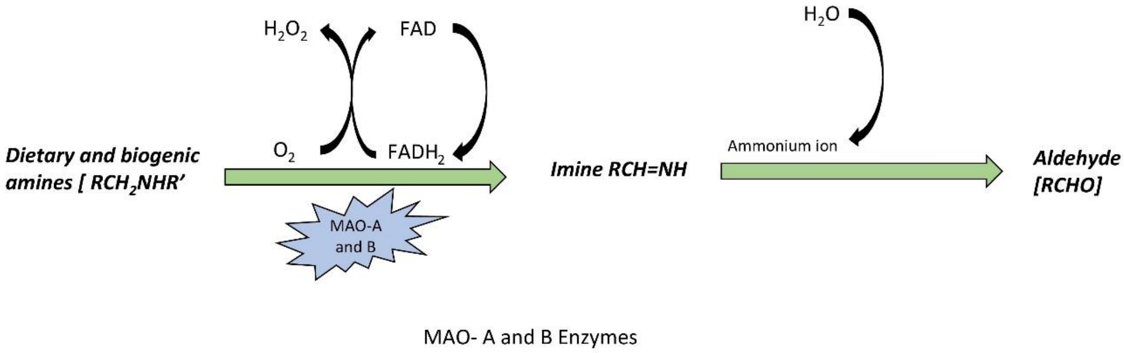

Figure 1.5. Reaction of MAO with amines

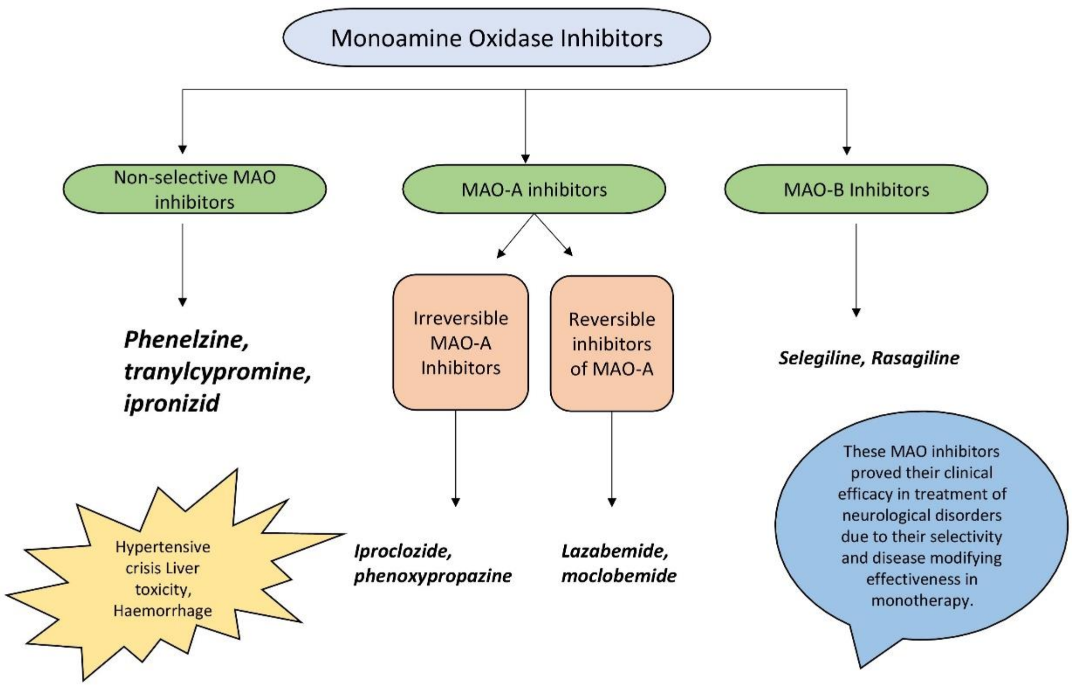

Figure 1.6. MAO inhibitors

The MAO-B isoform, which predominates in the human brain, breaks down dopamine into 3,4-dihydroxyphenylacetic acid and homovanillic acid. PD pathomechanism is strongly impacted by mitochondrial dysfunction, notably oxidative stress brought on by reactive dopamine metabolites and disruption of complex I of the mitochondrial electron transport chain. Because it catalytically converts both endogenous and exogenous dopamine to hydrogen peroxide, MAO-B is essential for the oxidative stress and oxidative damage mechanisms that occur in PD (Marti et al., 1990). MAO-B levels have been linked to ageing and various neurodegenerative conditions, including Alzheimer's Disease (AD) and PD; this phenomenon is assumed to be connected to the elevated oxidative stress that these conditions induce (Hauser and Hastings, 2013). It's noteworthy that 1-methyl-4-phenyl-1,2,3,6-tetrahydropyridine (MPTP) (William, 2017) is converted by the enzyme MAO-B into the neurotoxic metabolite 1-methyl-4-phenylpyridinium ion (MPP+), which might result in experimental or secondary parkinsonism (Figure 1.7) (He and Nakayama, 2009). Also, β-carbolines and isoquinolines, two more potential poisons, are activated by MAO-B which showed adverse effect (Chiba et al., 1984; Dézsi and Vécsei, 2014).

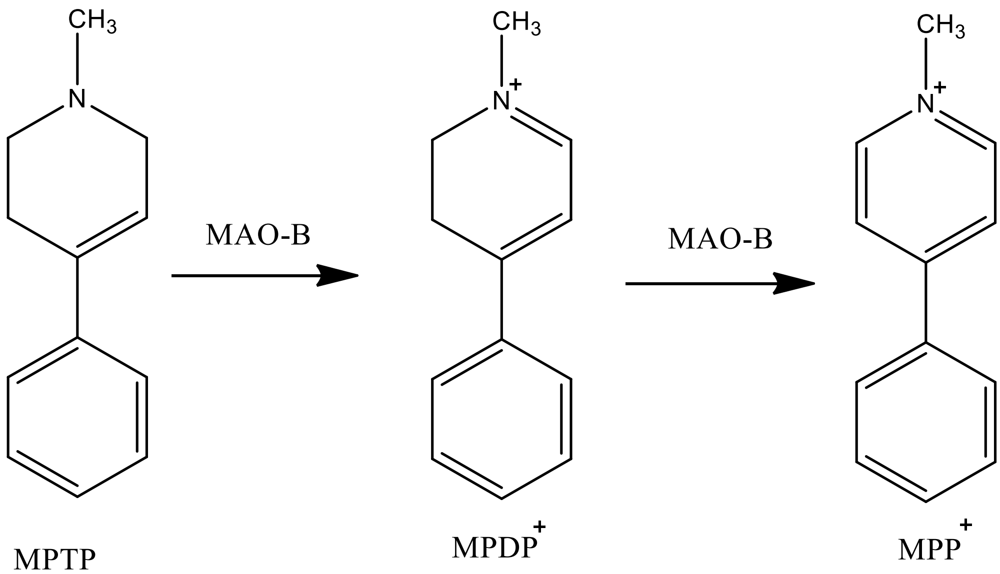

Figure 1.7. MPTP to MPP^+ transformation

Increased striatal dopaminergic activity brought on by MAO-B inhibition lowers dopamine breakdown and provides therapeutic advantages in dopamine-deficient diseases. As a result, levodopa's actions are enhanced and more dopamine is made available to interact with dopamine receptors (Dezsi and Vecsei, 2017). Inhibiting MAO-B limits the conversion of MPTP to MPP+ and lowers the amount of free radicals created by the oxidation of dopamine in animal models. Thus, MAO-B inhibition may have neuroprotective benefits, but more clinical studies are still required (Knoll et al., 1978; Cohen et al., 1984). The potential for some MAO-Bs to treat illness was examined in the data top study for selegiline and the delayed-start clinical trials for rasagiline. There are many scaffolds that have been synthesized and evaluated as MOA-B inhibitors (Pretorius et al., 2008; Borges et al., 2010; Carradori et al., 2014; Matos et al., 2014; Rodriguez-Enriquez et al., 2020; Boulaamane et al., 2022). Still, there is a lot of scope available to design, synthesize and evaluate MAO-B inhibitors to either treat completely or atleast hold the disease at diagnosed stage. To enrich the library of more MAO-B inhibitors, in the present work, conjugates of thiazole, pyrazole, and benzimidazole have been designed and *in-silico* studies have been done. The selected conjugates have been synthesized and evaluated.

1.4 Conclusions

The chapter covers the description of Parkinson's Disease (PD) and its possible pathways of treatment. PD was first medically described as a neurological syndrome by James Parkinson in 1817, though fragments of Parkinsonism can be found in earlier descriptions. This is the second most common neurodegenerative disorder worldwide, affecting 2–3 % of the population ≥ 65 years of age. There are different targets for the treatment of this disease which includes restoring dopamine synthesis, avoiding excess of dopamine breakdown, genetic neuromodulation, neuroprotection, and addressing disease-specific pathogenic variants. There are many targets for the treatment of PD, out of which MAO-B inhibitors have become recent target of research. MAOs are flavin adenine dinucleotide (FAD) containing enzymes that catalyze the oxidation of xenobiotics and endogenous monoamine neurotransmitters to modulate their levels and functions in peripheral and brain tissues. MAOs exist in two forms as MAO-A and MAO-B. The use of MAO-B inhibitors for the treatment of PD have been discussed in this chapter.

The present work has been carried out to design and synthesize the MAO-B inhibitors for PD. The conjugates of thiazole, pyrazole, and benzimidazole have been designed and *in-silico* studies have been done. The selected conjugates have been synthesized and evaluated. The work entitled "Synthesis and evaluation of heterocycles as anti-Parkinson agents" has been divided into four chapters excluding reference section:

Chapter 1: Parkinson's Disease: An overview
Chapter 2: Experimental Section
Chapter 3: Results and Discussion
Chapter 4: Conclusion

References

CHAPTER 2

Experimental Section

2.1 Materials and Instrumentation

All the chemicals, solvents and reagents were purchased from commercial suppliers and were used without further purifications. Reactions were performed in oven-dried glassware. Melting points were determined on a laboratory open-glass melting apparatus and were uncorrected. Thin-layer chromatography (TLC) was performed on aluminum-coated silica plates purchased from Merck (TLC Silica gel 60 F_{254}). UV-Visible spectrophotometer spectra were recorded on Perkin-Elmer Lambda-365. Fourier-transform infrared spectroscopy (FTIR) spectra were recorded in KBr on a Perkin-Elmer Spectrum II spectrophotometer, and proton nuclear magnetic resonance (^{1}H NMR) spectra were recorded on a Bruker Avance-300 spectrophotometer using tetramethylsilane (TMS) as an internal reference with chemical shift values being reported in ppm (δ value). The coupling constants are given in Hertz. Splitting patterns are designated as s (singlet), d (doublet), t (triplet), m (multiplet) etc. The elemental analysis was measured by Perkin Elmer 2400. The mass spectra were recorded by maXis impact and XEVO G-2-XS QTOF instruments. The RP-HPLC Thermofisher Ultimate 3000 UHPLC was used for purity check.

2.2 *In-silico* studies

2.2.1 Modelling platform

The computational analysis was carried out using the Schrödinger Maestro 16.4 trial version which included LigPrep, Glide XP docking, grid generation, free energy calculations, absorption, distribution, metabolism, and excretion (ADME) calculations, and MD simulations (Maestro 10.2 user manual). Windows 7 was used as the operating system.

2.2.2 Biological data

In this study, 3-D structure of the MAO-B target was retrieved from the Research Collaboratory for Structural Bioinformatics Protein Data Bank (www.rcsb.org). The conjugates of pyrazole and thiazole, benzimidazole and pyrazole, and benzimidazole and thiazole were used for further studies. The MAO-B targets were taken from the Protein Data Bank and its databank alpha-numeric identity is 4A7A for MAO-B.

2.2.3 Preparation of the protein

The crystallographic structure of enzyme MAO-B was retrieved from protein data bank (PDB) (PDB ID: 4A7A). The crystal structure of MAO-B is in complex with a rasagiline analogue as inhibitor with resolution of 1.7 Å (Binda et al., 2005). Before docking, the crystal structures of MAO-B were prepared using protein preparation wizard in Schrödinger Maestro 16.4 trial version (Maestro 10.2 user manual). The protein structure was optimized by removing the ligand, heteroatoms, water molecules, and co-factors. Missing atoms, hydrogen bonds, and charges were computed. Before generation of receptor grid, active sites were identified using sitemap.

2.2.4 Ligand preparation

The compounds **4a**, **4b**, **4f**, **4h**, **4m**, **7a**, **11** and **20-302** (total 304 compounds) were prepared using LigPrep module the Epik2.0 in the pH range of 7.0 ± 2.0. Preparation of ligands include generation of various tautomer's, assigning bond orders, stereochemistry and ring conformations to eliminate molecules on the basis of various criteria such as molecular weight or specified numbers. The OPLS-2005 force field was used for the optimization, which produced the low-energy isomer of the ligand (Vijayakumar et al., 2018).

2.2.5 Molecular docking

Molecular docking is a computational stimulation that predicts the preferred orientation of a ligand with a receptor during their interaction to form a complex with high stability. Docking studies were carried out using Glide tool of Schrödinger Maestro16.4 trial version to perform rigid, flexible docking for predicting the binding affinity, ligand efficiency, and inhibitory constant to the target. The compounds **4a**, **4b**, **4f**, **4h**, **4m**, **7a**, **11** and **20-302** (total 304 compounds) were docked to the active site of MAO-B using Glide Extra Precision (XP) mode, which docks to determine the ligand's flexibility. Only the active molecule would have available access to avoid the penalties and receive favourable docking scores with accurate hydrophobic contact between the protein and ligand. The obtained results were analysed considering the XP GScore (Vijayakumar et al., 2018; Schrodinger, LCC, PyMOL, 2015).

2.2.6 Prime molecular mechanics-generalized born surface area (MM-GBSA) calculations

The ligand binding energy of each compound **4a**, **4b**, **4f**, **4h**, **4m**, **7a**, **11** and **20-302** (total 304 compounds) required to inhibit MAO-B was estimated using Prime MMGBSA module in Schrödinger Maestro16.4 trial version. The binding mode for each compound was visualized using PyMOL. The total free energy binding (dG bind, kcal/mol) was estimated as follows using the software:

$$\Delta G\ bind = G\ complex - (G\ protein + G\ ligand)$$

where each energy term is a combination of G = molecular mechanics energies (MME) + GSGB (SGB solvation model for polar solvation) + GNP (non-polar solvation) coulomb energy, covalent binding energy, van der Waals energy, lipophilic energy, GB electrostatic solvation energy, prime energy, hydrogen-bonding energy, hydrophobic contact, self-contact correction (Vijayakumar et al., 2018). OPLS 2005 force field was used for the optimization, which produced the low-energy isomer of the ligand (Vijayakumar et al., 2018).

2.3 Synthesis of 5-amino-1*H*-pyrazole-4-carbonitrile derivatives (4a-n)

2.3.1 General procedure for the synthesis of catalytic MnO_2

In a solution of *n*-propanol and de-ionised water (70 mL, 1:1 v/v), manganese acetate tetrahydrate [$Mn(OAc)_2 \cdot 4H_2O$, 6 g] and silica and/or alumina (3 g) were added. The reaction mixture was stirred at 80 °C for 3 h. Further, an aqueous solution of $KMnO_4$ (1.5 g in 70 mL water) was added to the mixture and kept stirring for 2 h. A black precipitate was obtained. It was centrifuged and separated and then dried at 70 °C under vacuum for 5 h.

2.3.2 General procedure for synthesis of pyrazole derivatives (4a-n)

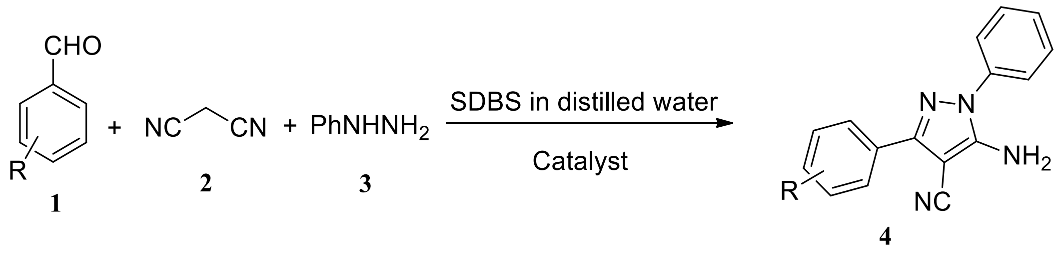

Scheme 2.1. Synthesis of pyrazole derivatives (**4a-n**)

Aldehyde (**1**, 1 mmol), malononitrile (**2**, 1 mmol), and catalyst (150 mg) were taken in distilled water (10 mL) into a round-bottomed flask. To the reaction mixture, sodium dodecylbenzene sulphonate (SDBS, 150 mg) was added and stirred at room temperature for 20 min till a white precipitate was obtained. At this point, phenylhydrazine (**3**, 1 mmol) was added, and the reaction mixture was further stirred at room temperature (35 °C) for 3–12 min. The progress of the reaction was monitored by TLC (hexane/ethyl acetate 7:3, v/v). After completion of the reaction, water and ethyl acetate (1:1, v/v, 30 mL) were added and filtered. The filtrate was put in a separating funnel to separate the ethyl acetate layer. The ethyl acetate was dried over anhydrous sodium sulfate (Na_2SO_4), filtered, and evaporated to give the final product that was further recrystallized with hot ethanol.

5-Amino-1,3-diphenyl-1H-pyrazole-4-carbonitrile (4a)

Yield: 91%; Mp.: 158-159 ^oC (Lit. Mp. 161 ^oC) (Mishra et al., 2017); FT-IR (KBr, cm^{-1}): 3458, 3344, 3026, 2926, 2865, 2209, 1615, 1594, 1562, 1493, 1257, 1195, 1138, 1088; ^1H NMR (DMSO-*d6*): δ 7.85 (s, 2H, NH_2), 7.64 (d, 2H, J = 7.2 Hz, ArH), 7.41–7.36 (m, 2H, ArH), 7.31–7.24 (m, 3H, ArH), 7.06 (d, 2H, J = 7.5 Hz, ArH), 6.74 (t, 1H, J = 7.2 Hz, ArH).

5-Amino-3-(4-nitrophenyl)-1-phenyl-1H-pyrazole-4-carbonitrile (4b)

Yield: 94%; Mp.: 161-162 ^oC (Lit. Mp. 164-165 ^oC) (Mishra et al., 2018); FT-IR (KBr, cm^{-1}): 3454, 3300, 3105, 2926, 2196, 1594, 1555, 1536, 1493, 1324, 1241, 1164, 1100, 915. ^1H NMR ($CDCl_3$): δ 8.24–8.21 (m, 2H, NH_2), 7.79–7.70 (m, 3H, ArH), 7.36–7.29 (m, 3H, ArH), 7.15 (dd, 2H, J = 9.0 and 1.2 Hz, ArH), 6.95 (t, 1H, J = 7.2 Hz, ArH).

5-Amino-3-(2-nitrophenyl)-1-phenyl-1H-pyrazole-4-carbonitrile (4c)

Yield: 90%; Mp.: 159 ^oC (Lit. Mp. 160-162 ^oC) (Kiyani and Bamdad, 2018); FT-IR (KBr, cm^{-1}): 3449, 3294, 3023, 2970, 2855, 2196, 1601, 1572, 1533, 1491, 1334, 1254, 1132, 903. ^1H NMR ($CDCl_3$): δ 8.36 (s, 2H, NH_2), 8.26–8.14 (m, 2H, ArH), 8.05–7.95 (m, 2H, ArH), 7.59–7.53 (m, 2H, ArH), 7.15–7.12 (m, 2H, ArH), 6.84 (t, 1H, J = 7.3 Hz, ArH).

5-Amino-3-(2-bromophenyl)-1-phenyl-1H-pyrazole-4-carbonitrile (4d)

Yield: 86%; Mp.: Semi solid (Lit. Mp. Semi solid) (Poonam and Singh, 2019); FT-IR (KBr, cm^{-1}): 3455, 3331, 3298, 3053, 2967, 2226, 1602, 1579, 1512, 1438, 1255, 1142, 1021. ^1H NMR ($CDCl_3$): δ 8.07–8.04 (m, 2H, NH_2), 7.52 (dd, 2H, J = 8.1 and 1.2 Hz, ArH), 7.30–7.24 (m, 4H, ArH), 7.25–7.15 (m, 2H, ArH), 6.86 (t, 1H, J = 7.2 Hz, ArH).

5-Amino-3-(2-fluorophenyl)-1-phenyl-1H-pyrazole-4-carbonitrile (4e)

Yield: 88%; Mp.: Viscous Oil (Lit. Mp. Oil) (Poonam and Singh, 2019); FT-IR (KBr, cm^{-1}): 3458, 3344, 3026, 2926, 2855, 2209, 1594, 1493, 1354, 1257, 1138, 1091. ^1H NMR ($CDCl_3$): δ 7.99–7.55 (m, 4H, NH_2, ArH), 7.27–7.25 (m, 2H, ArH), 7.11–6.88 (m, 5H, ArH).

5-Amino-3-(4-fluorophenyl)-1-phenyl-1H-pyrazole-4-carbonitrile (4f)

Yield: 93%; Mp.: Oil (Lit. Mp. Yellow oil) (Srivastava et al., 2014); FT-IR (KBr, cm^{-1}): 3465, 3311, 3053, 2924, 2208, 1597, 1502, 1445, 1229, 1089. ^1H NMR ($CDCl_3$): δ 7.87 (s, 2H, NH_2), 7.61–7.56 (m, 2H, Ar-H), 7.28–7.23 (m, 2H, ArH), 7.09–7.02 (m, 4H, ArH), 6.86 (t, 1H, J = 7.2 Hz, ArH).

5-Amino-3-(4-bromophenyl)-1-phenyl-1H-pyrazole-4-carbonitrile (4g)

Yield: 95%; Mp.: 164-165 ^oC (Lit. Mp. 164-165 ^oC) (Kiyani and Bamdad, 2018); FT-IR (KBr, cm^{-1}): 3465, 3310, 3043, 2926, 2210, 1600, 1501, 1493, 1320, 1202, 1150, 1062. ^1H NMR ($CDCl_3$): δ 7.83 (s, 2H, NH_2), 7.71–7.69 (m, 2H, ArH), 7.65–7.59 (m, 3H, ArH), 7.32–7.21 (m, 3H, ArH), 6.89–6.83 (m, 1H, ArH).

5-Amino-3-(4-chlorophenyl)-1-phenyl-1H-pyrazole-4-carbonitrile (4h)

Yield: 95%; Mp.: 128-129 ^oC (Lit. Mp. 129 ^oC) (Mishra et al., 2017); FT-IR (KBr, cm^{-1}): 3445, 3342, 3033, 2986, 2203, 1612, 1595, 1544, 1493, 1090. ^1H NMR ($CDCl_3$): δ 7.85 (s, 2H, NH_2), 7.70–7.49 (m, 5H, ArH), 7.38–7.24 (m, 3H, ArH), 6.88 (t, 1H, J = 7.3 Hz, ArH).

5-Amino-3-(2-chlorophenyl)-1-phenyl-1H-pyrazole-4-carbonitrile (4i)

Yield: 90%; Mp.: Semi solid (Lit. Mp. Semi solid) (Srivastava et al., 2014); FT-IR (KBr, cm^{-1}): 3455, 3341, 3022, 2921, 2853, 2204, 1591, 1497, 1355, 1257, 1130, 1091, 953. ^1H NMR ($CDCl_3$): δ 7.98 (s, 2H, NH_2), 7.62–7.55 (m, 2H, ArH), 7.40–7.34 (m, 3H, ArH), 7.25–7.15 (m, 3H, ArH), 6.76 (t, 1H, J = 7.3 Hz, ArH).

5-Amino-3-(4-methylphenyl)-1-phenyl-1H-pyrazole-4-carbonitrile (4j)

Yield: 96%; Mp.: 117-118 ^oC (Lit. Mp. 120 ^oC) (Mishra et al., 2017); FT-IR (KBr, cm^{-1}): 3455, 3310, 2924, 2205, 1595, 1505, 1256, 1128, 1069. ^1H NMR ($CDCl_3$): δ 8.26 (s, 2H, NH_2), 7.82–7.77 (m, 2H, ArH), 7.53–7.41 (m, 4H, ArH), 7.22–7.15 (m, 2H, ArH), 6.87 (t, 1H, J = 7.2 Hz, ArH), 2.33 (s, 3H, CH_3).

5-Amino-3-(4-methoxyphenyl)-1-phenyl-1H-pyrazole-4-carbonitrile (4k)

Yield: 96%; Mp.: 107-108 ^oC (Lit. Mp. 110 ^oC) (Mishra et al., 2017); FT-IR (KBr, cm^{-1}): 3455, 3300, 2962, 2889, 2198, 1603, 1556, 1519, 1483, 1303, 1122, 1011, 993. ^1H NMR ($CDCl_3$): δ 7.94 (s, 2H, NH_2), 7.69–7.61 (m, 2H, ArH), 7.57–7.52 (m, 3H, ArH), 7.13– 7.00 (m, 3H, ArH), 6.76 (t, 1H, J = 7.3 Hz, ArH), 3.74 (s, 3H, OCH_3).

5-Amino-3-(2-methoxyphenyl)-1-phenyl-1H-pyrazole-4-carbonitrile (4l)

Yield: 90%; Mp.: 130-131 ^oC (Lit. Mp. 130-132 ^oC) (Srivastava et al., 2014); FT-IR (KBr, cm^{-1}): 3453, 3297, 2962, 2919, 2198, 1596, 1519, 1493, 1333, 1128, 1016, 997. ^1H NMR ($CDCl_3$): δ 7.84 (s, 2H, NH_2), 7.66–7.61 (m, 2H, ArH), 7.50–7.44 (m, 2H, ArH), 7.13–7.01 (m, 4H, ArH), 6.89–6.93 (m, 1H, ArH), 3.84 (s, 3H, OCH_3).

5-Amino-3-(3,4-dimethoxyphenyl)-1-phenyl-1H-pyrazole-4-carbonitrile (4m)

Yield: 94%; Mp.: 120-122 ^oC (Lit. Mp. 120-123 ^oC) (Srivastava et al., 2014); FT-IR (KBr, cm^{-1}): 3463, 3294, 2972, 2939, 2201, 1596, 1511, 1494, 1330, 1128, 1016. ^1H NMR ($CDCl_3$): δ 8.45 (s, 2H, NH_2), 7.69–7.63 (m, 2H, ArH), 7.35–7.29 (m, 3H, ArH), 7.16–6.97 (m, 3H, ArH), 3.79–3.76 (m, 6H, 2×OCH_3).

5-Amino-3-(3-nitrophenyl)-1-phenyl-1H-pyrazole-4-carbonitrile (4n)

Yield: 93%; Mp.: 127-129 °C (Lit. Mp. 128-130 °C) (Srivastava et al., 2014); FT-IR (KBr, cm^{-1}): 3450, 3284, 3023, 2972, 2855, 2206, 1601, 1572, 1555, 1533, 1490, 1334, 1251, 1130, 943. ^1H NMR ($CDCl_3$): δ 8.16 (s, 2H, NH_2), 7.76–7.64 (m, 2H, ArH), 7.45–7.35 (m, 2H, ArH), 7.19–7.03 (m, 2H, ArH), 6.99–6.84 (m, 3H, ArH).

2.4 Synthesis of phenyl-1,3-thiazole-2-amine derivatives (7a-l)

2.4.1 Procedure for the synthesis of MoS_2 quantum dots

The MoS_2 QDs were prepared through facile hydrothermal route. The sodium molybdate (24 mM) and thioacetamide (55 mM) were taken in a certain amount and stirred for 30 min under inert environment. Then, 1,4-diamino butane (DAB, 1.4 mL) was added to the above mixture and stirred for another 10 min. Afterwards, the mixture was transferred to the Teflon lined hydrothermal reactor at 200 °C for 24 h. The mixture was allowed to cool naturally to the room temperature and then, the surfactant was purified through dialysis process for 48 h. The cellulose membrane of 1 kda was used to eliminate impurities and unreacted reagents. The DI water used for dialysis was changed at an interval of 2 h. The final product obtained is the pale-yellow colloidal solution which exhibit bright blue fluorescence under UV illumination. The purified QDs were then kept at 4 °C until further characterizations and reactions.

2.4.2 Procedure for the synthesis phenyl-1,3-thiazole-2-amine derivatives (7a-l)

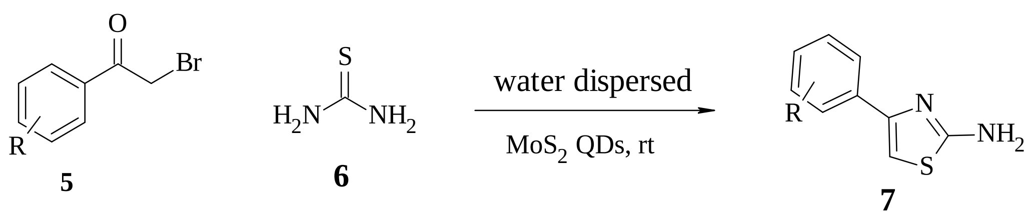

Scheme 2.2. Synthesis of pyrazole derivatives (**7a-l**)

2.5 Synthesis of 2-(4-nitrophenyl)-1H-benzoimidazole

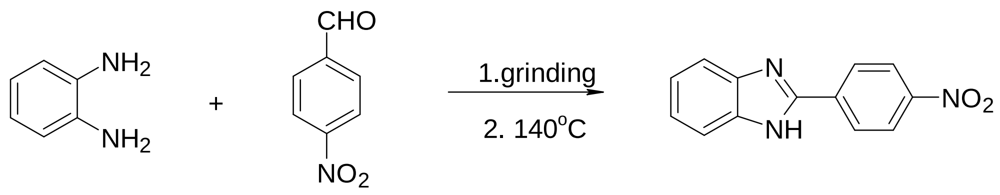

8 **1b** **9**

Scheme 2.3. Synthesis of 2-(4-nitrophenyl)-1H-benzoimidazole (**9**)

Benzene-1,2-diamine (**8**, 9.2 mmol) and 4-nitrobenzaldehyde (**1b**, 9.2 mmol) was thoroughly ground with a pestle in a mortar at room temperature until the overall mixture turned into a melt. The melt was then heated at 140 °C for 2 h. The progress of reaction was monitored by TLC. After completion, the compound was extracted with ethyl acetate and was purified by column chromatography.

2-(4-Nitrophenyl)-1H-benzo[d]imidazole (9)

Yield: 88%; Mp.: >300 °C (Lit. Mp. 324-326 °C) (Patil et al., 2016); FT-IR (KBr, cm^{-1}): 3337, 2963, 1604, 1511, 1433, 1337, 1281, 1101, 1008, 968, 852, 744, 709, 681, 614; ^{1}H NMR (DMSO-*d6*, 400 MHz) δ: 13.30 (s, 1H, NH), 8.44-8.39 (m, 4H, ArH), , 7.74 (d, *J* = 8.0 Hz, 1H, ArH), 7.60 (d, *J* = 8.0 Hz, 1H, ArH), 7.31-7.23 (m, 2H, ArH).

2.6 Synthesis of 2-(4-aminophenyl)-1H-benzo[d]imidazole (10)

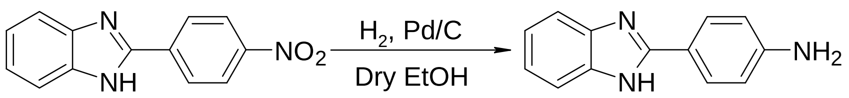

9 **10**

Scheme 2.4. Synthesis of 2-(4-aminophenyl)-1H-benzo[d]imidazole (**10**)

A solution of 2-(4-nitrophenyl)-1H-benzoimidazole (**9**, 500 mg, 2.0 mmol) in dry ethanol (50 mL) was taken in a glass reaction bottle (500 mL). To this solution Pd/charcoal (10%) (0.01 g) was added. The reaction mixture was hydrogenated at an ambient temperature and at 60 psi pressure for 7 h. After completion of the reaction, the catalyst was filtered using a celite pad. The solvent was evaporated under reduced pressure to obtain the desired product **10**.

2-(4-Aminophenyl)-1H-benzo[d]imidazole (10)

Yield: 90%; Mp.: 242-244 °C (Lit. Mp. 246-248 °C) (Khan et al., 2009); FT-IR (KBr, cm^{-1}): 3361, 2964, 1607, 1497, 1442, 1398, 1273, 1181, 1044, 831, 744, 697, 615; ^{1}H NMR (DMSO-*d6*, 300 MHz): δ 12.40 (s, 1H, NH) , 7.84 (d, *J* = 9.0 Hz, 2H, ArH), 7.50 (d, *J* = 9.0 Hz, 2H, ArH), 7.11-7.08 (m, 2H, ArH), 6.67 (d, *J* = 9.0 Hz, 2H, ArH), 5.57 (s, 2H, NH_2).

2.7 Synthesis of thiazole-pyrazole amide conjugate (11): Method-I

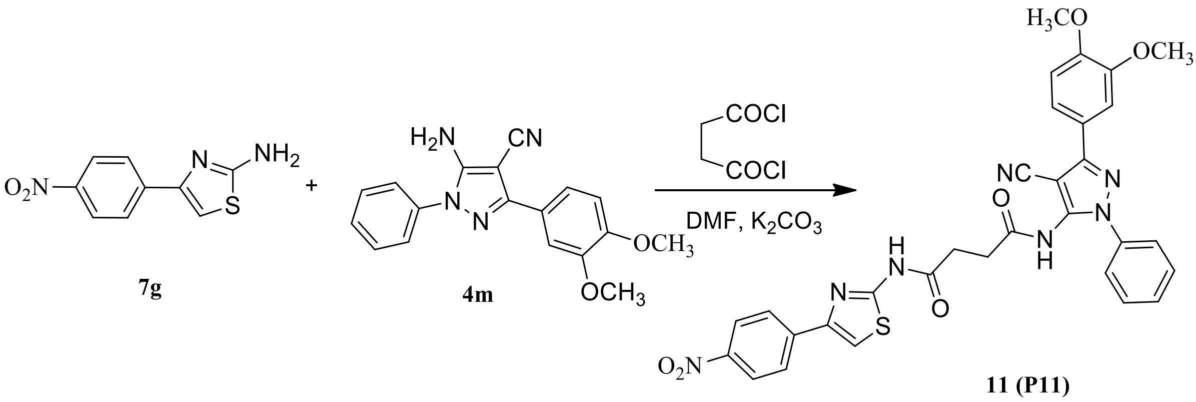

Scheme 2.5. Synthesis of thiazole-pyrazole amide conjugates (**11**)

Succinyl dichloride (148 mmol) was diluted with DMF (25 mL). This solution was added dropwise to a solution of 4-(4-nitrophenyl)-1,3-thiazol-2-amine (**7g**, 156 mmol) in DMF (100 mL) at room temperature during 25 min. After the addition was completed, the pyrazole **4m** was added dropwise and after addition temperature of the reaction mixture was increased to 60 °C. The content was stirred at room temperature for 24 h and then cold 2% sodium bicarbonate was added. The product that was separated, filtered, washed thoroughly with water, ethanol (100 mL), acetone (100 mL) and finally with hexane (50 mL). It was dried under vacuum and subjected to column chromatography to get the desired conjugate **11**.

2.8 Synthesis of thiazole-pyrazole amide conjugates: Method - II

2.8.1 *Synthesis using step-wise methods*

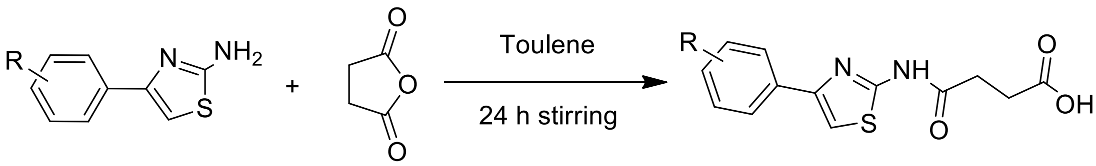

7 12 13

a. R = H (P7)
b. R = 4-OCH_3 (P8)
c. R = 4-NO_2

Scheme 2.6. Synthesis of 4-oxo-4-((4-arylthiazol-2-yl)amino)butanoic acid (**13**)

2-Aminothiazole derivative (**7**, 284 mmol) was dissolved in THF (10 mL). After dissolution, succinic anhydride (**12**, 189 mmol) was added to the reaction mixture. The reaction mixture was kept on stirring for 24 h. Progress of the reaction was monitored by TLC (MeOH-CH_3Cl - 1:9 v/v). After completion, the crude product was obtained by solvent extraction and dried over reduced pressure.

4-Oxo-4-((4-nitrophenyl)thiazol-2-yl)amino)-4-oxobutanoic acid (13c)

2.9 Synthesis of thiazole-pyrazole and thiazole-benzimidazole amide conjugates

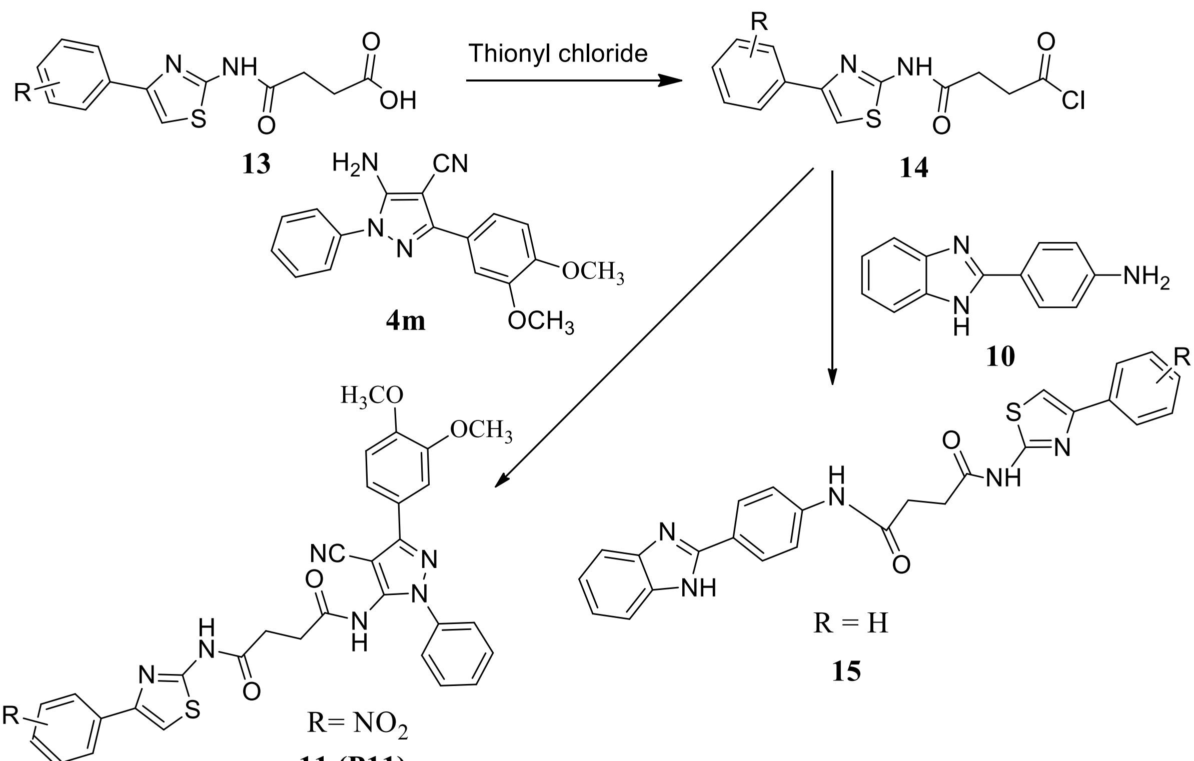

Scheme 2.7. Synthesis of thiazole-pyrazole (**11**) and thiazole-benzimidazole amide (**15**) conjugates

Thionyl chloride (60 mmol) was added to 4-oxo-4-((4-arylthiazol-2-yl)amino)butanoic acid (**13**, 3.0 mmol) and the resulting suspension was refluxed for 3 h to give a clear light yellow solution. Excess thionyl chloride was removed *in vacuo*. The obtained acid chloride without further characterisation was mixed with dry DMF (15 mL) and cooled to 0 – 4 ^{o}C. A solution of amine (**10**, 5.0 mmol) and triethylamine (6.0 mmol) in dry DMF (2.5 mL) was added. The resulting mixture was stirred at room temperature for 12 h. The solvent was removed with rotatory evaporator. The solid obtained was washed with aqueous ammonium chloride solution and water, then dried to get the amide conjugates which was recrystallised to get the pure compounds.

N[1]-(4-(1H-benzo[d]imidazol-2-yl)phenyl)-N[4]-(4-phenylthiazol-2-yl)succinimide (15) (P15)

2.10 Synthesis of thiazole-thiazole and thiazole-pyrazole amine conjugates

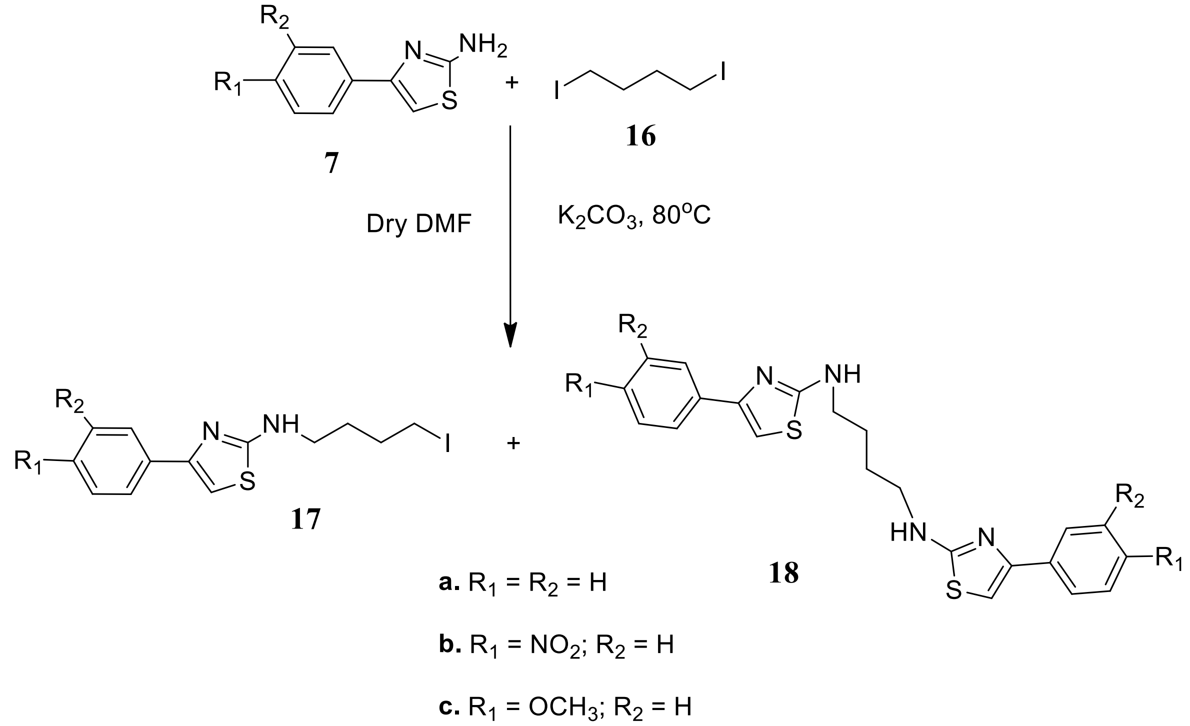

Scheme 2.8. Synthesis of thiazole derivatives (**17** and **18**)

4-Aryl-1,3-thiazol-2-amine (**7**, 100 mmol) was dissolved in dry DMF (5 mL). After dissolution, fused K_2CO_3 (2.8 g) was added to the solution. The reaction was stirred at 80 ^oC for 20 min. After that, 1,4-diiodobutane (**16**, 100 mmol) was added dropwise to the reaction mixture and the temperature was raised to 105 ^oC. The heating was continued for 15 h. Progress of the reaction was monitored by TLC (hexane: ethylacetate 7:3, v/v). After the reaction, the solvent was removed under reduced pressure. The crude product was purified by column chromatography.

N-(4-Iodobutyl)-4-phenylthiazol-2-amine (17a)

Yield: 42%; Mp.: 178-179 ^{o}C; FTIR (KBr, cm^{-1}): 3305, 3250, 3100, 2924, 2862, 1605, 1514, 1485, 1405, 1350, 1226, 1080, 914, 845, 772, 515; ^{1}H NMR (DMSO-d_6, 300 MHz) δ: 7.79-7.74 (m, 2H, ArH), 7.48-7.43 (m, 2H, ArH), 7.25-7.22 (m, 1H, ArH), 7.05 (s, 1H, H-thiazole), 3.35 (m, 2H, CH_2), 3.14 (t, 2H, CH_2), 1.86 (m, 2H, CH_2), 1.50 (m, 2H, CH_2); ESI-Mass (m/z): 358 (M^+).

N-(4-Iodobutyl)-4-(4-nitrophenyl)thiazol-2-amine (17b)

Yield: 40%; Mp.: 195-196 ^{o}C; FTIR (KBr, cm^{-1}): 3298, 3150, 3100, 2914, 1605, 1550, 1514, 1486, 1405, 1350, 1320, 1226, 1086, 917, 848, 772, 521; ^{1}H NMR (DMSO-d_6, 300 MHz) δ: 8.20-8.02 (m, 3H, Ar-H), 7.38-7.24 (m, 2H, H-thiazole, ArH), 3.32 (m, 2H, CH_2), 3.10 (t, 2H, CH_2), 1.84 (m, 2H, CH_2), 1.52 (m, 2H, CH_2); ESI-Mass (m/z): 403 (M^+).

N-(4-Iodobutyl)-4-(4-methoxyphenyl)thiazol-2-amine (17c)

Yield: 41%; Mp.: 189-190 ^{o}C; FTIR (KBr, cm^{-1}): 3296, 3120, 2945, 1601, 1523, 1481, 1337, 1218, 1076, 914, 773, 530; ^{1}H NMR (DMSO-d_6, 300 MHz) δ: 7.84 (d, 2H, J = 9.0 Hz, ArH), 7.30 (s, 1H, H-thiazole), 6.96 (d, 2H, J = 9.0 Hz, ArH), 3.78 (s, 3H, OCH_3), 3.28 (m, 2H, CH_2), 3.10 (t, 2H, CH_2), 1.80 (m, 2H, CH_2), 1.50 (m, 2H, CH_2); ESI-Mass (m/z): 388 (M^+).

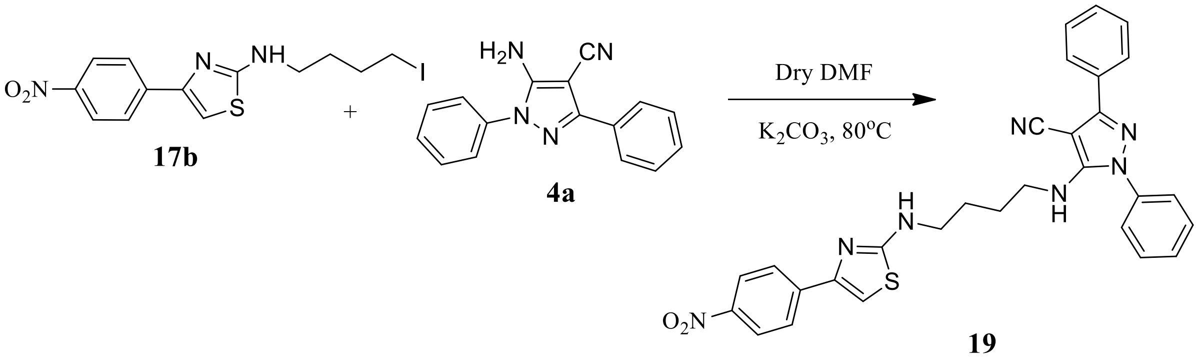

Scheme 2.9. Synthesis of thiazole-pyrazole amine conjugate (**19**)

5-Amino-1,3-diphenyl-1H-pyrazole-4-carbonitrile (**4a**, 100 mmol) was dissolved in dry DMF (10 mL). After dissolution, fused K_2CO_3 (2.8 g) was added to the solution. The reaction was stirred at 80 ^oC for 30 min. After that, N-(4-Iodobutyl)-4-(4-nitrophenyl)thiazol-2-amine (**17b**, 100 mmol) was added to the reaction mixture and the temperature was raised to 105 ^oC. The heating was continued for 20 h. Progress of the reaction was monitored by TLC (benzene:ethyl acetate 9:1, v/v). After the reaction, the solvent was removed under reduced pressure. The crude product was washed with cold water and dried. This was further recrystallized with hot ethanol to get the pure compound **19**.

2.11 Biological screening methods

2.11.1 *In-vitro* studies

The potential effect of the synthesized compounds on *h*MAO-B enzyme were evaluated according to the previously reported fluorometric assay (Can et al., 2017). For the experiment, commercially available Amplex™ Red Monoamine Oxidase Assay kit (Invitrogen™ by Thermo Fisher Scientific) and *h*MAO-B enzyme (recombinant, expressed in baculovirus infected BTI insect cells from Sigma Life Science) were used. The fluorescence measurements were taken by a Bio Tek-Synergy H1 microplate reader (Can et al., 2017).

a) Inhibitor solutions: Different concentrations (10^{-3}-10^{-9} M) of the synthesized compounds and reference compounds (Pargyline hydrochloride and Safinamide mesylate) were prepared in 2% DMSO (vehicle).
b) Enzyme solution: Recombinant *h*MAO-B enzyme (0.64 U/mL) was dissolved in 1X Reaction Buffer (prepared by dissolving 5 mL of 0.25 M sodium phosphate buffer stock solution available in assay kit to 20 mL deionized water).
c) Working solution: Working solution was prepared by adding 200 µL of Amplex Red reagent stock solution (~20 mM), 100 µL of Horseradish peroxidase stock solution (200 U/mL) and 200 µL of substrate stock solution (benzylamine, 100 mM) to 9.5 mL 1X Reaction Buffer.

In flat black bottom 96-well micro test plate, we added inhibitor solution (20 µL/well) and *h*MAO-B enzyme (100 µL/well), which was incubated at 37°C for 15 minutes. After this incubation period, the reaction was started by adding the working solution (100 µL/well). The mixture was incubated for 30 minutes at 37°C and fluorescence (Excitation: 535 nm, Emission: 587 nm) was measured at 5 minutes intervals to follow the kinetics of the reaction (Can et al., 2017). The control experiments were carried out by replacing the inhibitor solution with vehicle. A positive control was prepared by diluting 20 mM H_2O_2 working solution to 10 µM in 1X Reaction Buffer. 1X Reaction Buffer without H_2O_2 was negative control. Further, to check the possibility of non-enzymatic inhibition by the inhibitor solution, the inhibitor solution and working solution was mixed (Can et al., 2017). The background activity was determined from the vials containing all the components except the *h*MAO-B enzyme which was replaced by 1X Reaction Buffer (Can et al., 2017). The blank, control and the different concentrations of inhibitor solutions were analyzed in triplicates and percent inhibition was calculated using following equation:

$$\%\ \text{Inhibition} = \frac{(\text{Fluoroscence of control}) - (\text{Fluoroscence of inhibitor})}{(\text{Fluoroscence of control})} \times 100$$

The IC_{50} values were determined from a dose-response curve obtained by plotting the percentage inhibition versus log concentration and were expressed as mean ± SEM (standard error of means) (Can et al., 2017).

2.11.2 Antioxidant Test

2,2-Diphenyl-1-picrylhydrazyl (DPPH) Scavenging Activity

Each compound (1 mL) was mixed with freshly prepared DPPH solution (3 mL) and allowed to react for 30 minutes at room temperature in the dark. After that, the mixture was tested for DPPH radical scavenging activity on a double beam UV-visible spectrophotometer at a wavelength of 517 nm. The solution of DPPH in methanol (1.2 mg in 50 mL) was used as blank and studied at the same wavelength. The samples were run in triplicate, and the mean value of three of them was recorded, and results are calculated. Percentage of antioxidant activity was calculated using the formula:

$$AA\ (\%) = [(A_b - A_s) / A_b] \times 100$$

where AA = Antioxidant activity; A_b = Absorbance of blank; A_s = Absorbance of sample

The AA (%) of the samples was compared with gallic acid (0.3 mg in 20 mL methanol).

*****

CHAPTER 3

RESULTS AND DISCUSSION

3.1 *In-silico* interaction studies

3.1.1 Preparation of the protein

The protein preparation wizard in Schrödinger Maestro 16.4 version (Maestro 10.2 user mannual) was used for the preparation of protein of MAO-B (PDB ID: 4A7A). The proteins are the clusters of amino acids that are bonded together by peptide bonds (Bhagavan and Ha, 2015). The carbonyl oxygen and amine hydrogen of peptide bond are *trans* in the position. The C-N bond in the peptide bond possess partial double bond character. Therefore, it is rigid, planar and not free to rotate but the N-C_α and C_α-C bonds (Figure 3.1) are not rigid and hence possess the ability to rotate freely (Bhagavan and Ha, 2015; Choudhari, 2014). The angle of rotation or dihedral angle around N-C_α bond is called phi (φ) and that around C_α-C bond is called psi (ψ). The bulkiness of R groups attached to the N-C_α and C_α-C bonds may impose some restrictions on the rotation leading to certain combinations of φ and ψ which is preferred for stability of protein. The φ/ψ plot of amino acid residues in a peptide is called the Ramachandran plot (Bhagavan and Ha, 2015; Choudhari, 2014).

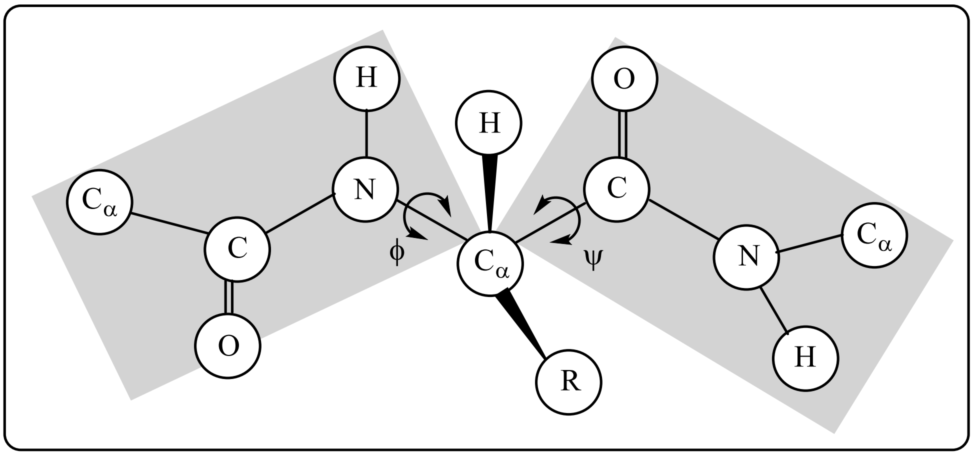

Figure 3.1. Peptide bond showing peptide plane, φ and ψ and bond rotation involving two amino acids (Choudhari, 2014)

3.1.2 Active site prediction

The first step is the preparation of protein. After the preparation of protein, the active sites for MAO-B protein were identified using sitemap tool. The site score above 1, was selected for grid generation in Glide application of Maestro and then receptor grid was generated around the most active site with a grid box by receptor grid generation tool in Glide. Once receptor grid was generated, docking studies were carried out.

3.1.3 Molecular docking

In the *in-silico* study, benzimidazole, pyrazole, thiazole, and their amide and amine linked conjugates were docked using Glide tool of Schrödinger Maestro 16.4 version (Tables 3.1-3.4). The docking score of compounds **4a**, **4b**, **4f**, **4h**, **4m**, **7a**, **11** and **20** – **154** varied from -13.427 to -3.626 (Table 3.1). The compound **11** have the highest docking score value of -13.427 and the MMGBSA dG bind score is -72.967856 showing the good binding affinities of compound **11** with the amino acid residues of MAO-B enzyme. Therefore, this compound was selected for the synthesis. In another series of the compounds **155** – **176** (Table 3.2), the compound **155** showed highest docking score of -14.435 with the MMGBSA dG bind score of -67.215204. This also showed good binding affinities with the amino acid residues of MAO-B enzyme. In the series of pyrazole-thiazole amine conjugates, the compounds **19**, **177** – **280** (Table 3.3) have been docked. The compound **177** has highest docking score of – 11.318 with the MMGBSA dG bind score of – 53.163778 also showed good binding affinities with the amino acid residues of MAO-B enzyme. In the series of pyrazole/thiazole-benzimidazole amine conjugates, the compounds **281** – **302** (Table 3.4) have been docked. The compound **282** has highest docking score of – 13.600 with the MMGBSA dG bind score of – 57.154 also showed good binding affinities with the amino acid residues of MAO-B enzyme.

All the compounds were analysed and then among them some of the compounds were selected for the synthesis (Table 3.5). Not all the compounds having highest docking score have been selected for synthesis. The selected compounds exhibited docking score between -10.678 to -7.836 which was comparable with the standard drug safinamide (-10.600). The compounds also showed good measurable binding affinities to the target residues. The binding affinities indicate the flexibility and contribution of ligand for the target enzyme (Subramaniyana et al., 2018). The chemical structures of all the compounds docked have been given in Figures 3.2 – 3.6.

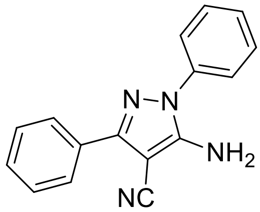

4a (P1)

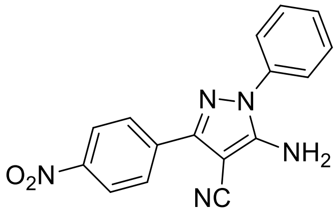

4b (P2)

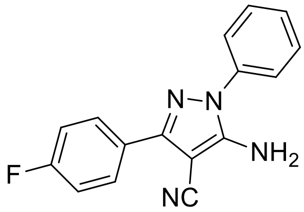

4f (P3)

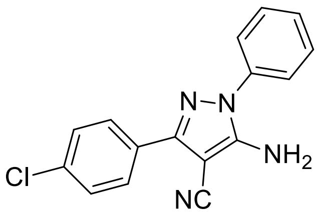

4h (P4)

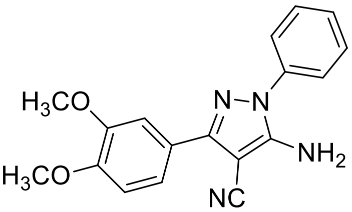

4m (P5)

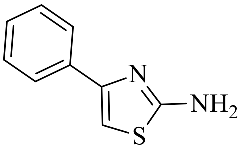

7a (P6)

Figure 3.2. Chemical structures of docked pyrazole and thiazole derivatives

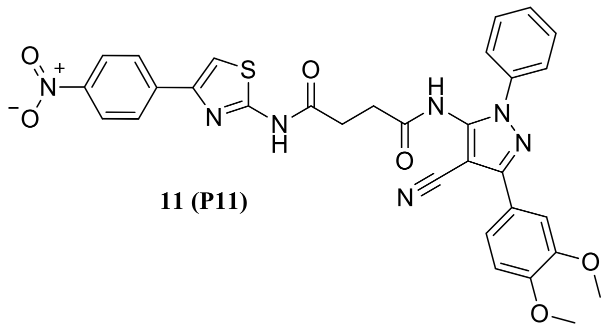

11 (P11)

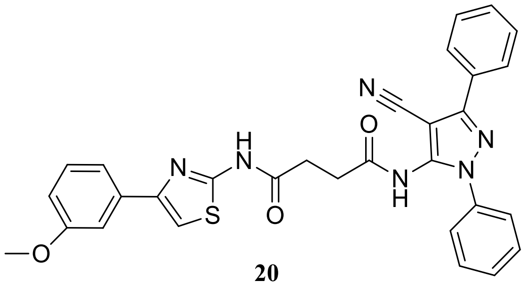

20

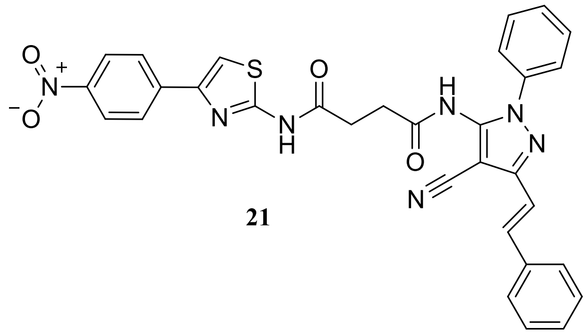

21

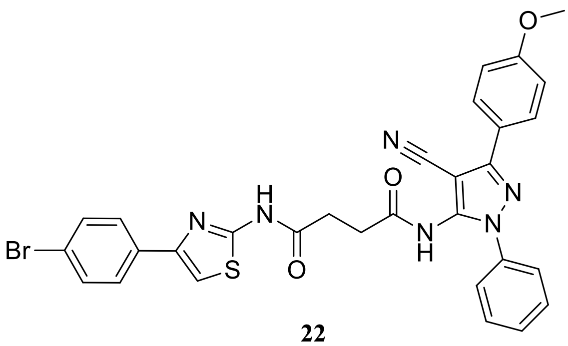

22

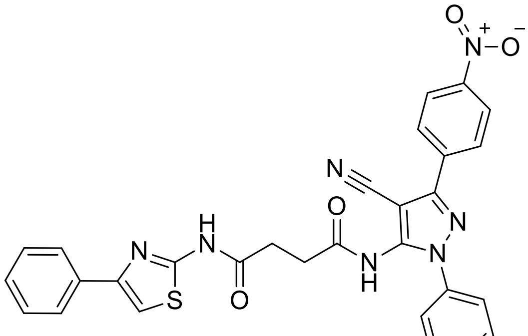

23

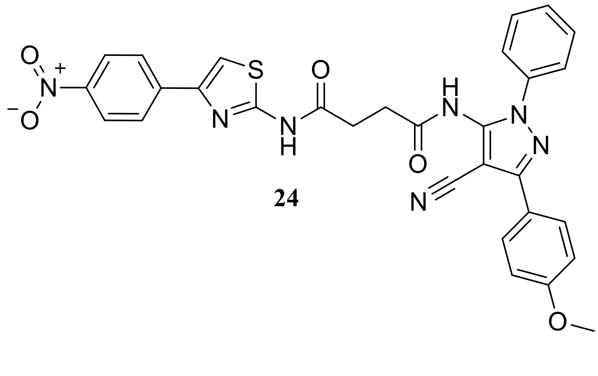

24

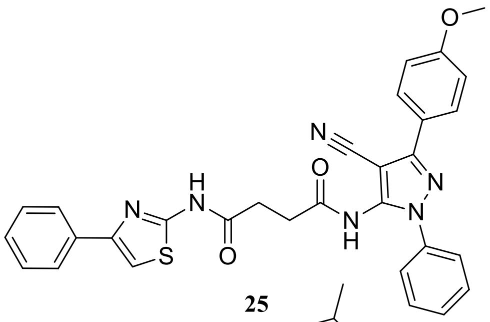

25

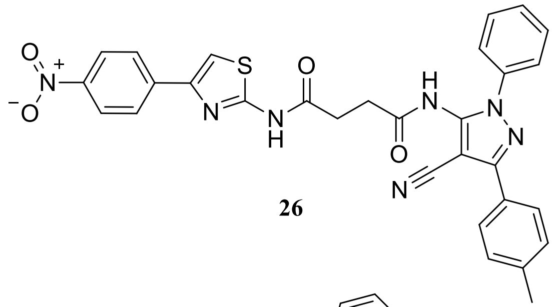

26

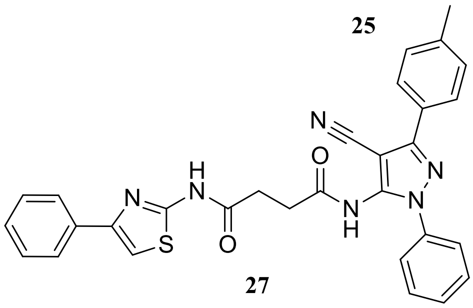

27

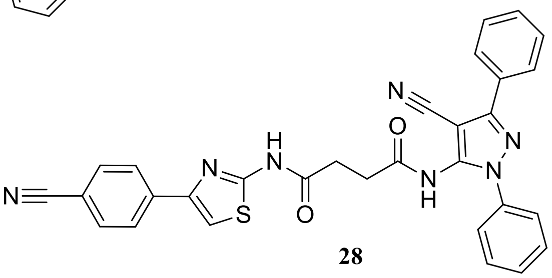

28

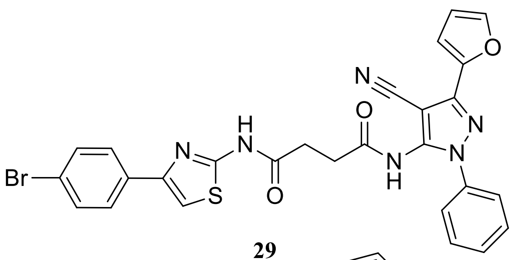

29

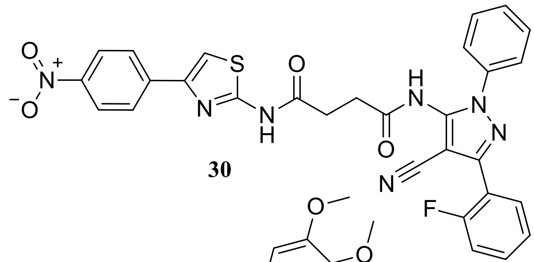

30

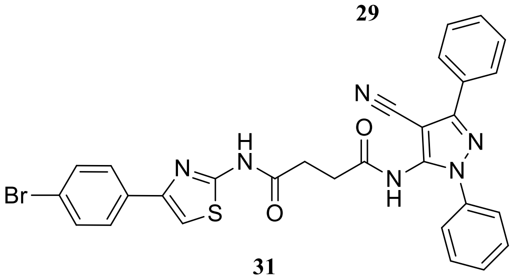

31

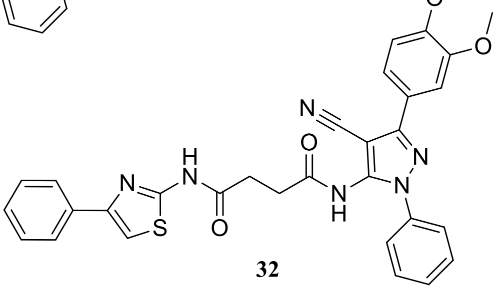

32

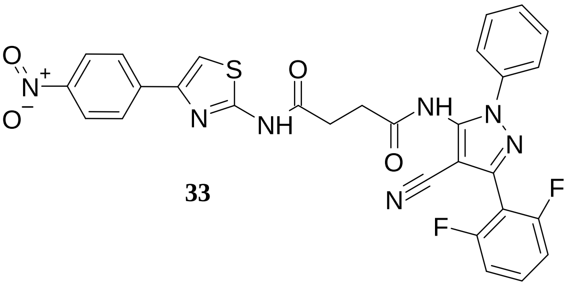

33

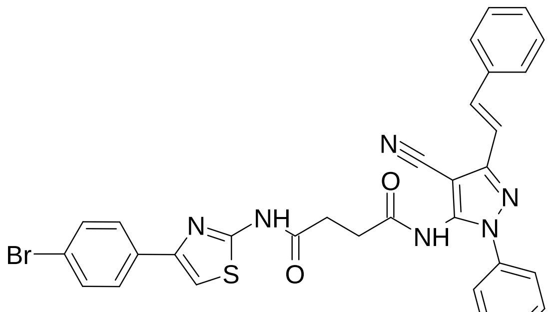

34

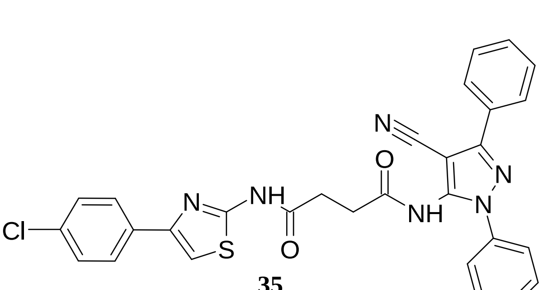

35

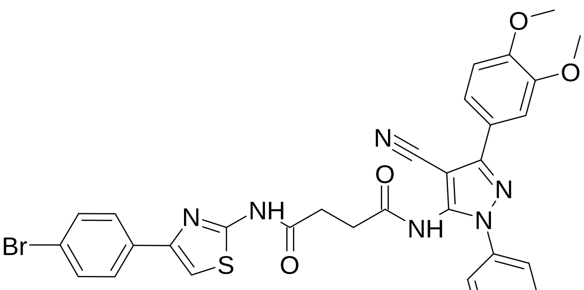

36

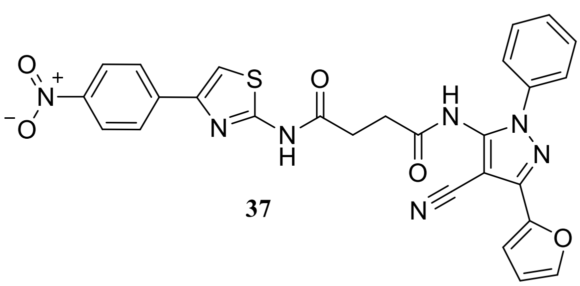

37

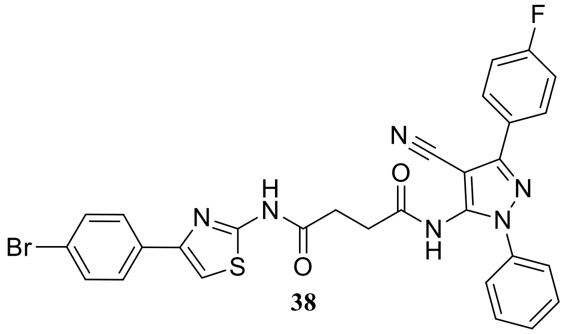

38

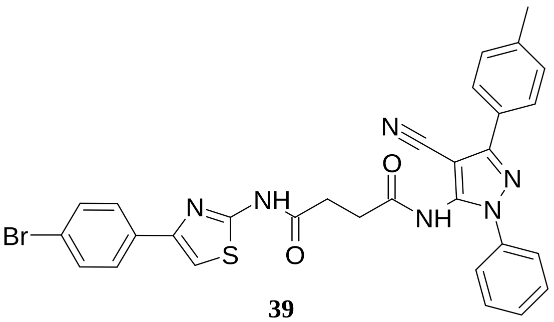

39

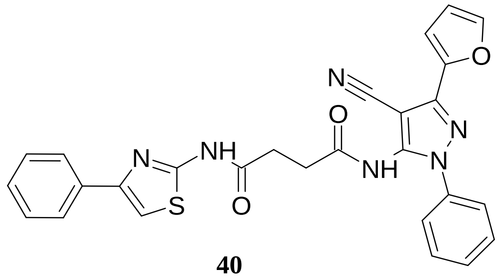

40

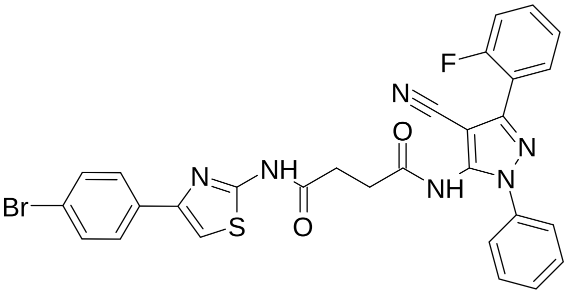

41

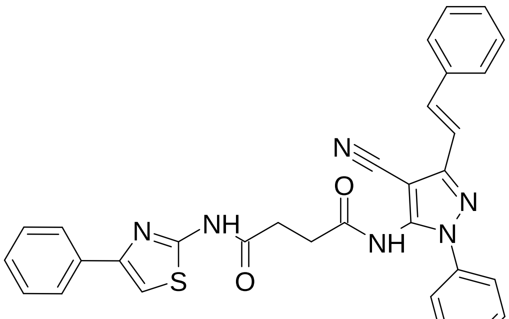

42

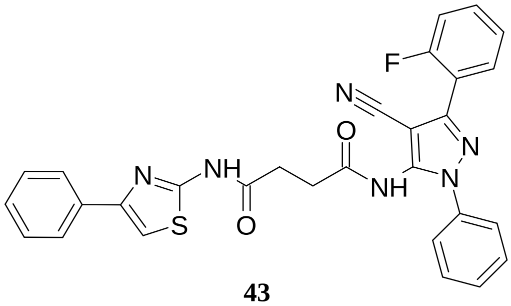

43

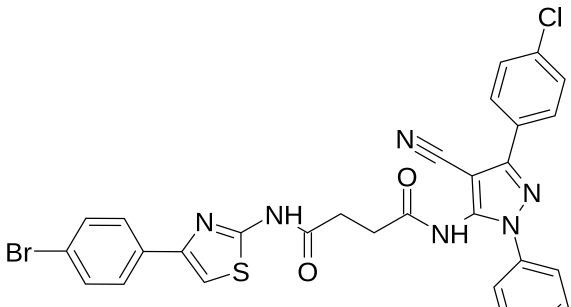

44

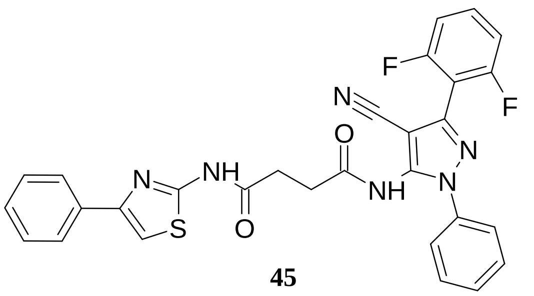

45

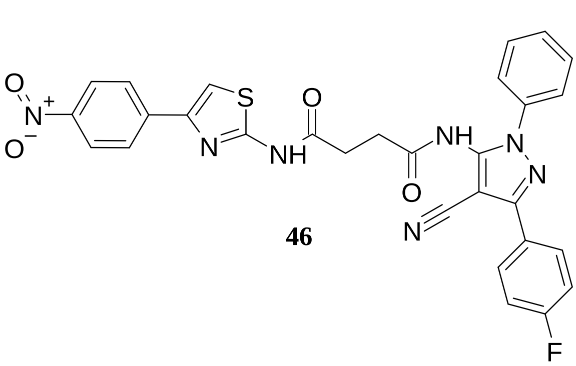

46

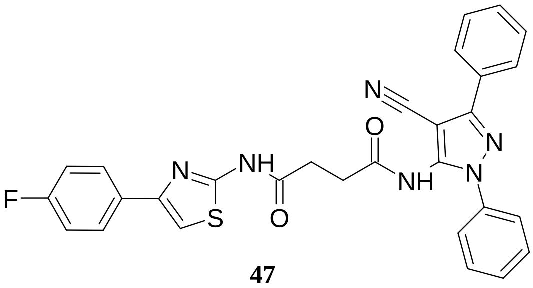

47

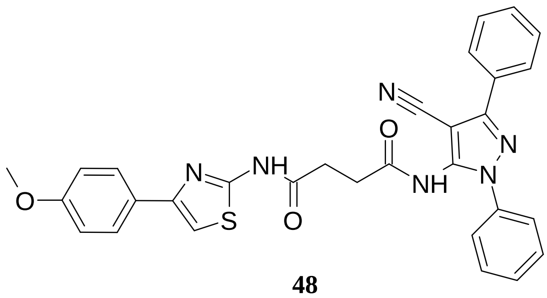

48

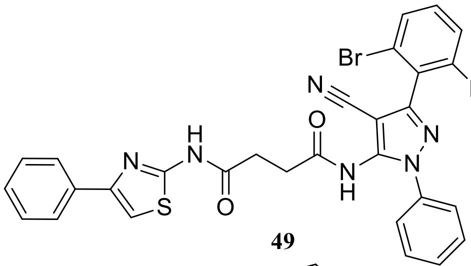

49

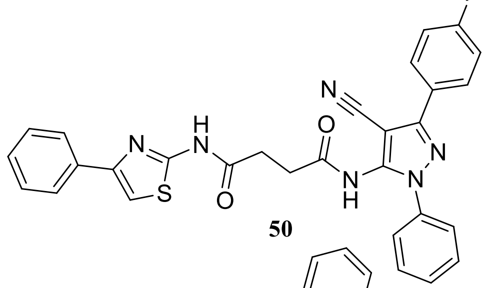

50

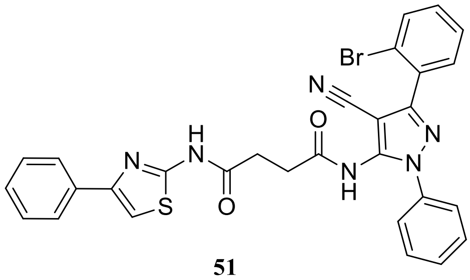

51

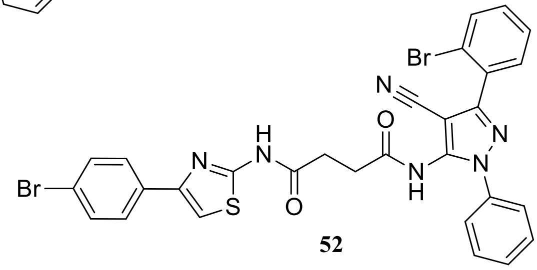

52

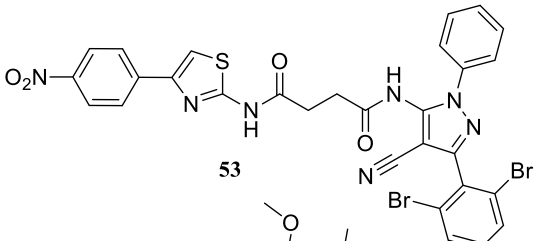

53

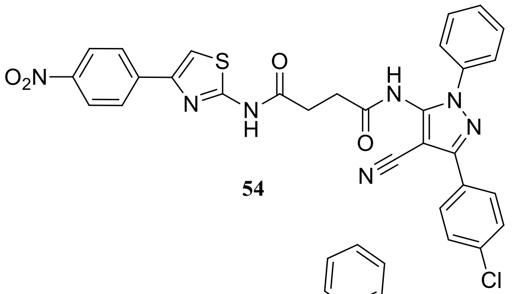

54

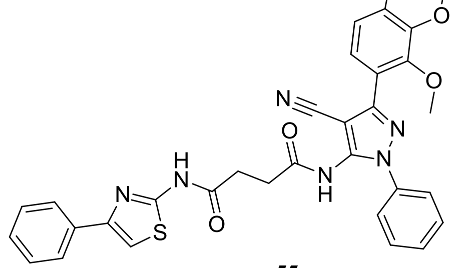

55

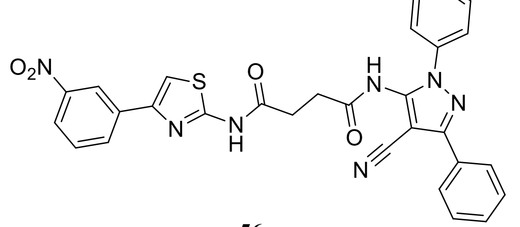

56

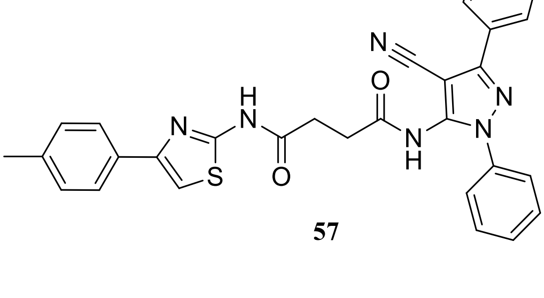

57

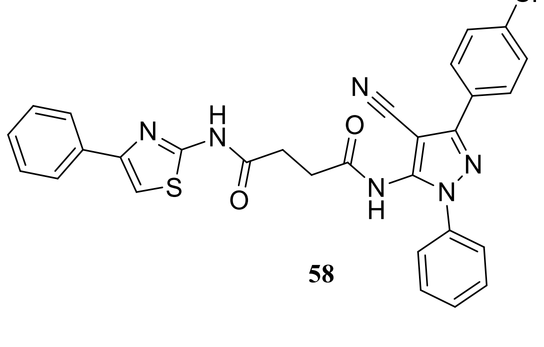

58

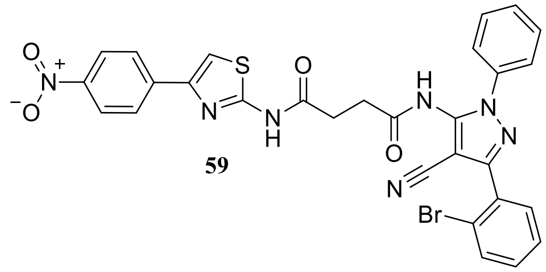

59

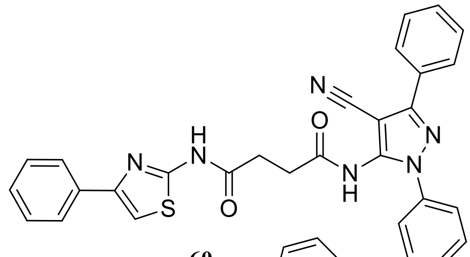

60

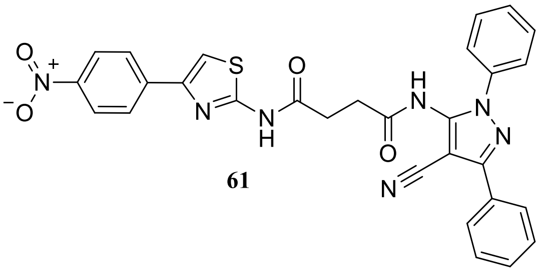

61

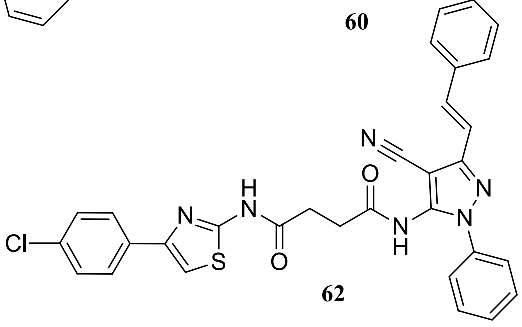

62

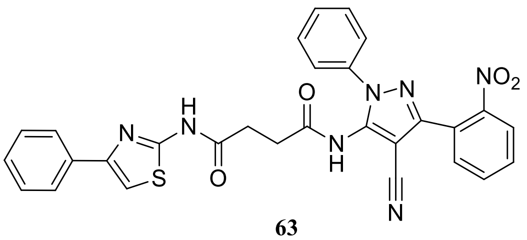

63

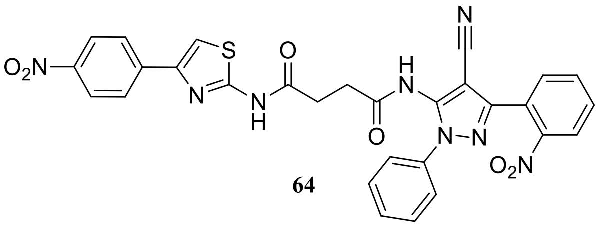

64

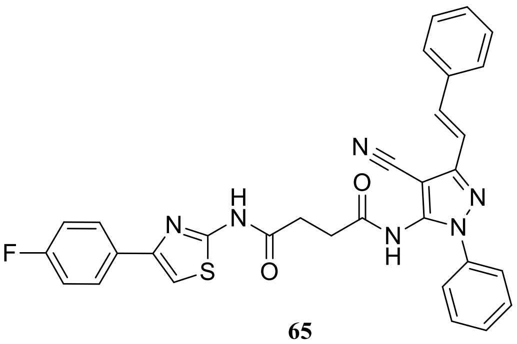

65

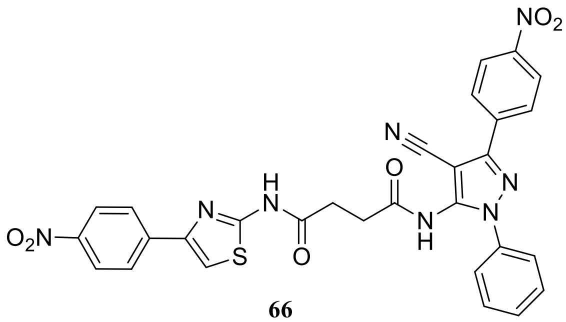

66

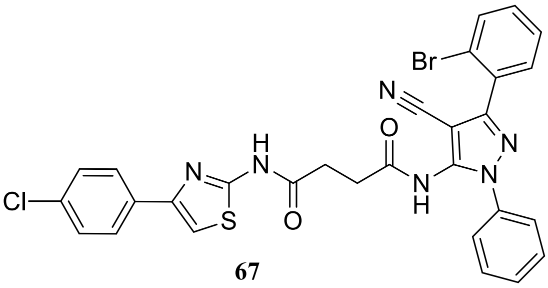

67

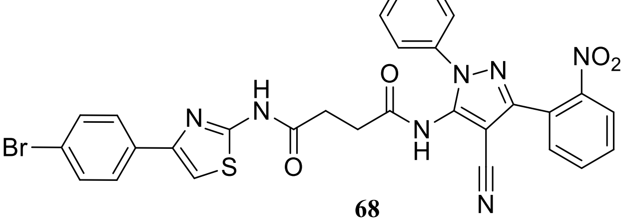

68

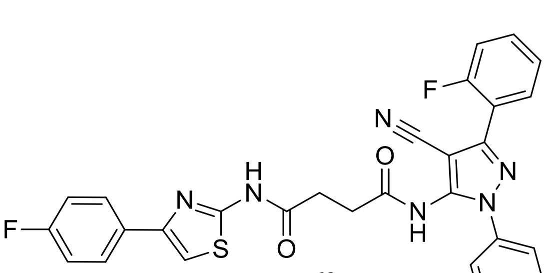

69

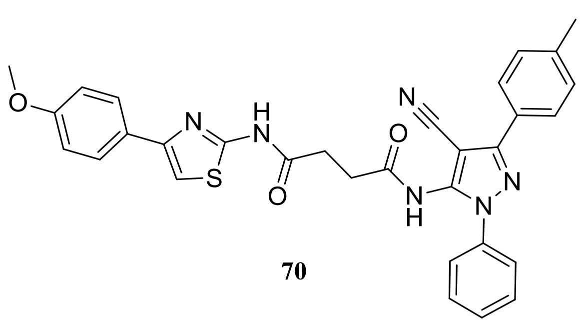

70

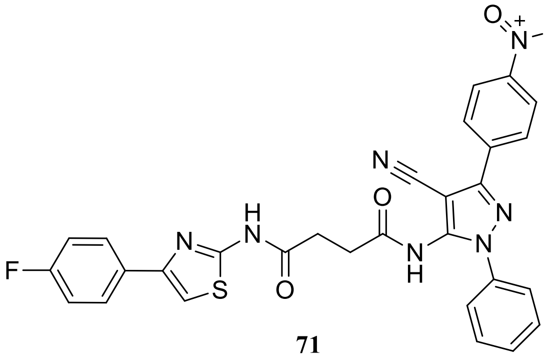

71

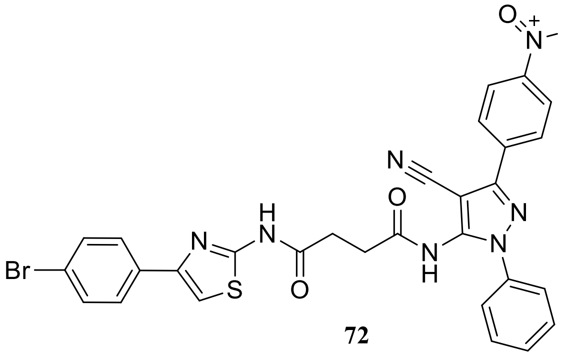

72

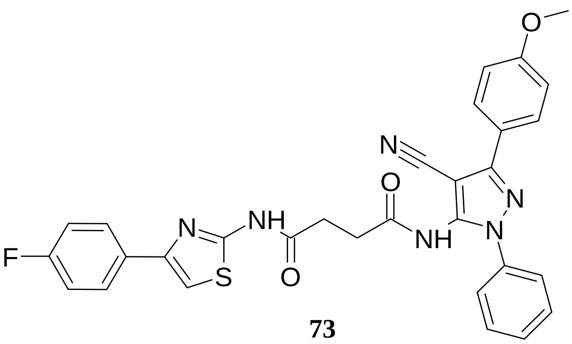

73

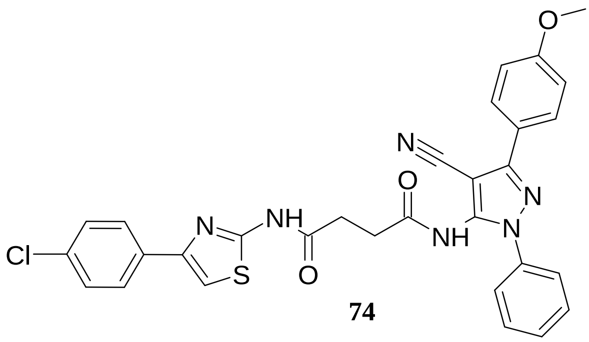

74

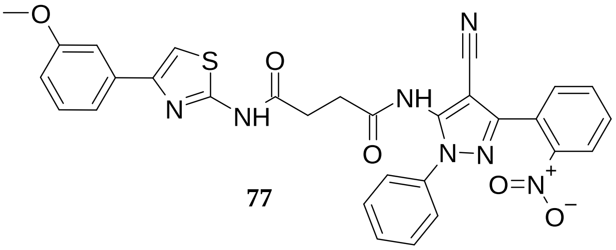

77

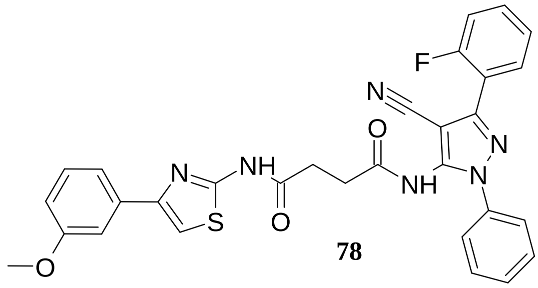

78

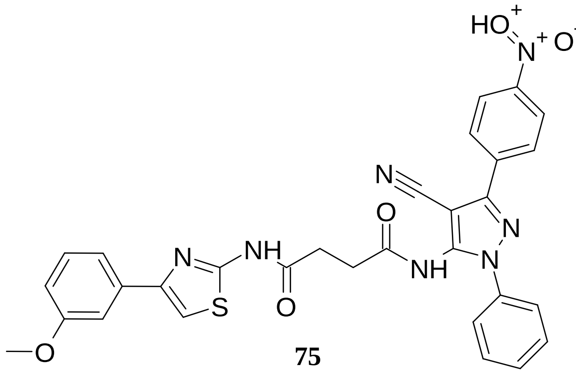

75

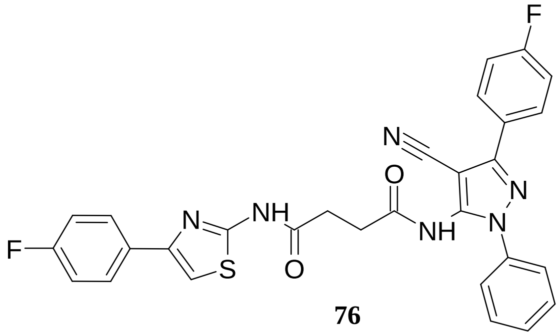

76

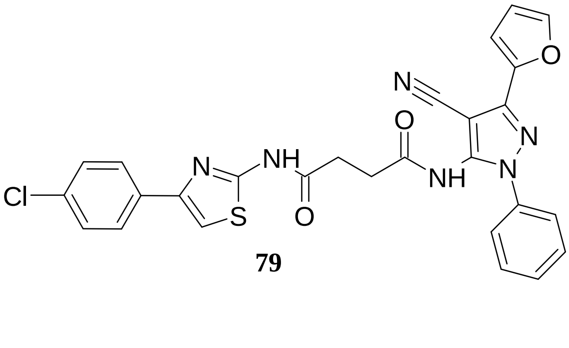

79

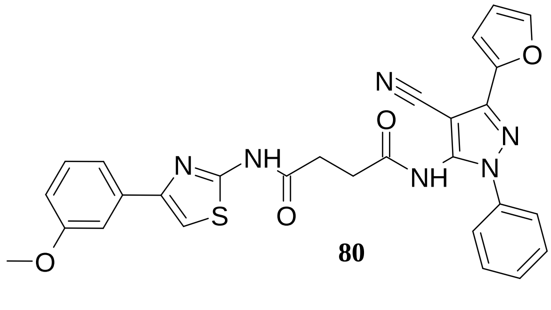

80

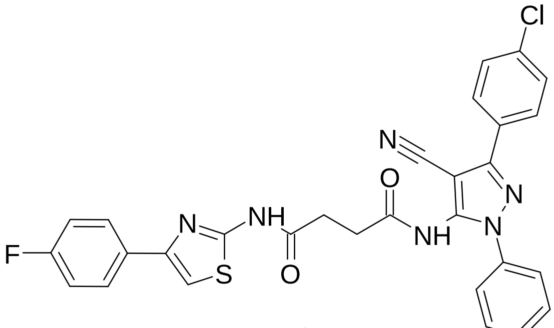

81

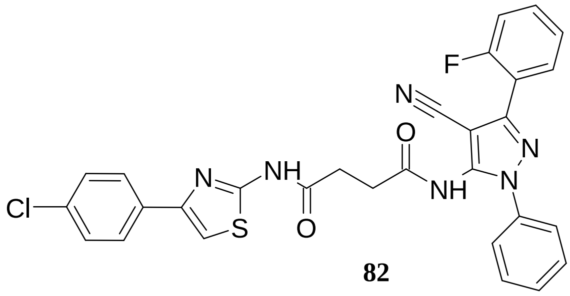

82

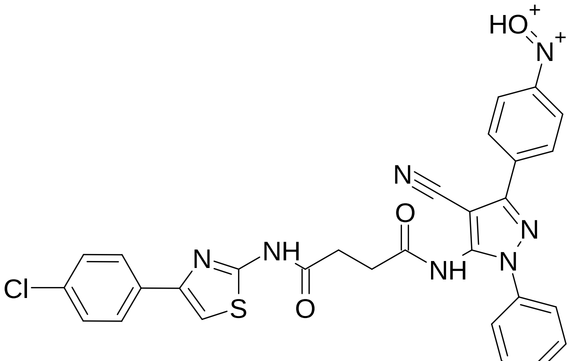

83

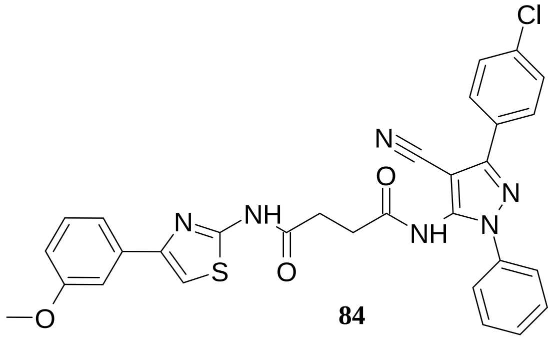

84

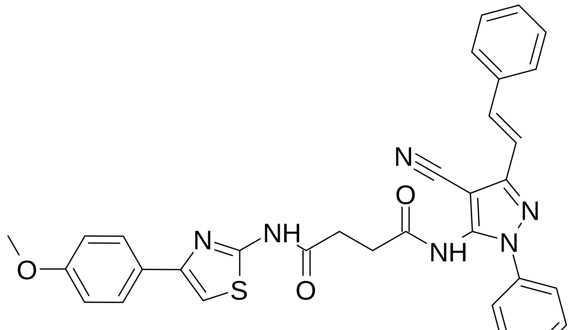

85

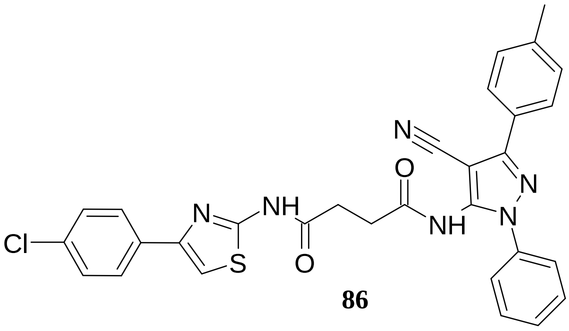

86

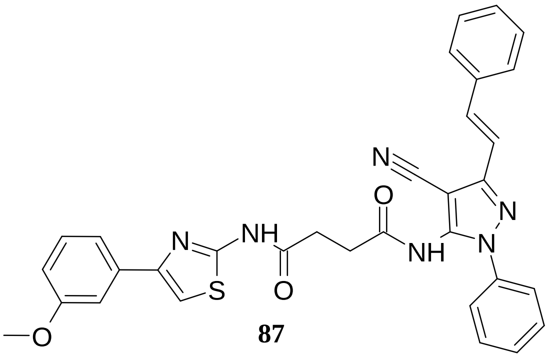

87

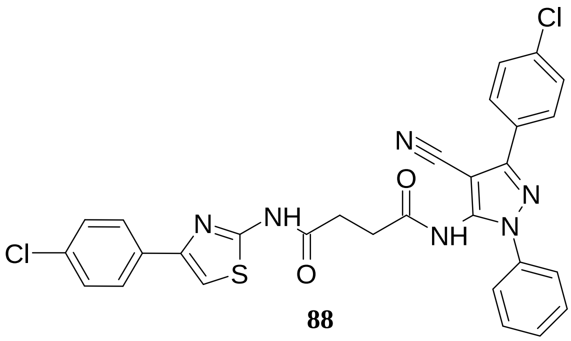

88

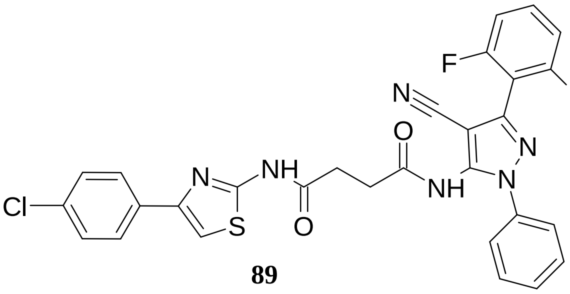

89

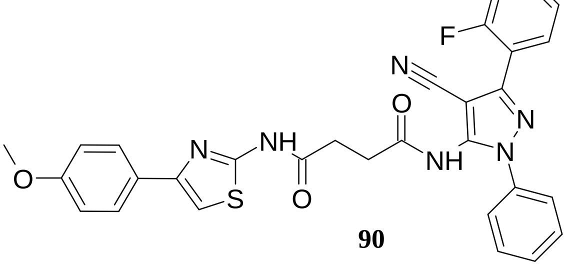

90

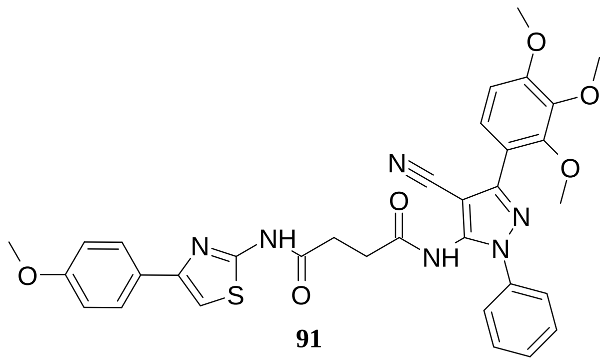

91

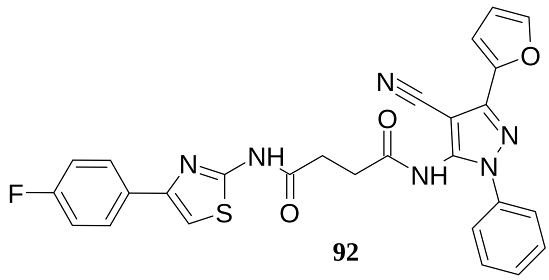

92

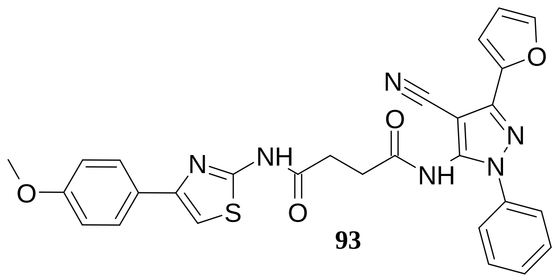

93

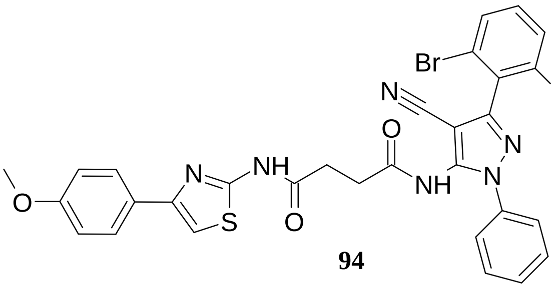

94

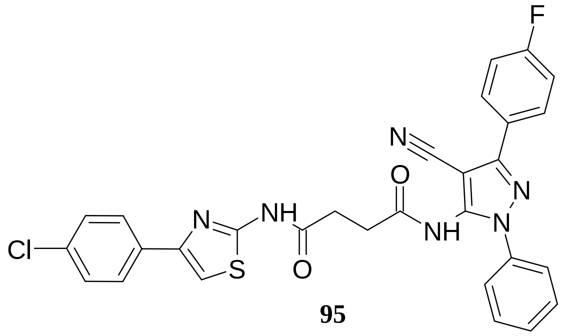

95

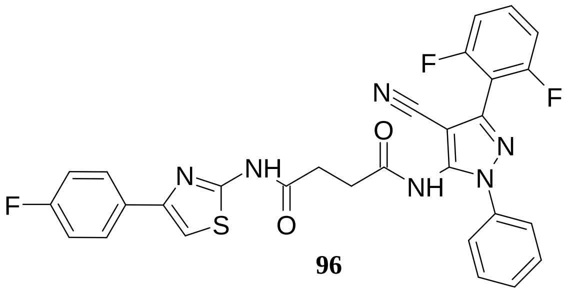

96

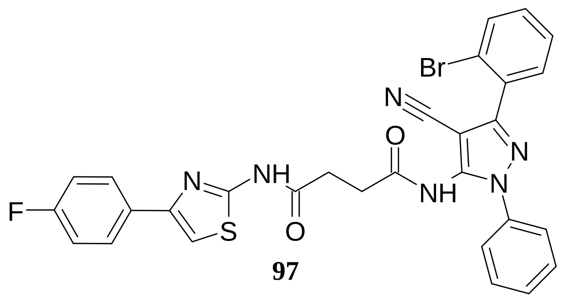

97

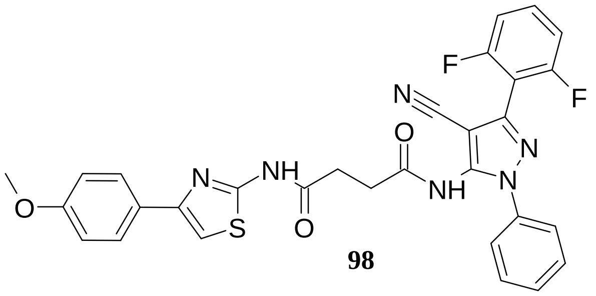

98

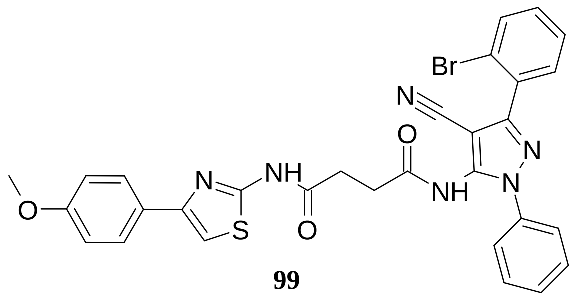

99

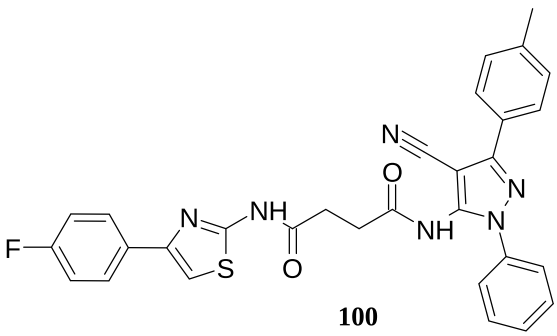

100

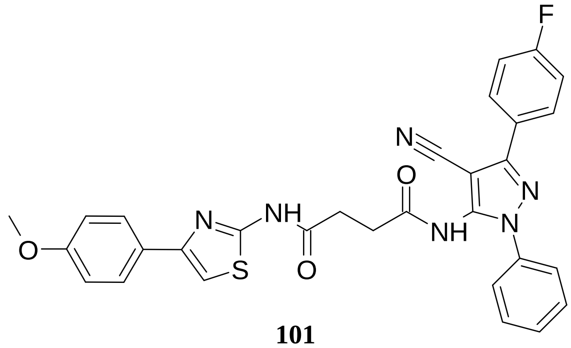

101

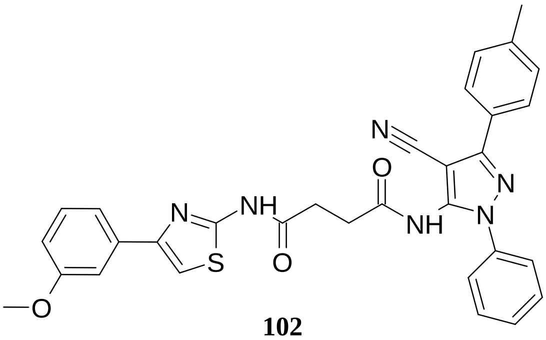

102

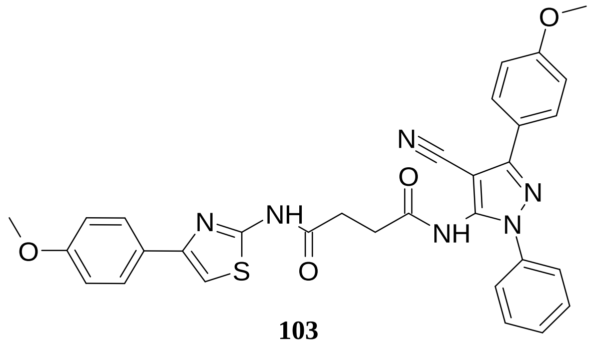

103

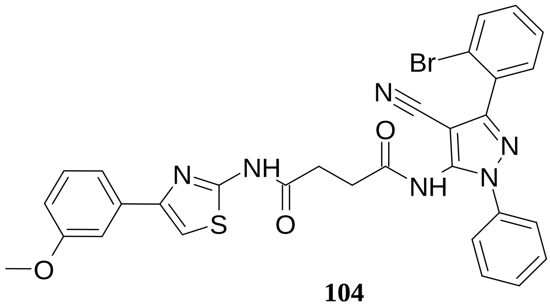

104

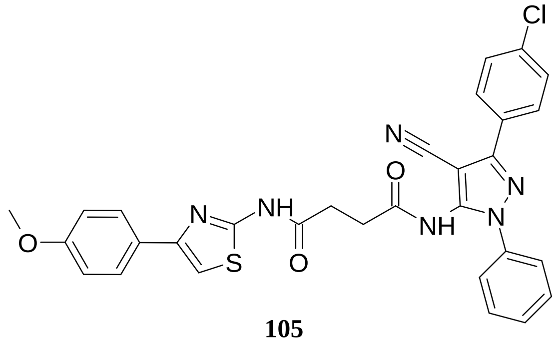

105

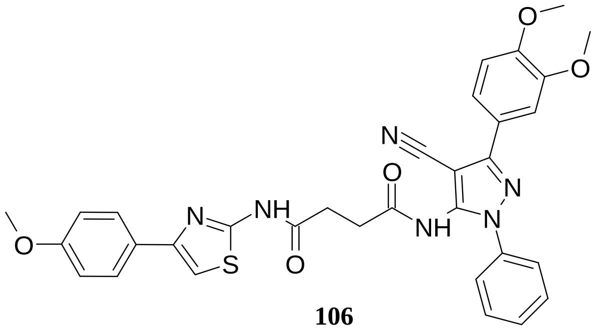

106

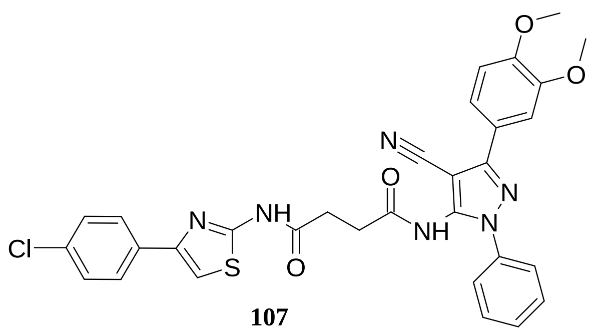

107

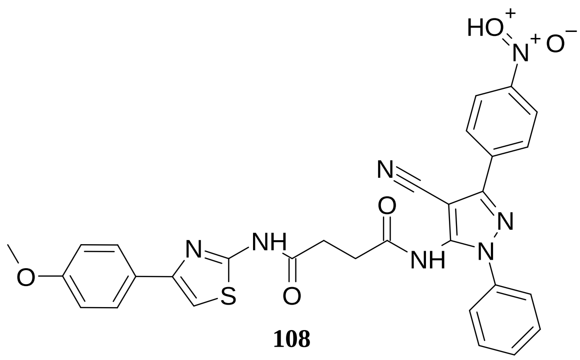

108

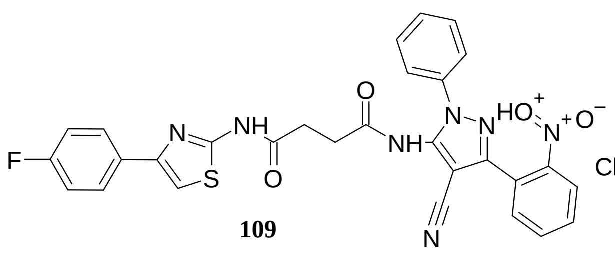

109

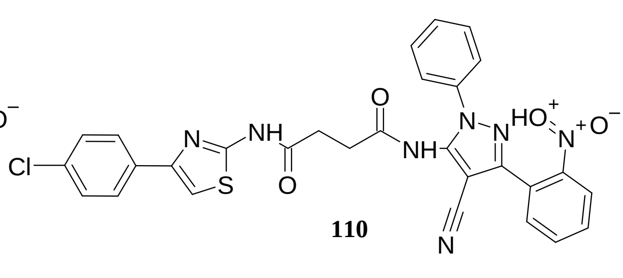

110

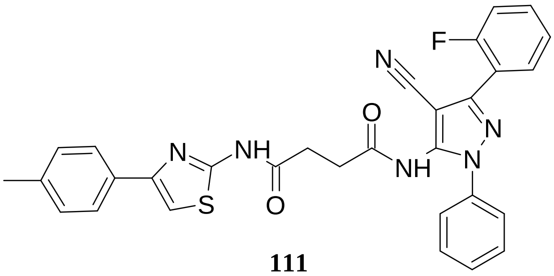

111

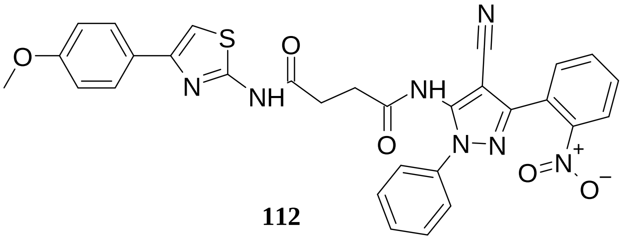

112

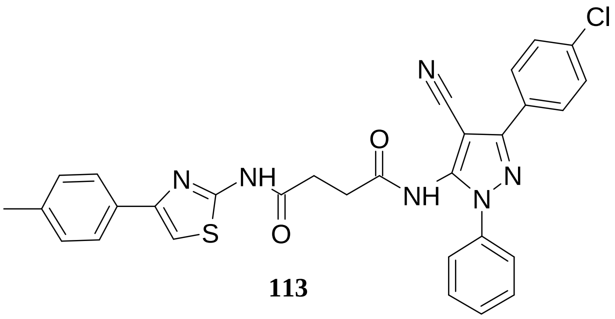

113

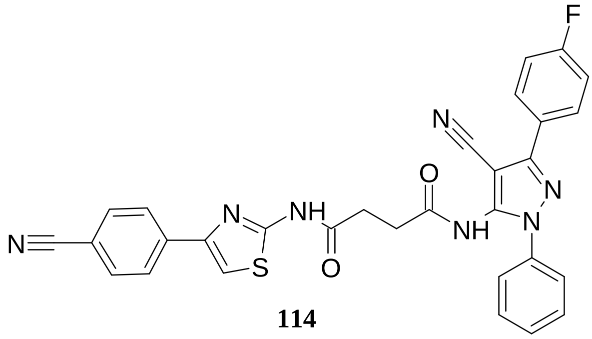

114

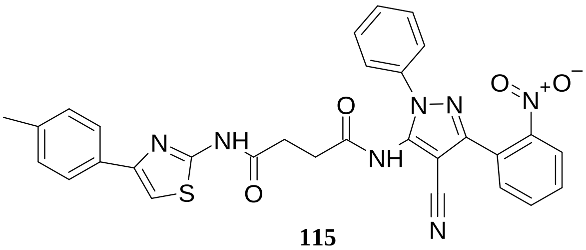

115

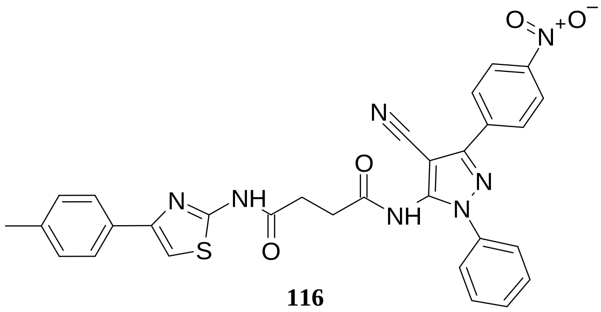

116

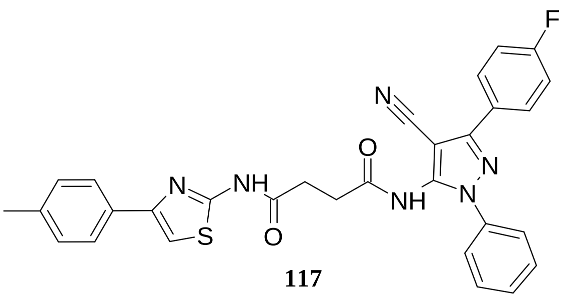

117

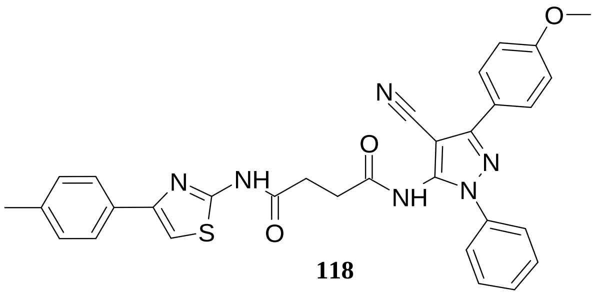

118

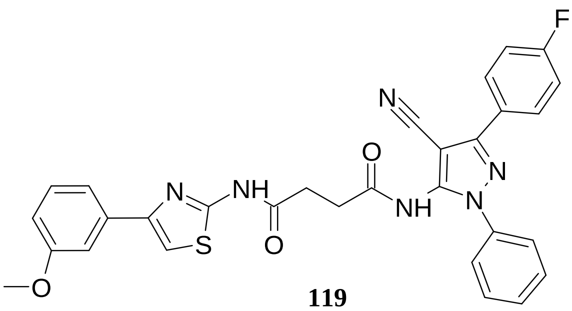

119

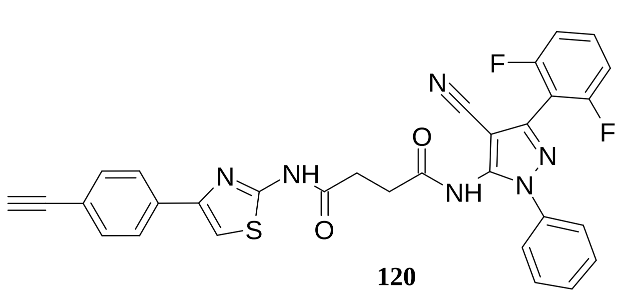

120

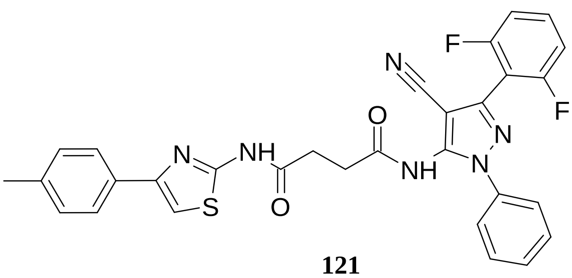

121

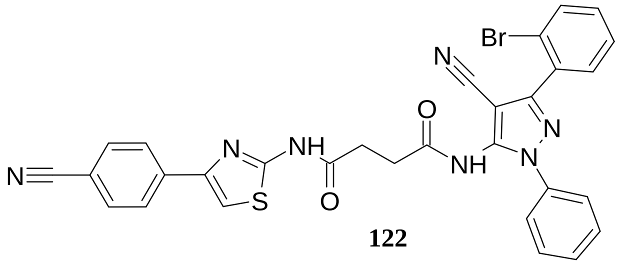

122

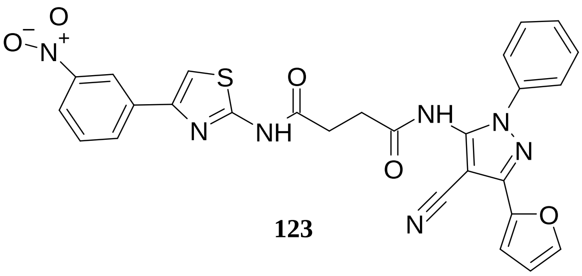

123

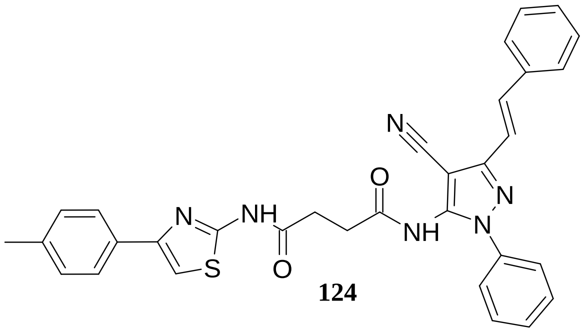

124

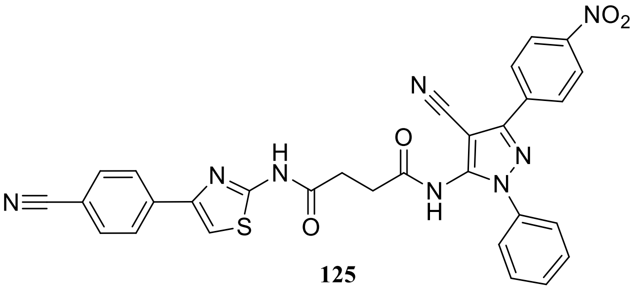

125

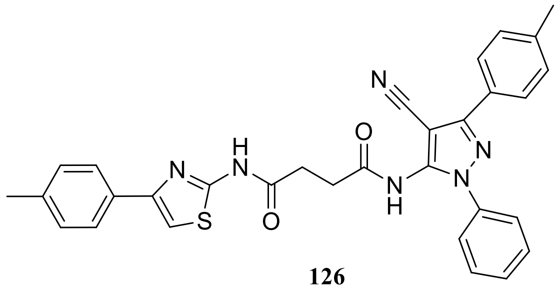

126

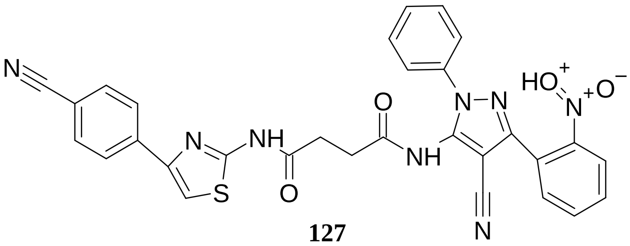

127

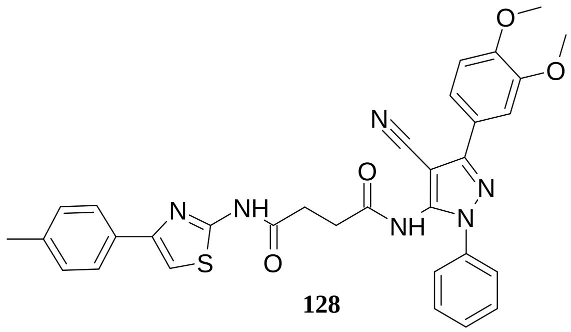

128

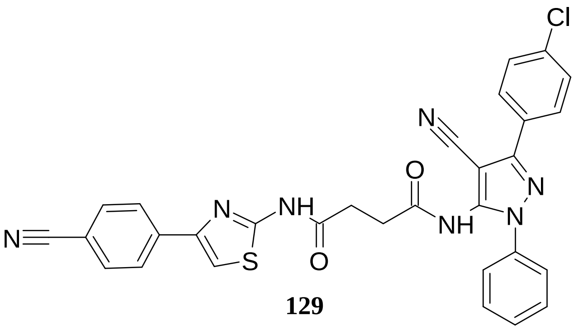

129

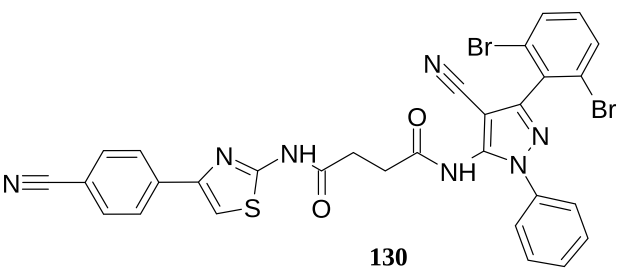

130

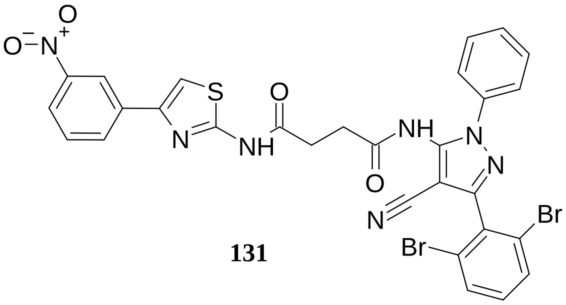

131

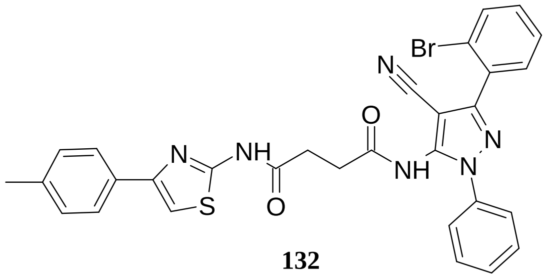

132

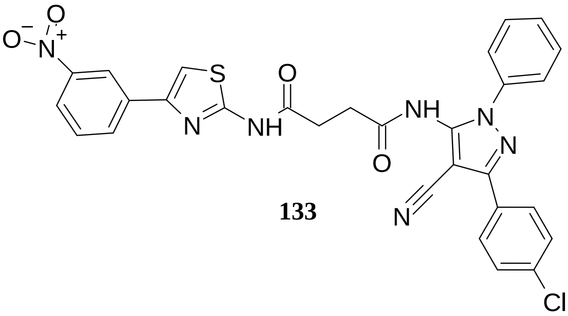

133

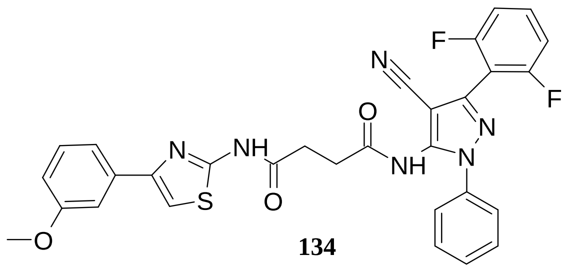

134

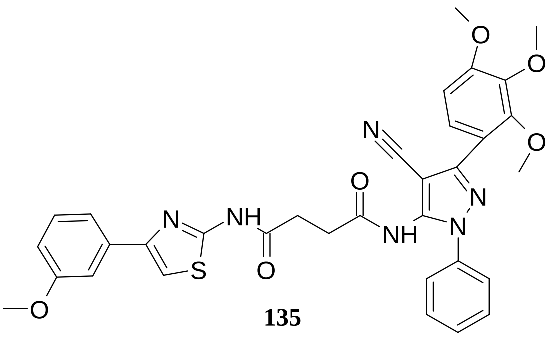

135

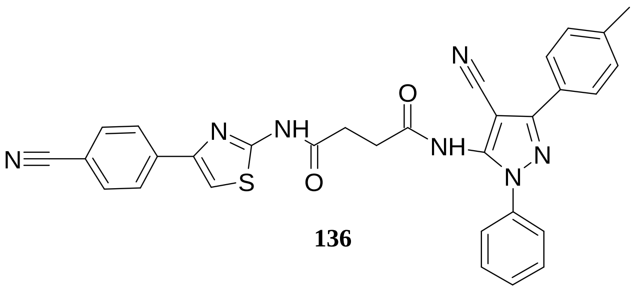

136

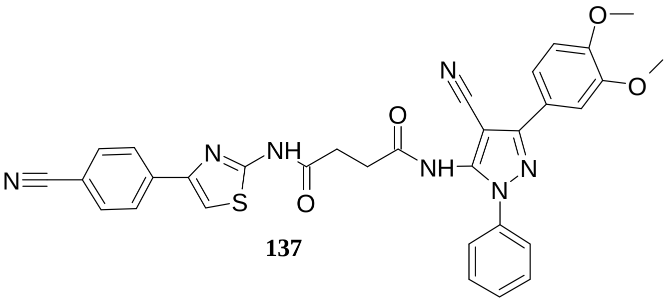

137

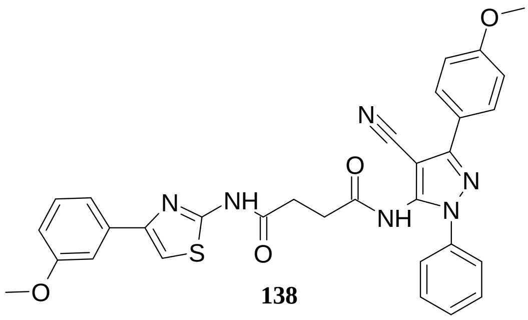

138

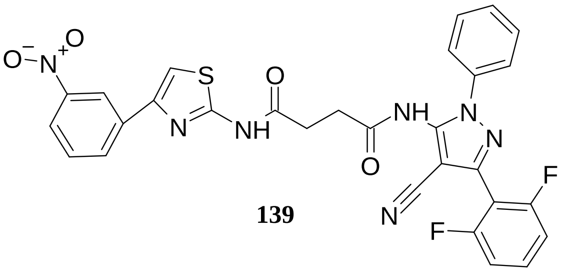

139

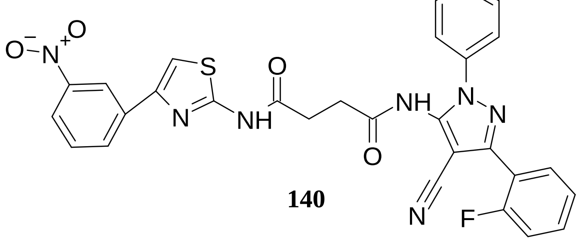

140

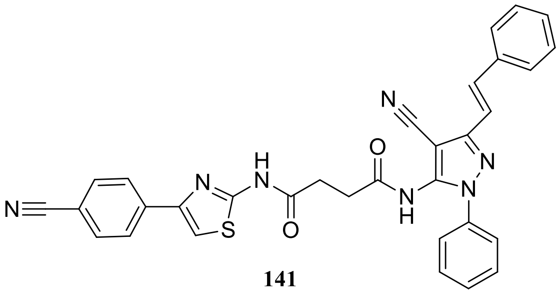

141

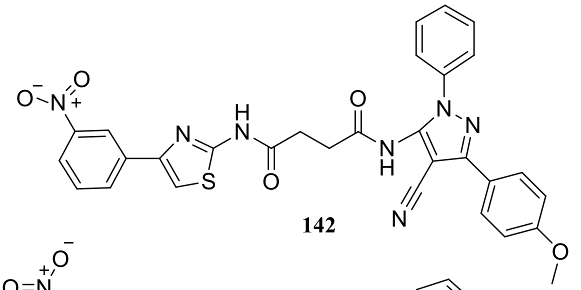

142

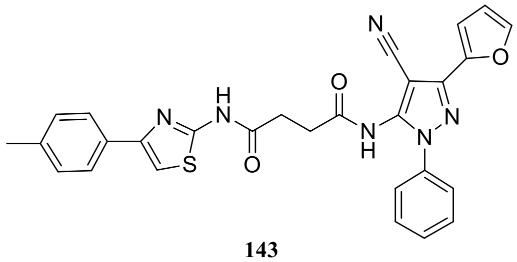

143

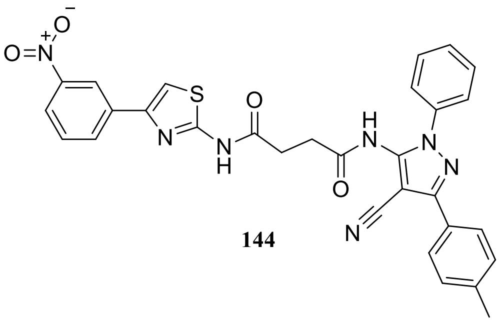

144

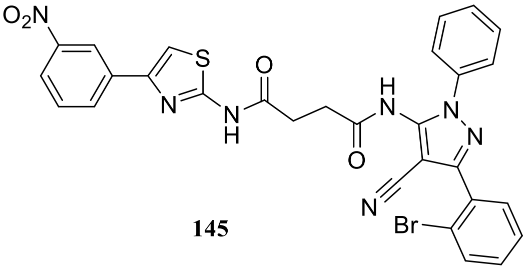

145

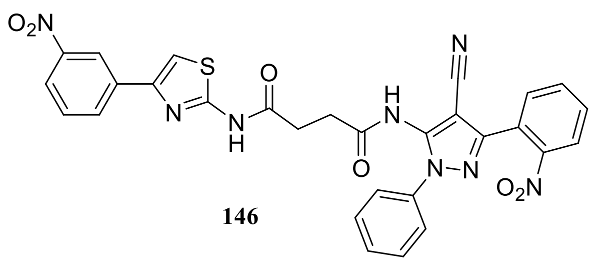

146

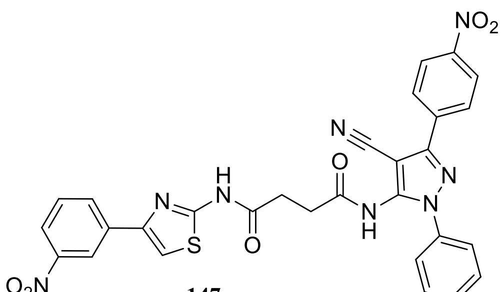

147

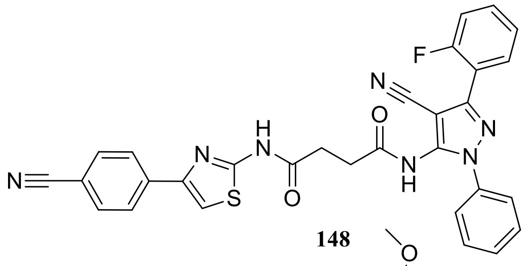

148

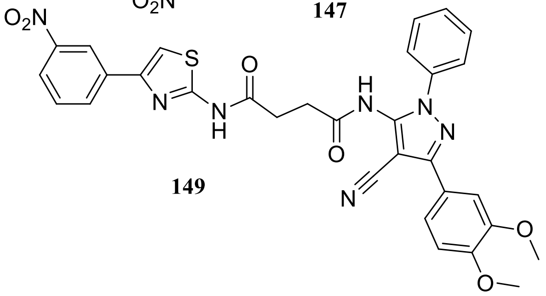

149

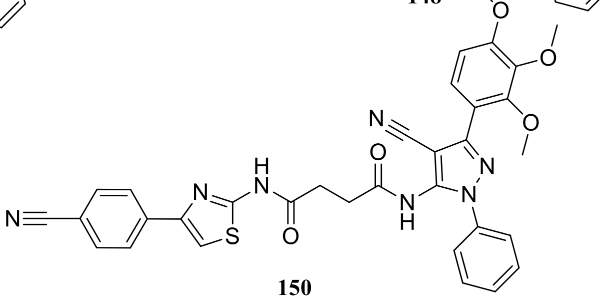

150

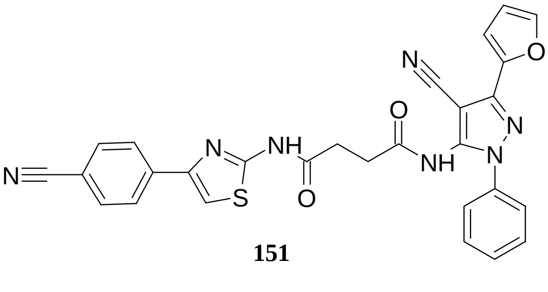

151

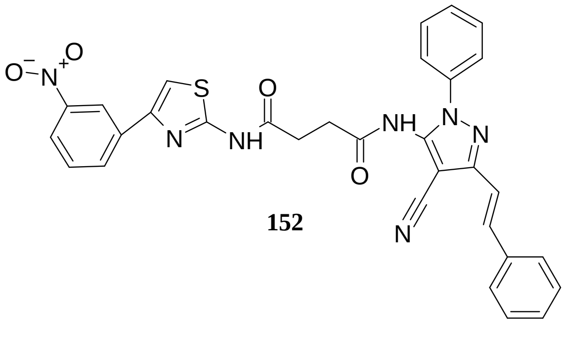

152

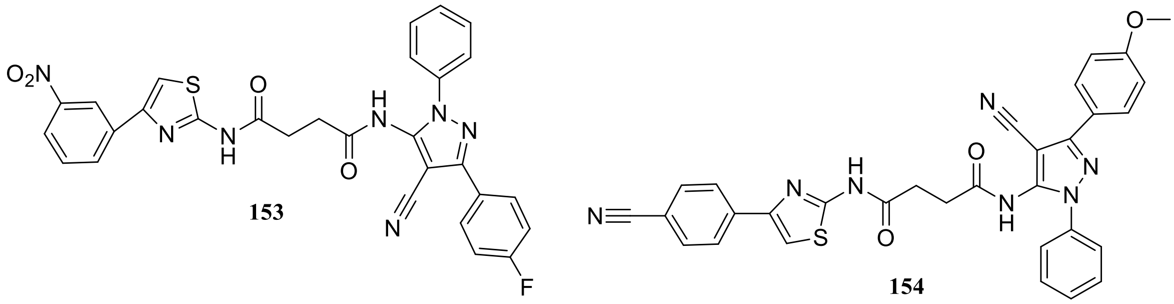

Figure 3.3. Chemical structures of docked thiazole-pyrazole amide conjugates

Table 3.1. Docking Score and MMGBSA dG binding energy of pyrazole - thiazole conjugates

S. No.	Comp. No.			S. No.	Comp. No.		
1	**4a (P1)**			73	**85**		
2	**4b (P2)**			74	**86**		
3	**4f (P3)**			75	**87**		
4	**4h (P4)**			76	**88**		
5	**4m (P5)**			77	**89**		
6	**7a (P6)**			78	**90**		
7	**11 (P11)**			79	**91**		
8	**20**			80	**92**		
9	**21**			81	**93**		
10	**22**			82	**94**		
11	**23**			83	**95**		
12	**24**			84	**96**		
13	**25**			85	**97**		
14	**26**			86	**98**		
15	**27**			87	**99**		
16	**28**			88	**100**		
17	**29**			89	**101**		
18	**30**			90	**102**		
19	**31**			91	**103**		
20	**32**			92	**104**		
21	**33**			93	**105**		
22	**34**			94	**106**		
23	**35**			95	**107**		
24	**36**			96	**108**		
25	**37**			97	**109**		
26	**38**			98	**100**		
27	**39**			99	**111**		
28	**40**			100	**112**		
29	**41**			101	**113**		
30	**42**			102	**114**		
31	**43**			103	**115**		

32	**44**			104	**116**		
33	**45**			105	**117**		
34	**46**			106	**118**		
35	**47**			107	**119**		
36	**48**			108	**120**		
37	**49**			109	**121**		
38	**50**			110	**122**		
39	**51**			111	**123**		
40	**52**			112	**124**		
41	**53**			113	**125**		
42	**54**			114	**126**		
43	**55**			115	**127**		
44	**56**			116	**128**		
45	**57**			117	**129**		
46	**58**			118	**130**		
47	**59**			119	**131**		
48	**60**			120	**132**		
49	**61**			121	**133**		
50	**62**			122	**134**		
51	**63**			123	**135**		
52	**64**			124	**136**		
53	**65**			125	**137**		
54	**66**			126	**138**		
55	**67**			127	**139**		
56	**68**			128	**140**		
57	**69**			129	**141**		
58	**70**			130	**142**		
59	**71**			131	**143**		
60	**72**			132	**144**		
61	**73**			133	**145**		
62	**74**			134	**146**		
63	**75**			135	**147**		
64	**76**			136	**148**		
65	**77**			137	**149**		
66	**78**			138	**150**		
67	**79**			139	**151**		
68	**80**			140	**152**		
69	**81**			141	**153**		
70	**82**			142	**154**		
71	**83**						
72	**84**						

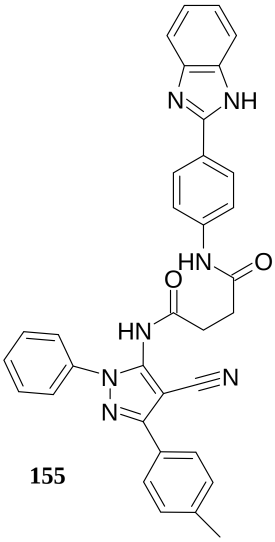

155

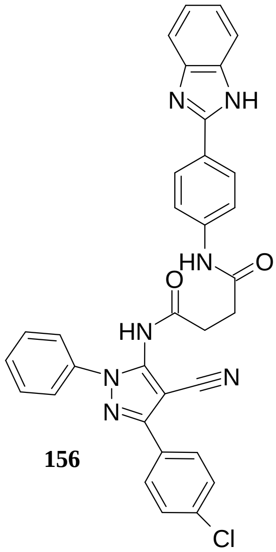

156

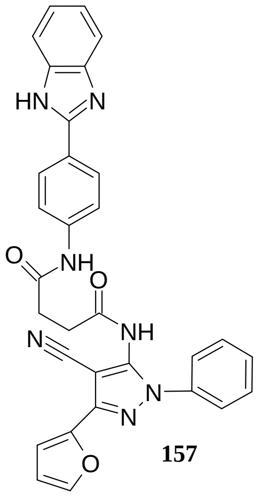

157

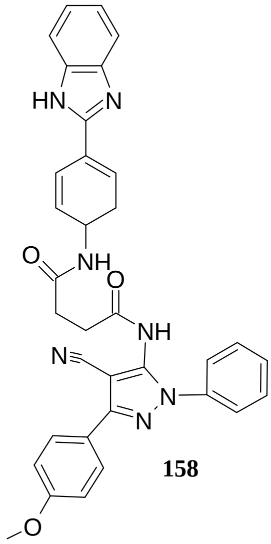

158

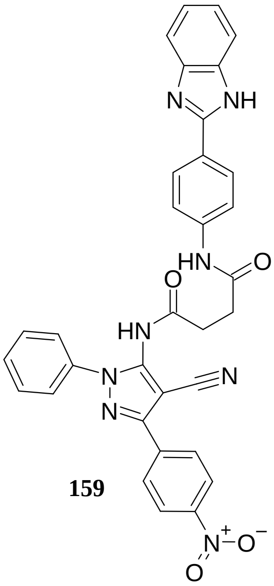

159

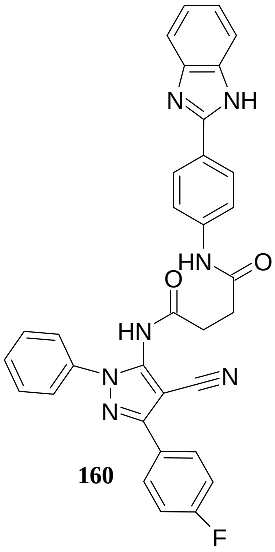

160

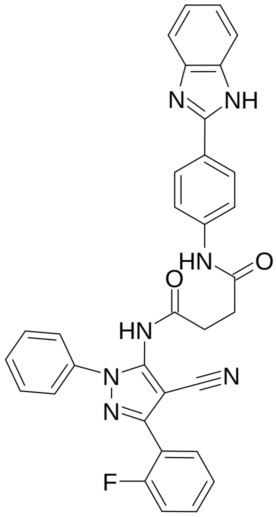

161

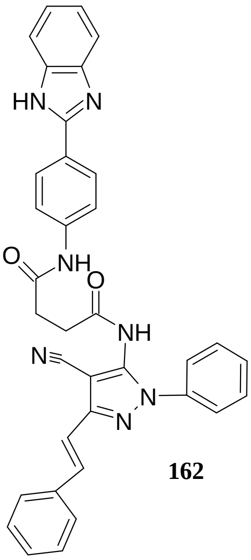

162

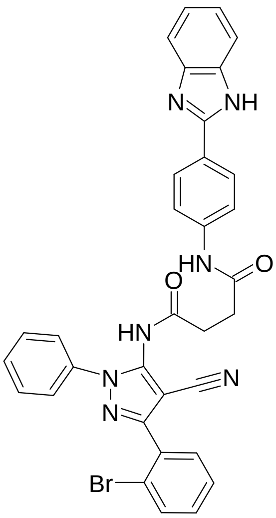

163

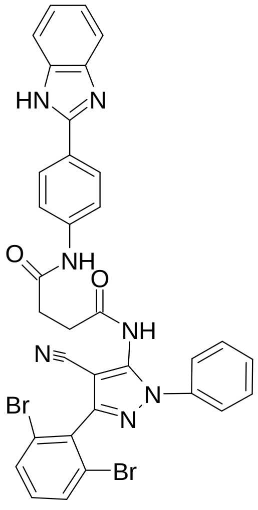

164

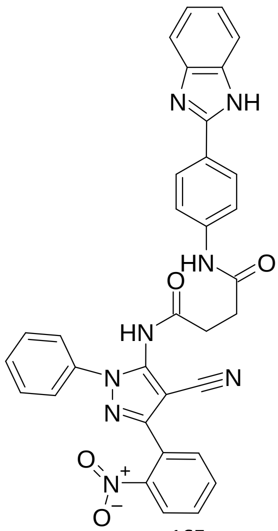

165

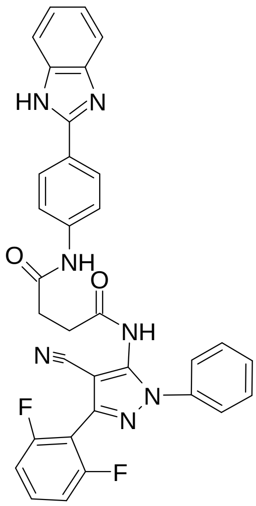

166

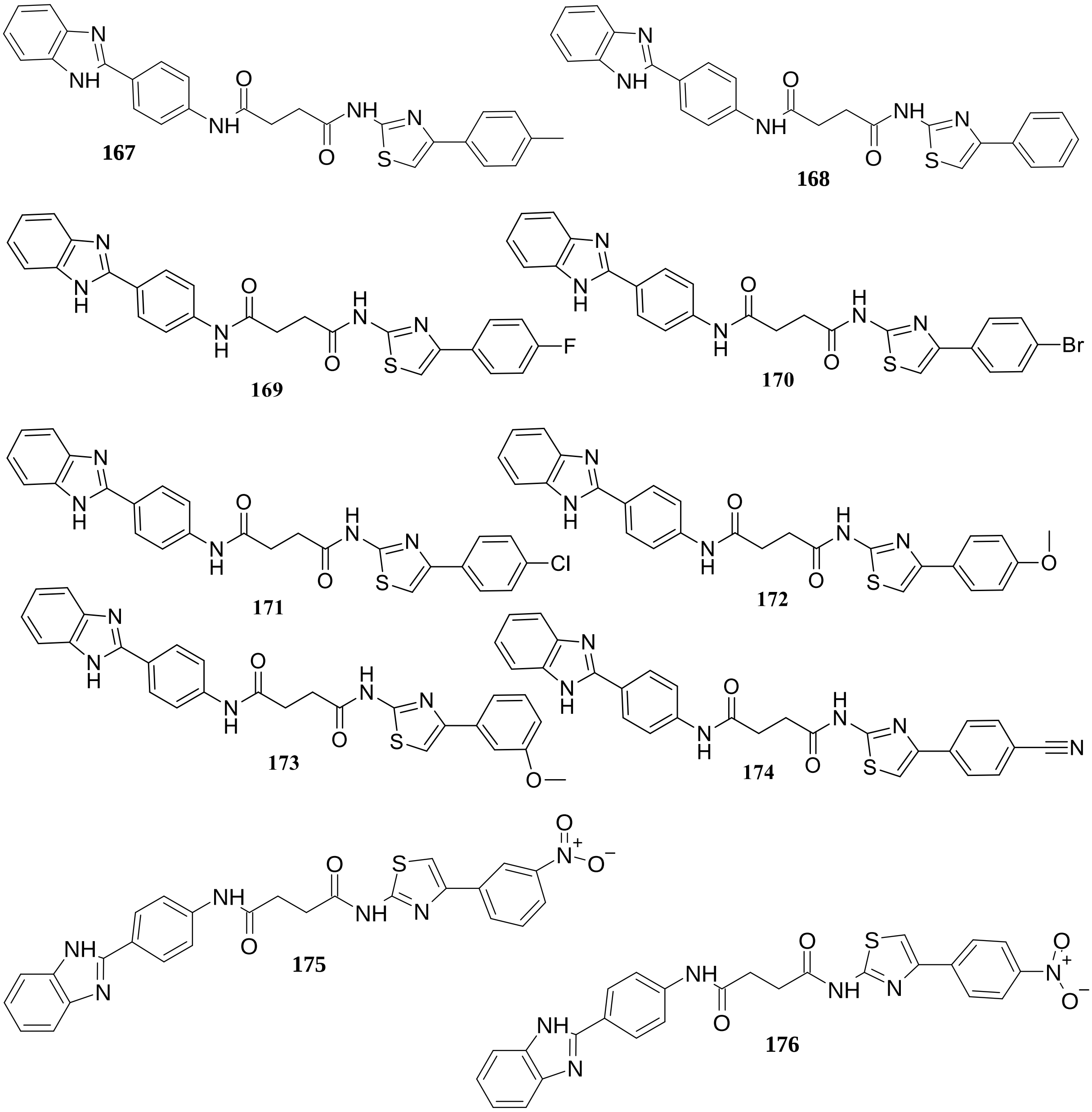

Figure 3.4. Chemical structures of docked thiazole/pyrazole and benzimidazole amide conjugates

Table 3.2. Docking Score, and MMGBSA dG binding energy of benzimidazole and pyrazole/ thiazole amide conjugates

S.No.	**Comp. No.**			**S.No.**	**Comp. No.**	**Docking Score**	**MMGBSA dG Bind**
1.	**155**			12.	**166**		
2.	**156**			13.	**167**		
3.	**157**			14.	**168**		
4.	**158**			15.	**169**		
5.	**159**			16.	**170**		

6.	**160**			17.	**171**		
7.	**161**			18.	**172**		
8.	**162**			19.	**173**		
9	**163**			20.	**174**		
10.	**164**			21.	**175**		
11.	**165**			22.	**176**		

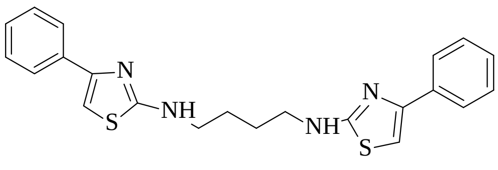

18a (P9)

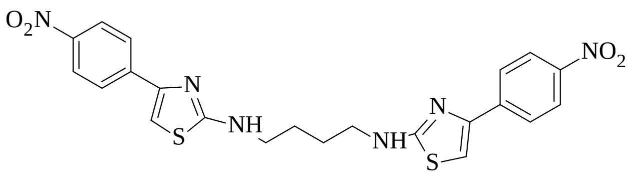

18b (P12)

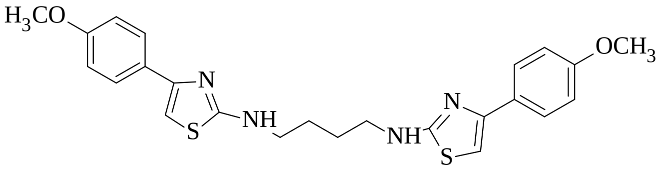

18c (P13)

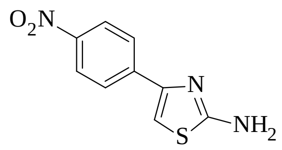

7g (P14)

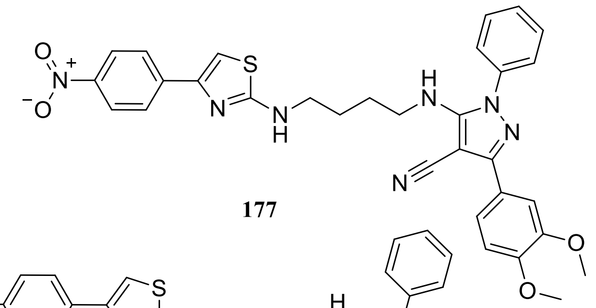

177

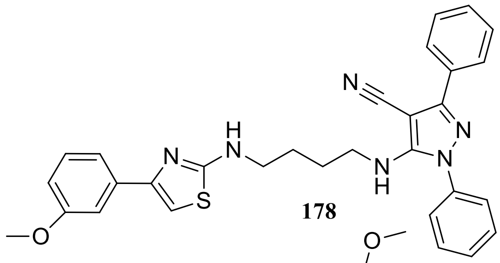

178

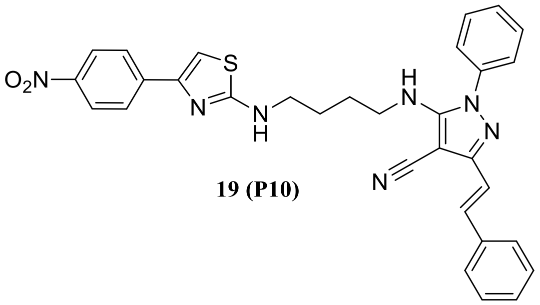

19 (P10)

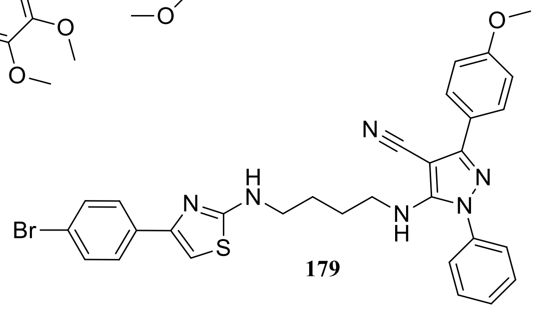

179

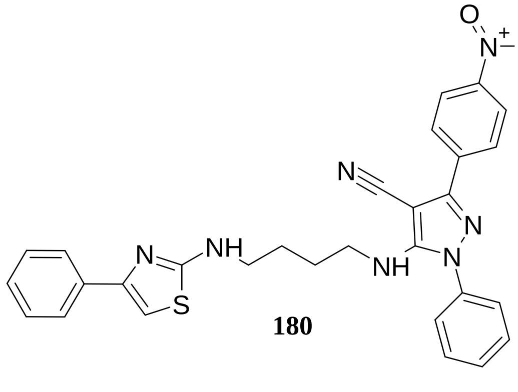

180

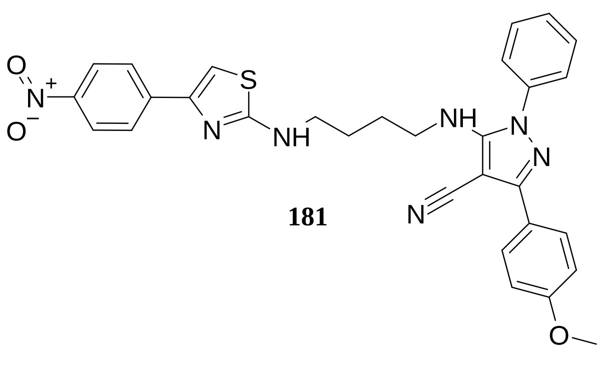

181

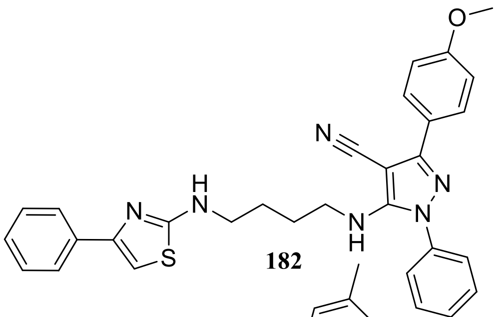

182

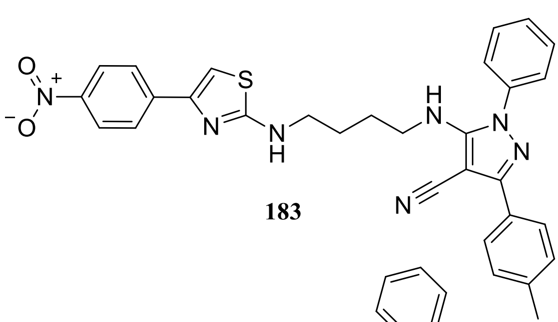

183

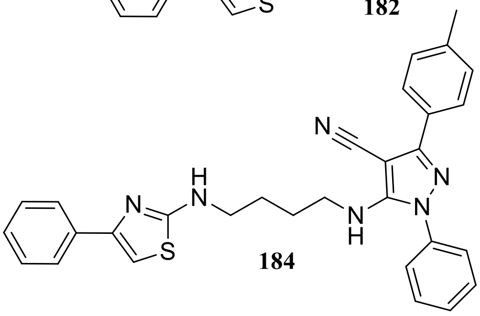

184

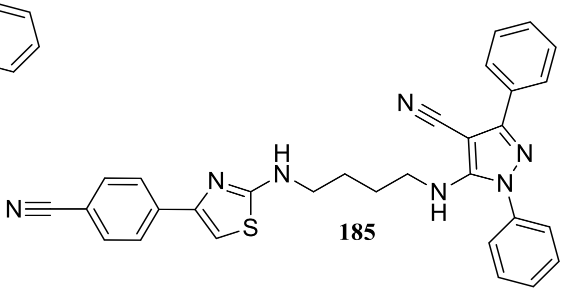

185

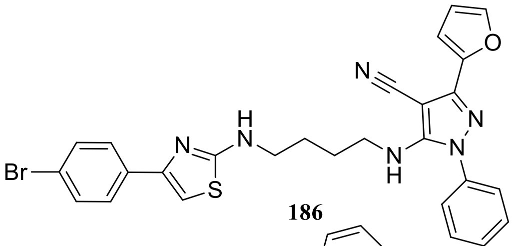

186

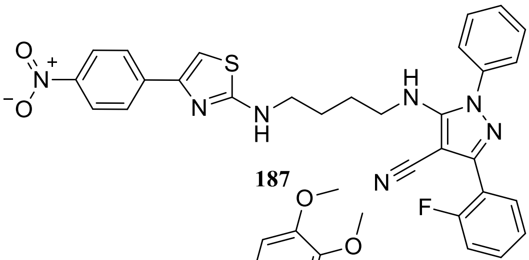

187

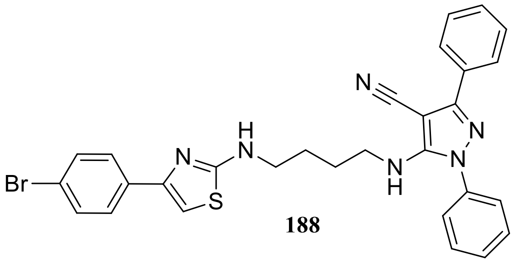

188

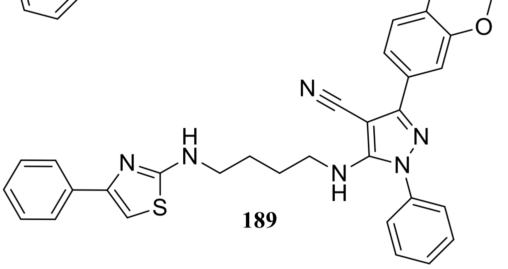

189

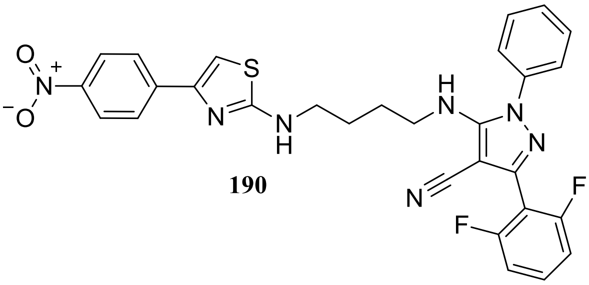

190

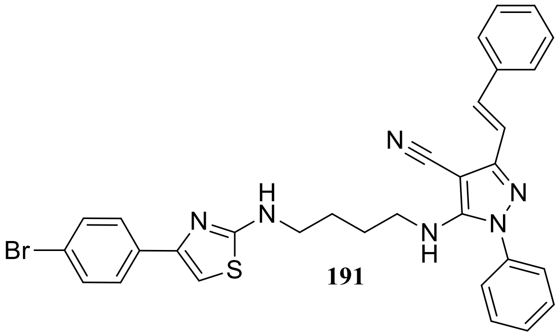

191

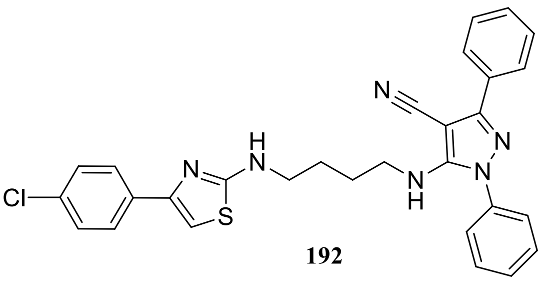

192

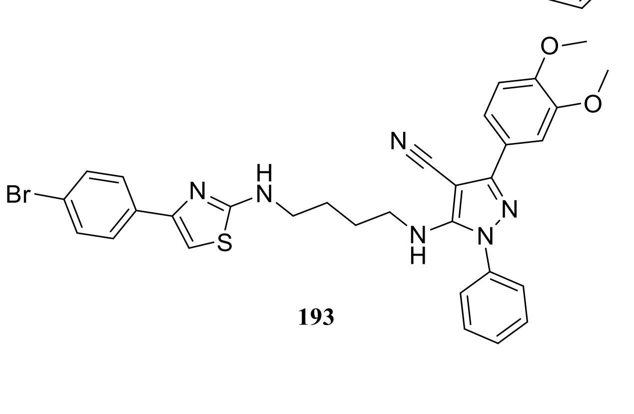

193

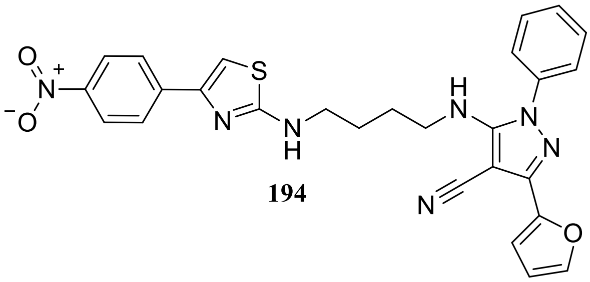

194

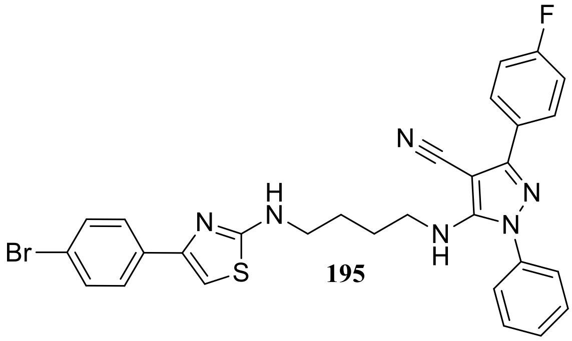

195

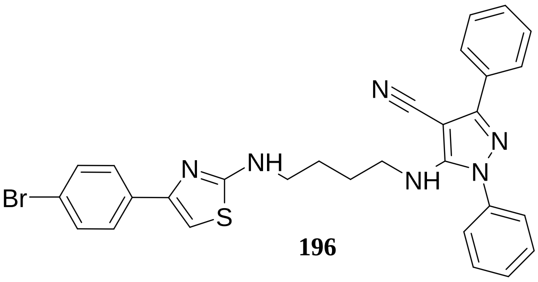

196

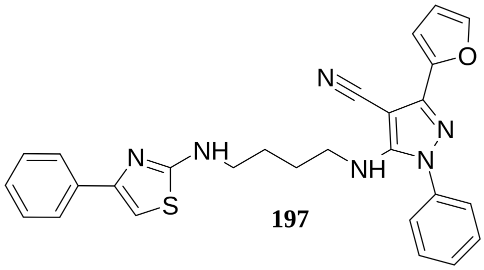

197

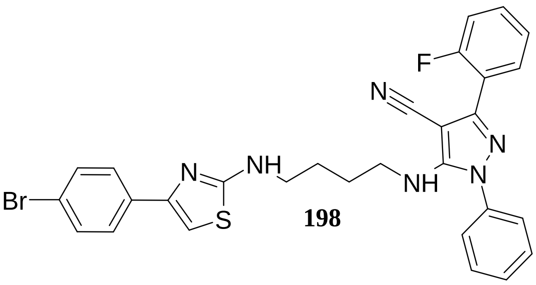

198

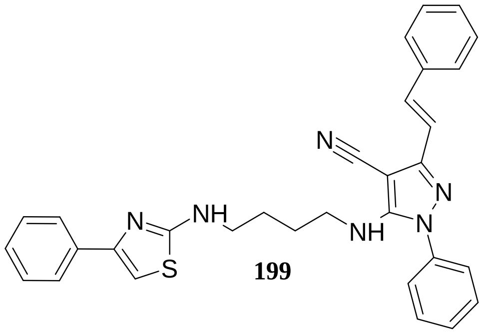

199

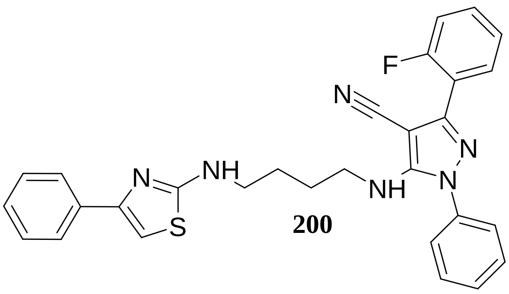

200

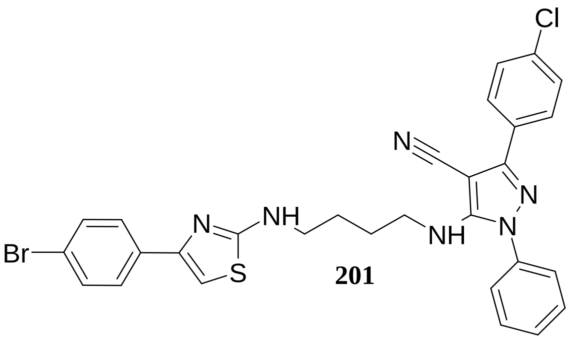

201

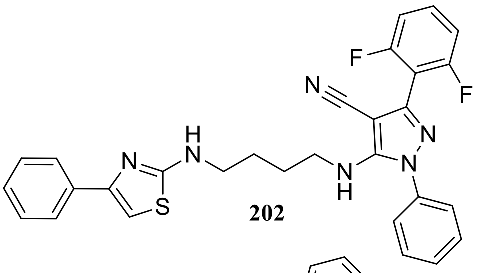

202

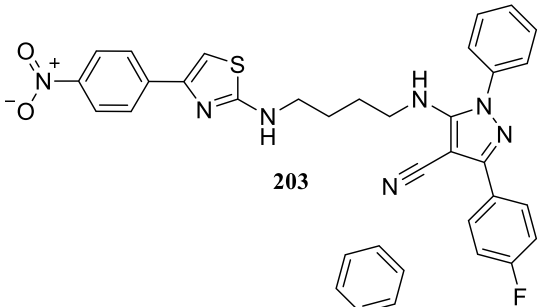

203

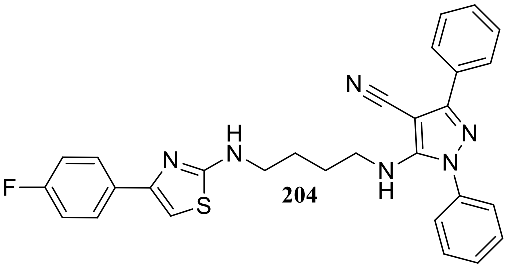

204

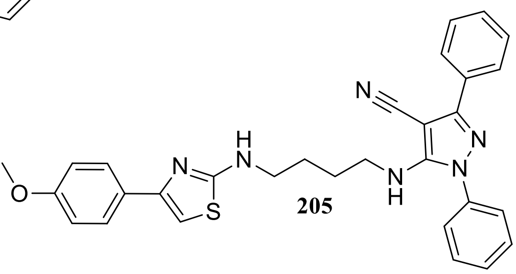

205

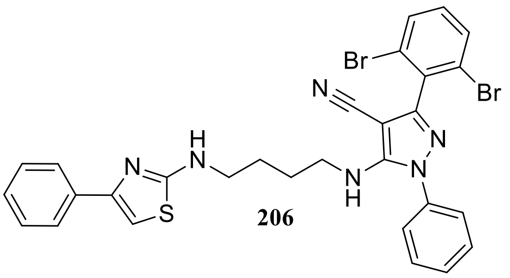

206

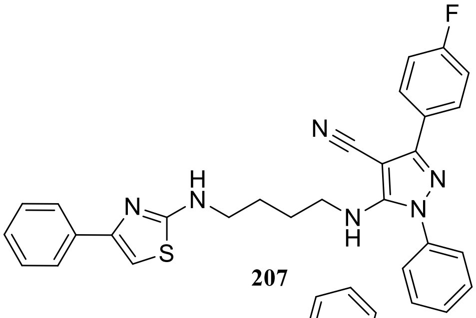

207

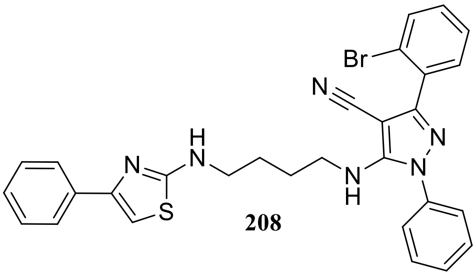

208

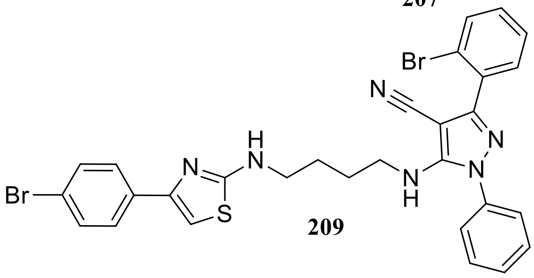

209

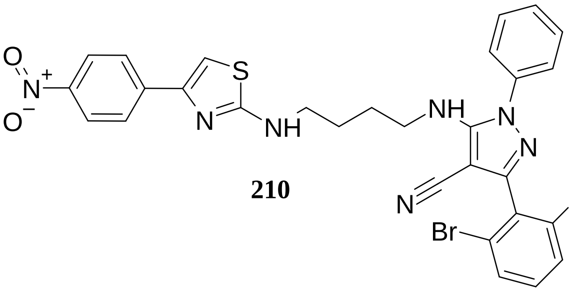

210

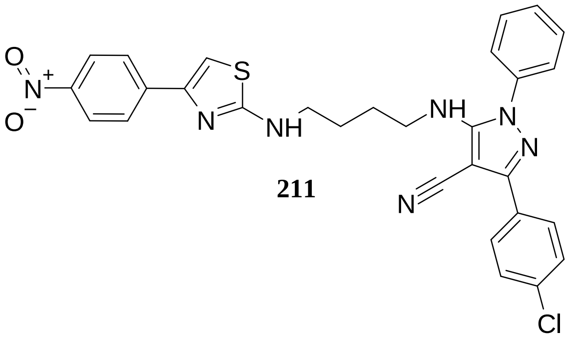

211

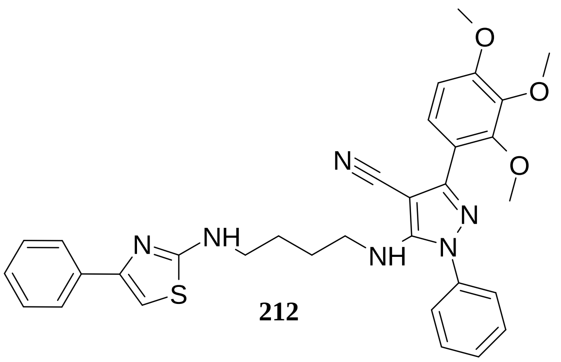

212

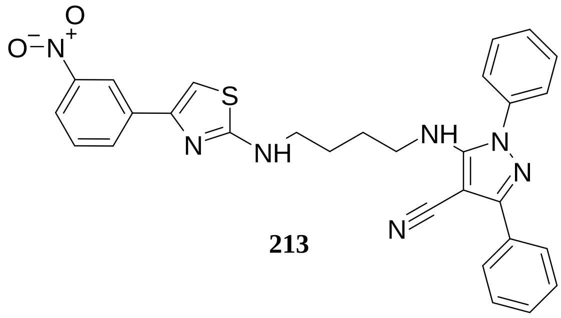

213

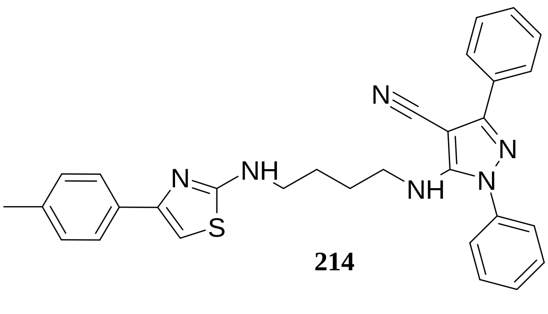

214

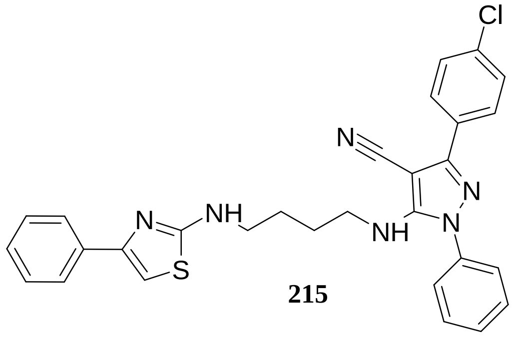

215

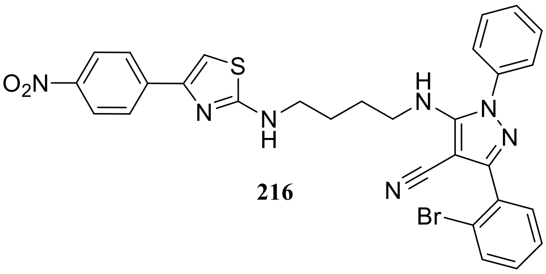

216

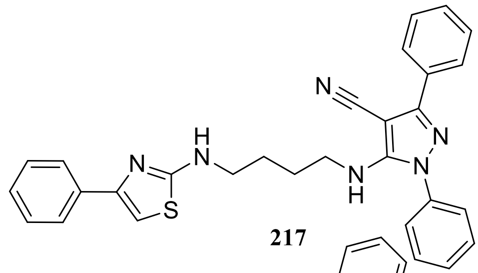

217

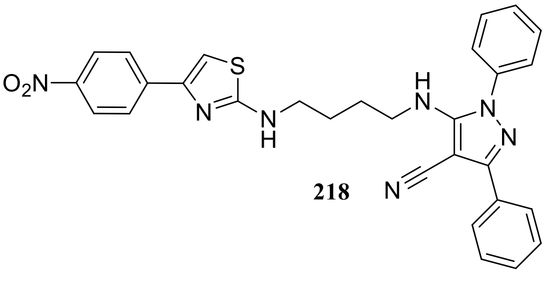

218

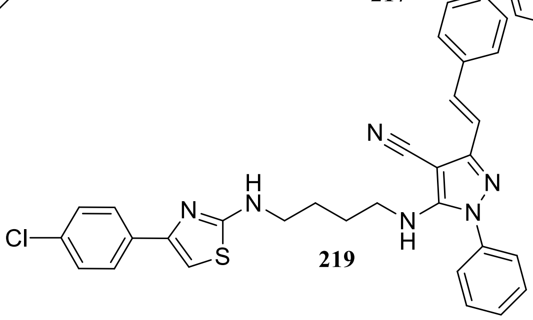

219

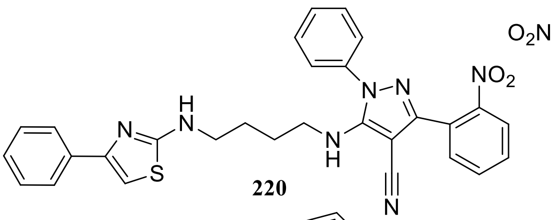

220

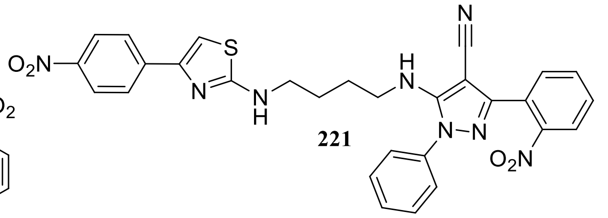

221

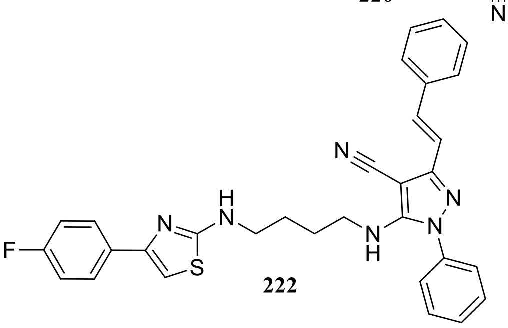

222

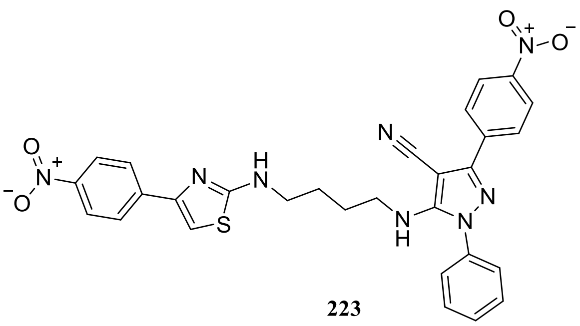

223

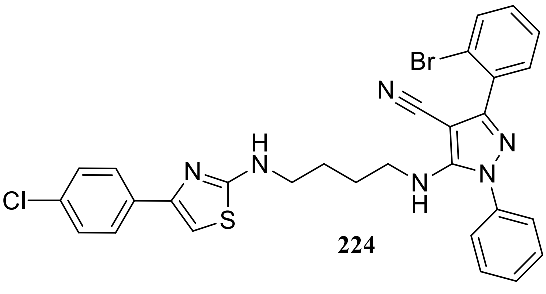

224

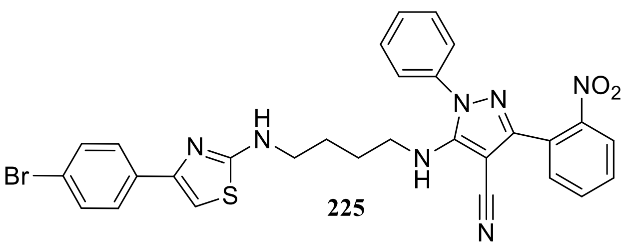

225

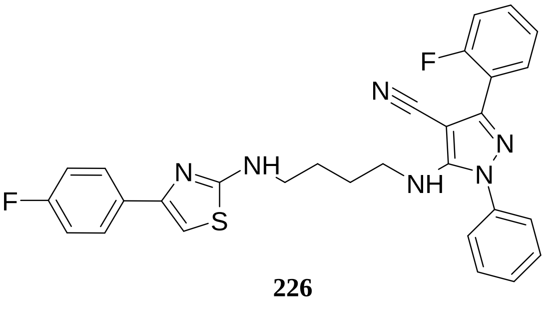

226

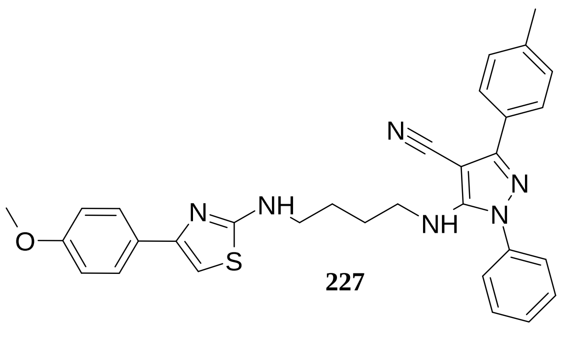

227

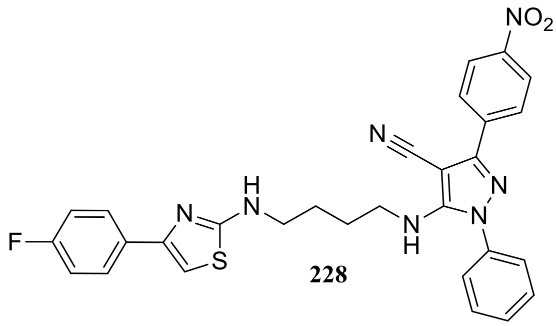

228

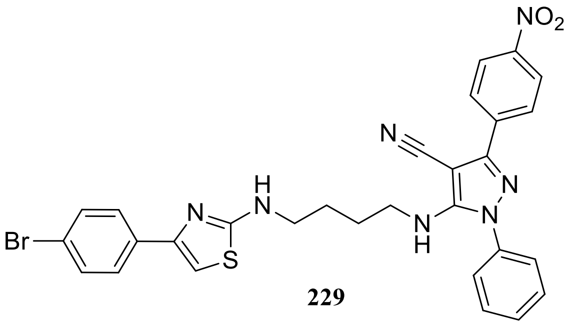

229

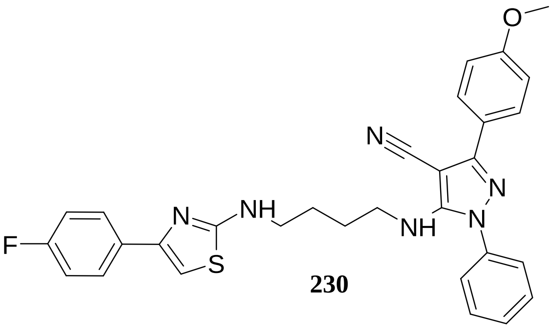

230

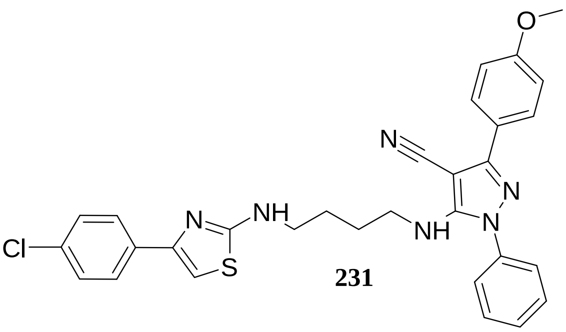

231

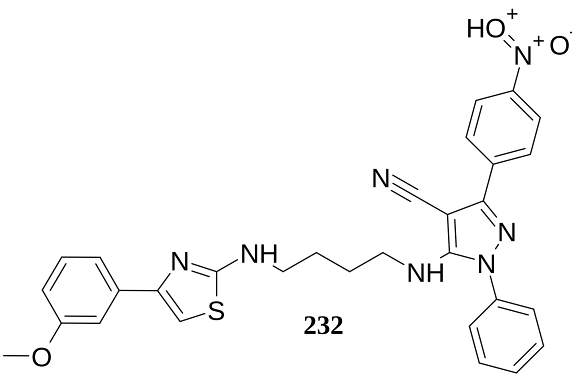

232

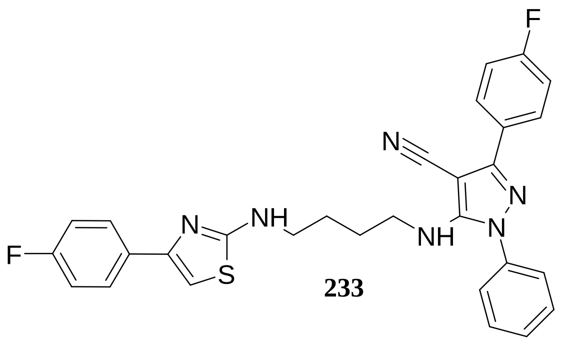

233

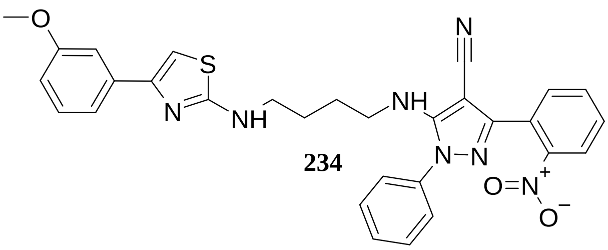

234

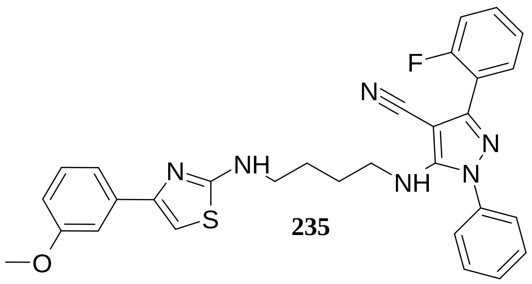

235

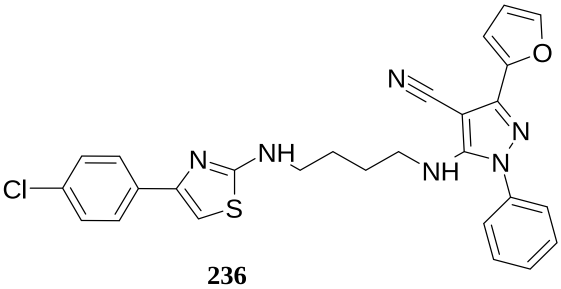

236

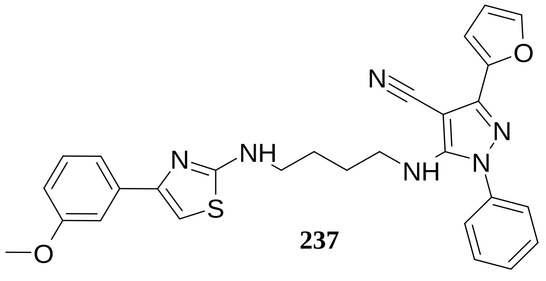

237

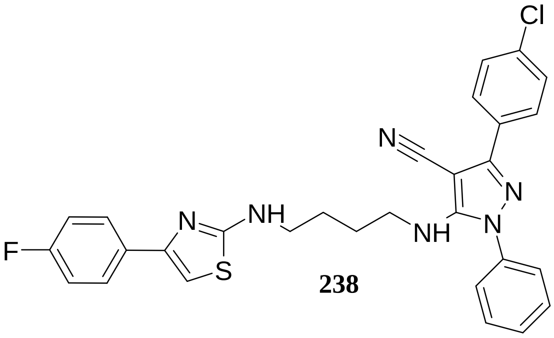

238

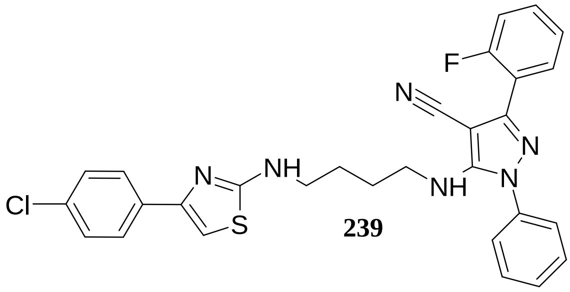

239

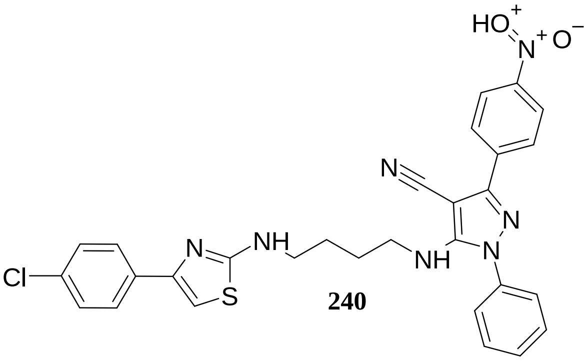

240

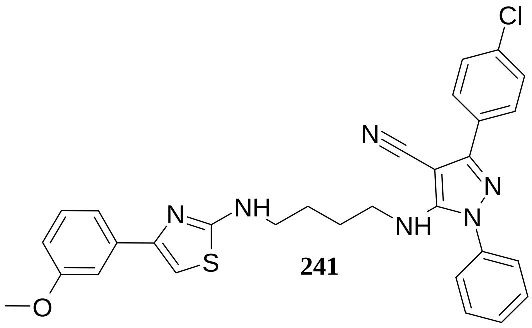

241

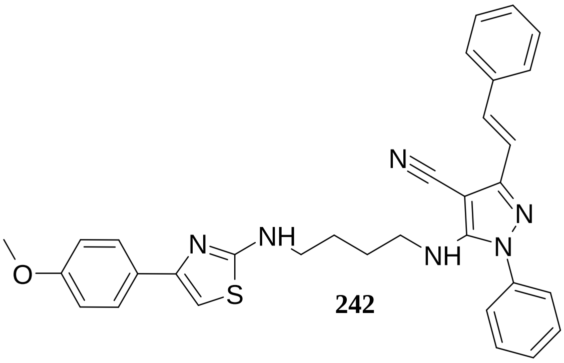

242

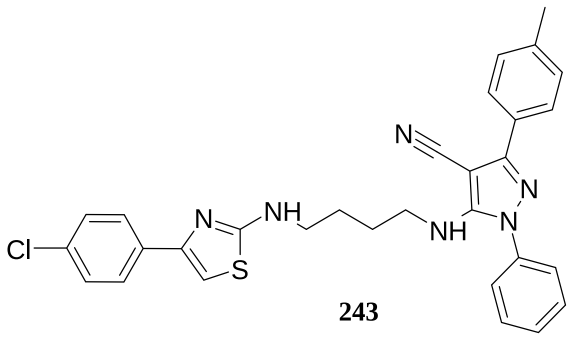

243

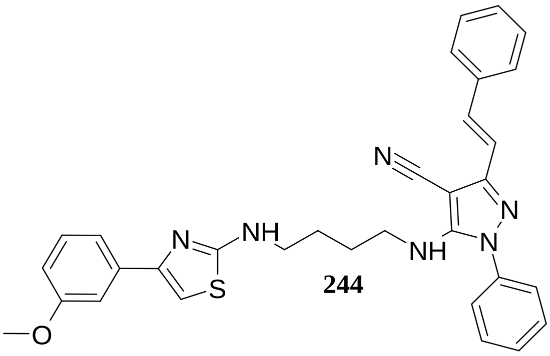

244

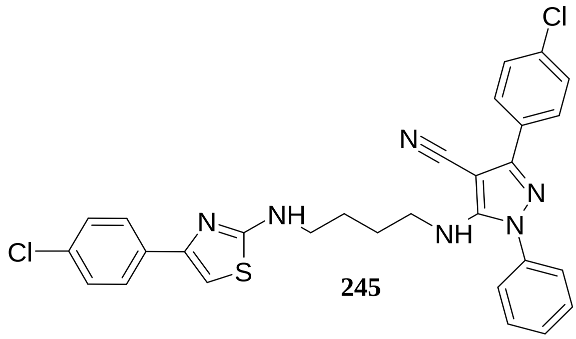

245

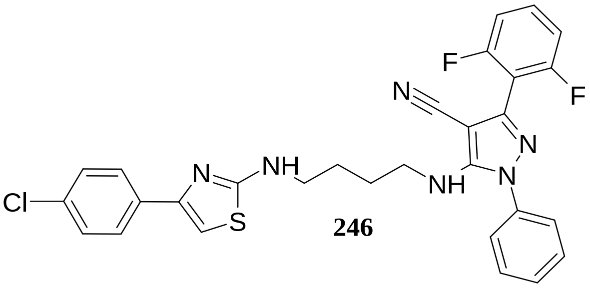

246

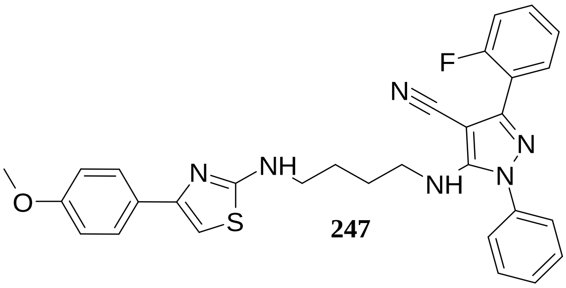

247

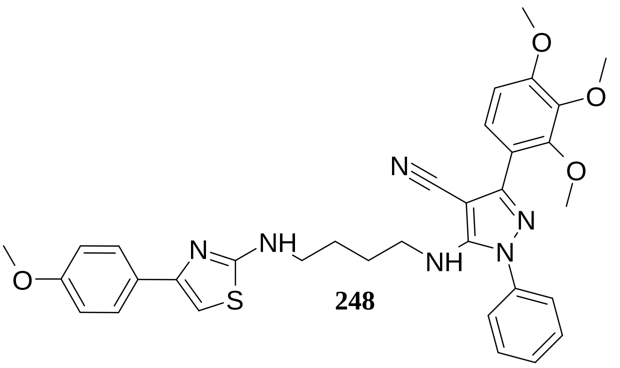

248

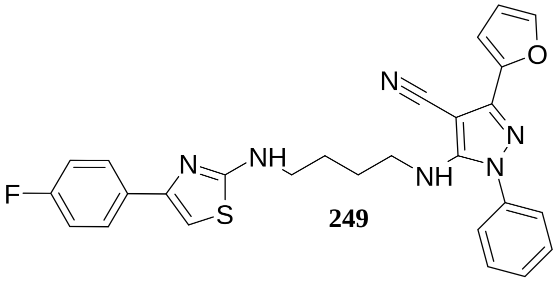

249

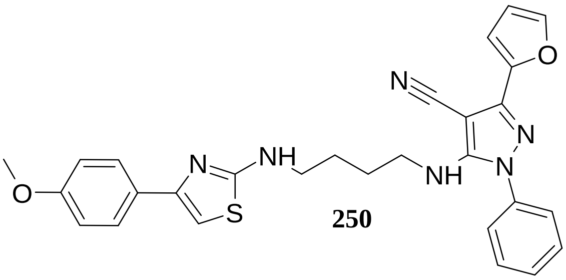

250

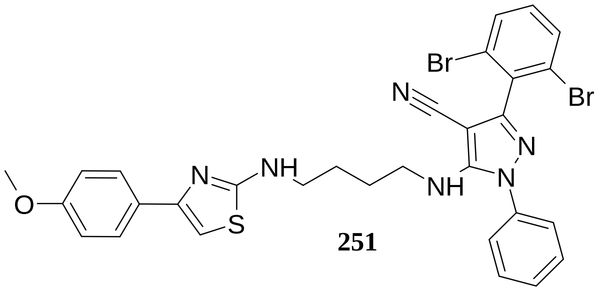

251

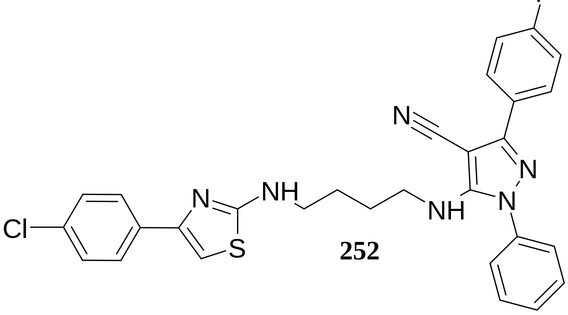

252

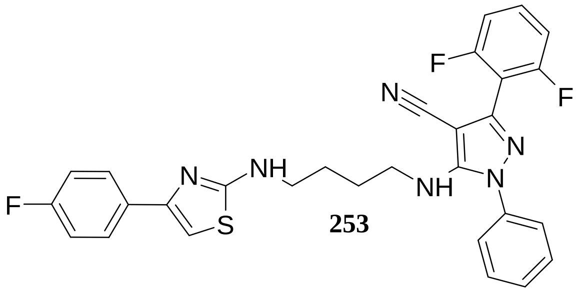

253

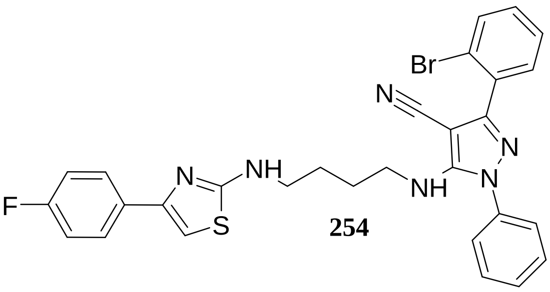

254

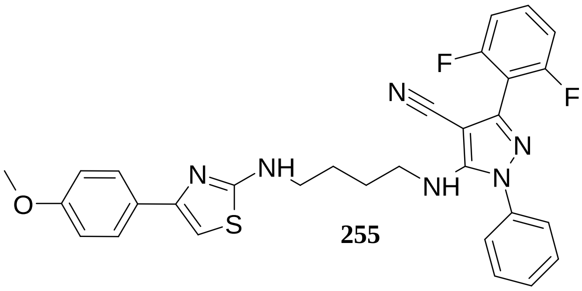

255

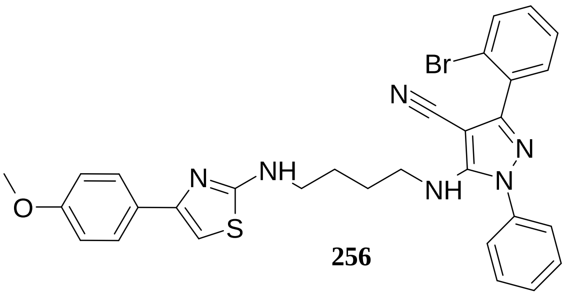

256

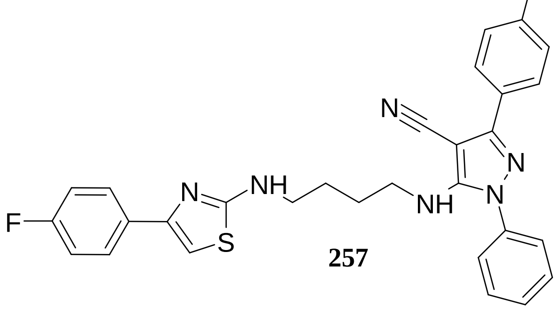

257

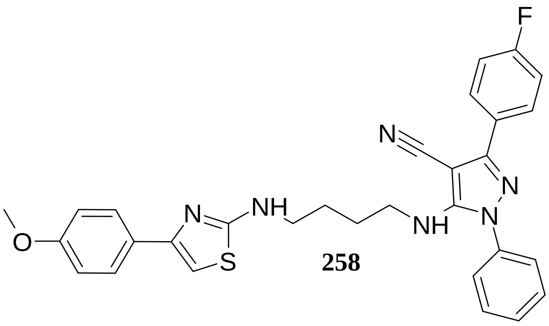

258

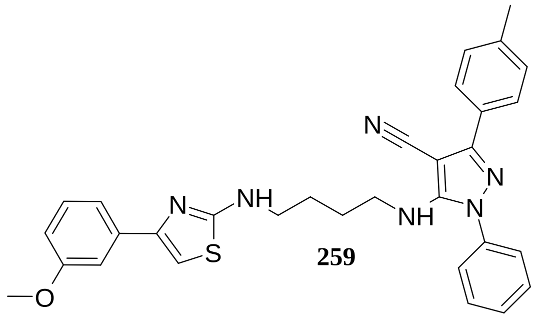

259

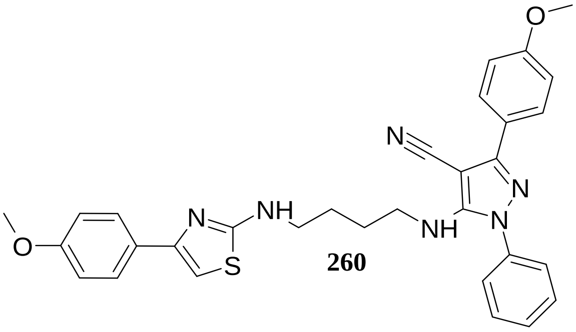

260

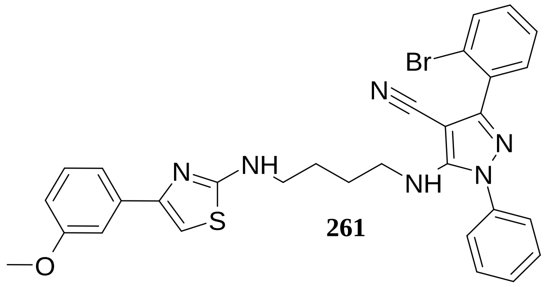

261

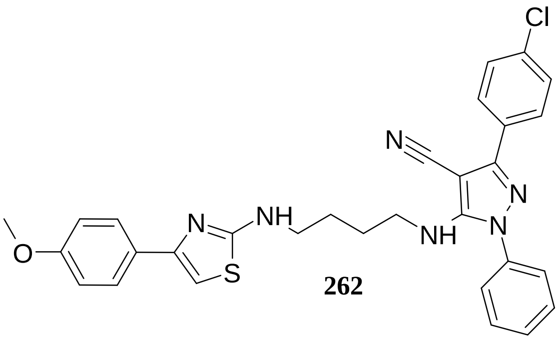

262

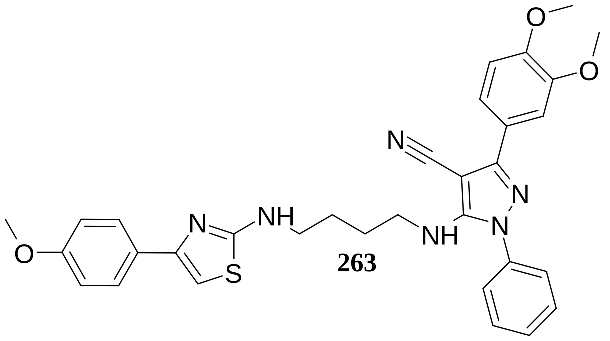

263

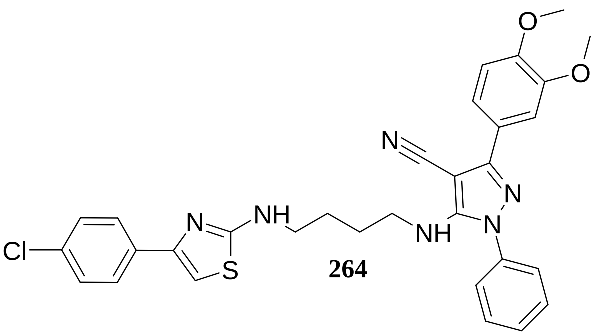

264

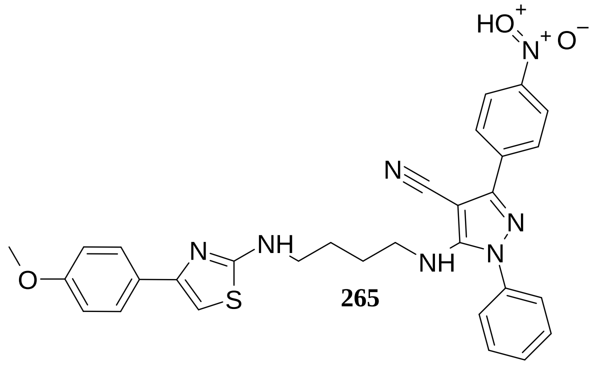

265

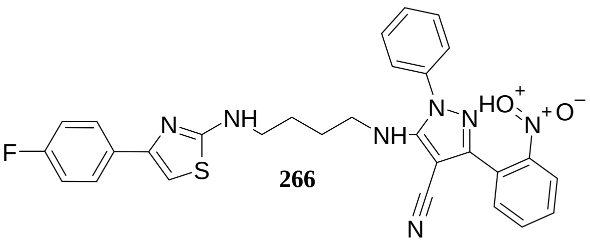

266

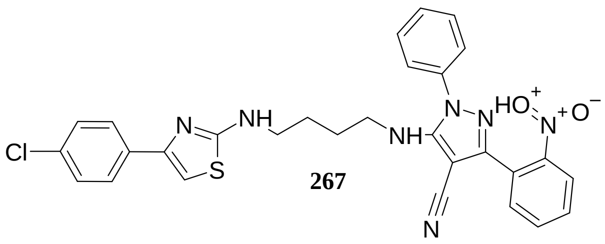

267

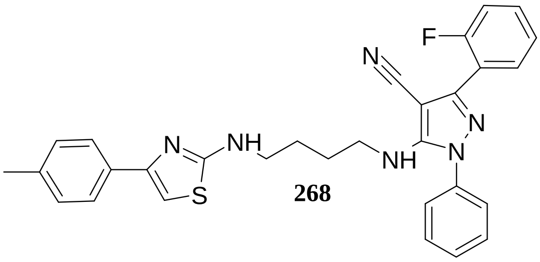

268

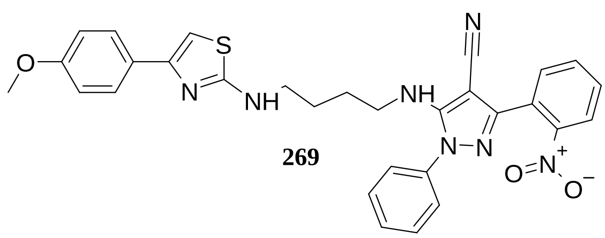

269

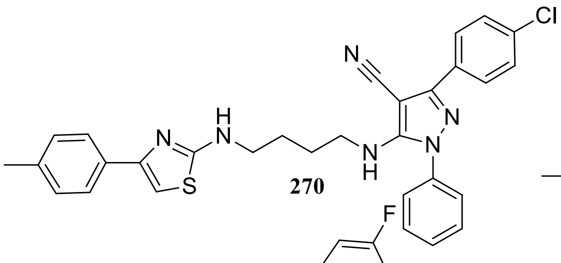

270

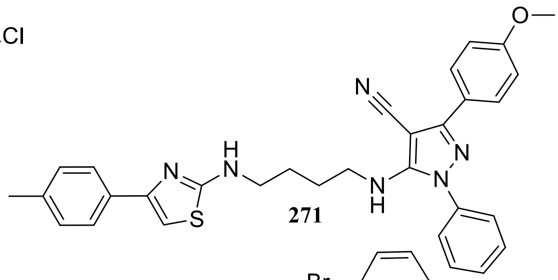

271

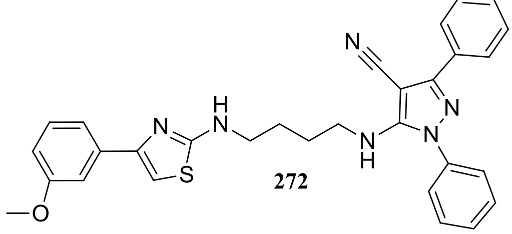

272

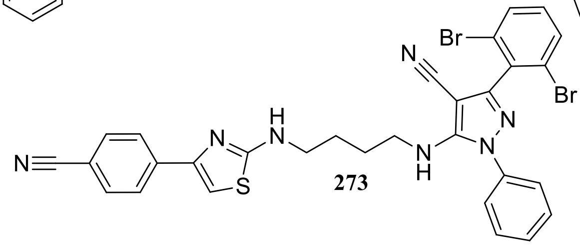

273

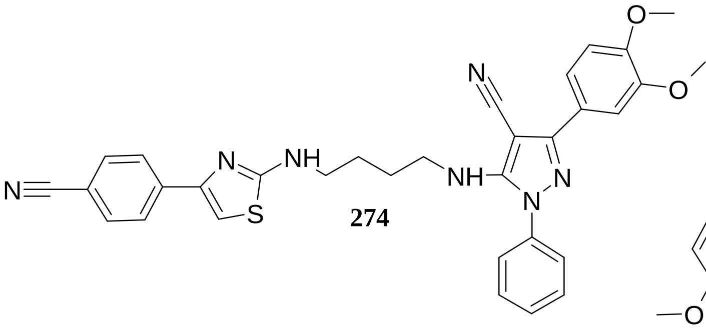

274

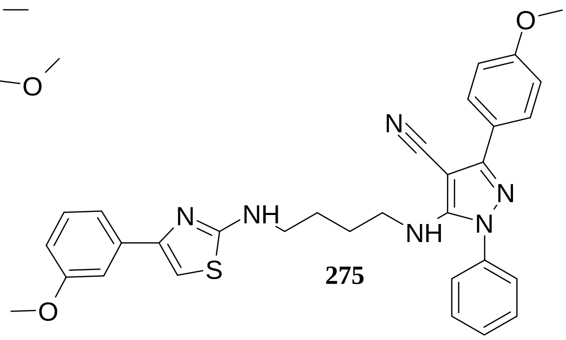

275

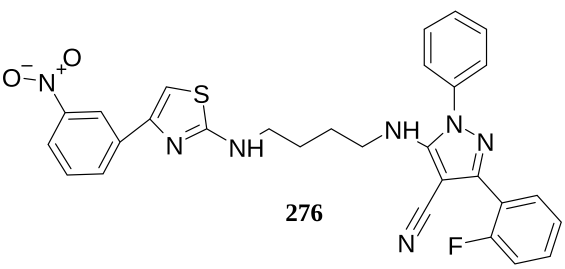

276

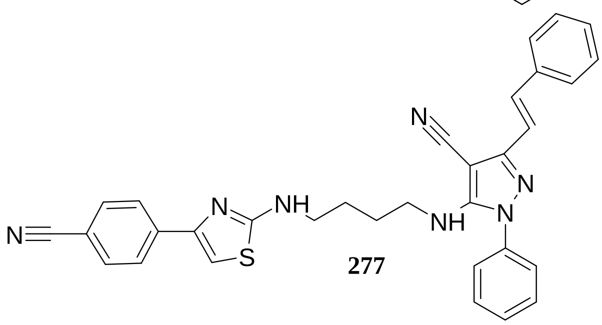

277

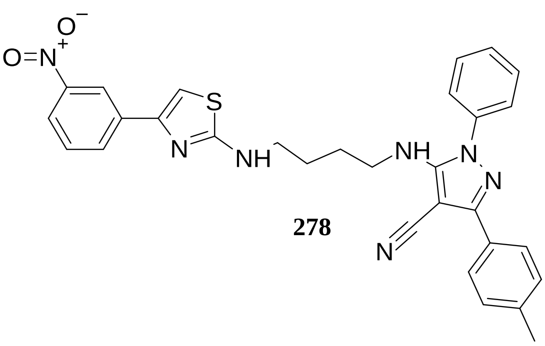

278

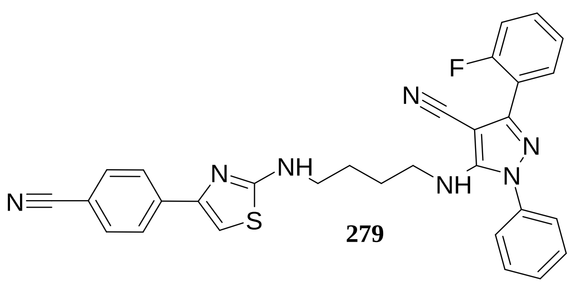

279

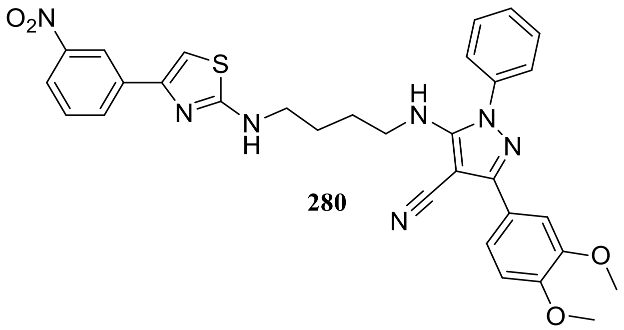

280

Figure 3.5. Chemical structures of docked thiazole-pyrazole amine conjugates

Table 3.3. Docking Score, and MMGBSA dG binding energy of pyrazole - thiazole amine conjugates

S.No.	Comp. No.			S.No.	Comp. No.		
1	**177**			54	**229**		
2	**178**			55	**230**		
3	**19 (P10)**			56	**231**		
4	**179**			57	**232**		
5	**180**			58	**233**		
6	**181**			59	**234**		
7	**182**			60	**235**		
8	**183**			61	**236**		
9	**184**			62	**237**		
10	**185**			63	**238**		
11	**186**			64	**239**		
12	**187**			65	**240**		
13	**188**			66	**241**		
14	**189**			67	**242**		
15	**190**			68	**243**		
16	**191**			69	**244**		
17	**192**			70	**245**		
18	**193**			71	**246**		
19	**194**			72	**247**		
20	**195**			73	**248**		
21	**196**			74	**249**		
22	**197**			75	**250**		
23	**198**			76	**251**		
24	**199**			77	**252**		
25	**200**			78	**253**		
26	**201**			79	**254**		
27	**202**			80	**255**		
28	**203**			81	**256**		
29	**204**			82	**257**		
30	**205**			83	**258**		

31	**206**			84	**259**		
32	**207**			85	**260**		
33	**208**			86	**261**		
34	**209**			87	**262**		
35	**210**			88	**263**		
36	**211**			89	**264**		
37	**212**			90	**265**		
38	**213**			91	**266**		
39	**214**			92	**267**		
40	**215**			93	**268**		
41	**216**			94	**269**		
42	**217**			95	**270**		
43	**218**			96	**271**		
44	**219**			97	**272**		
45	**220**			98	**273**		
46	**221**			99	**274**		
47	**222**			100	**275**		
48	**223**			101	**276**		
49	**224**			102	**277**		
50	**225**			103	**278**		
51	**226**			104	**279**		
52	**227**			105	**280**		
53	**228**						

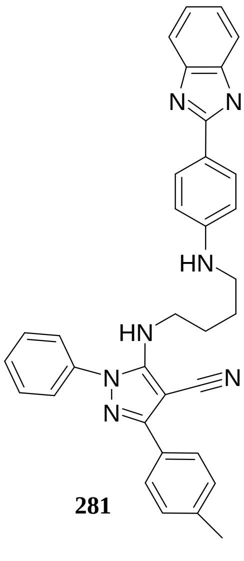

281

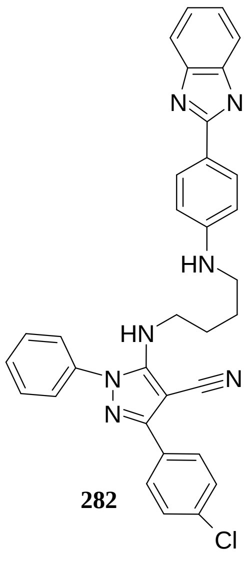

282

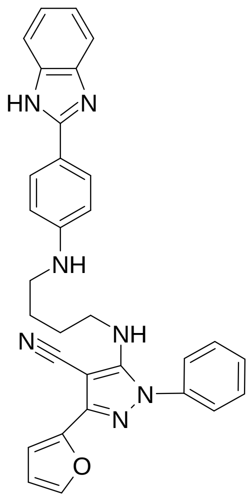

283

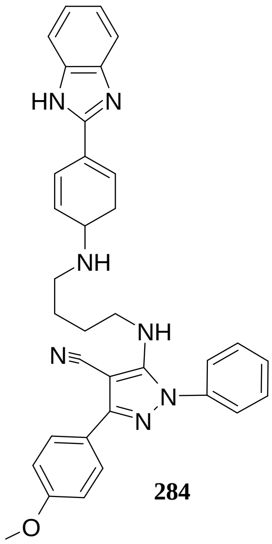

284

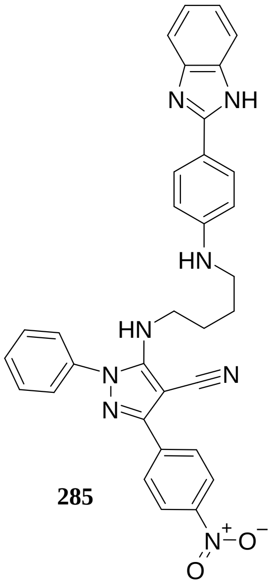

285

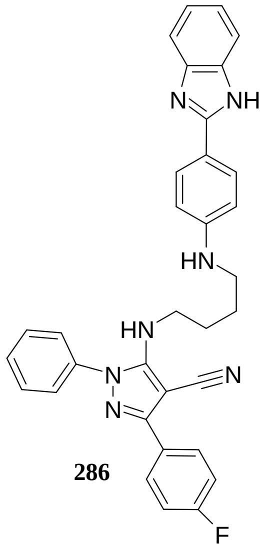

286

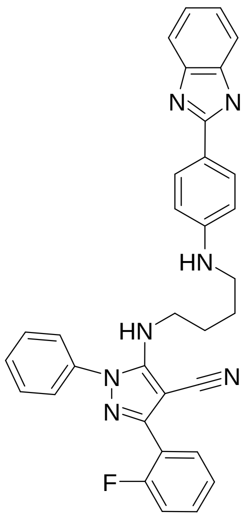

287

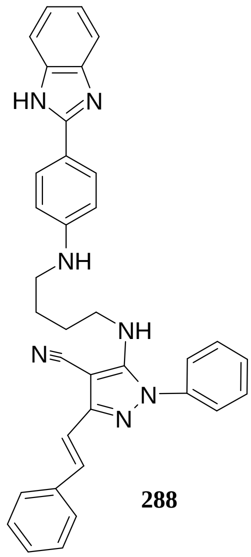

288

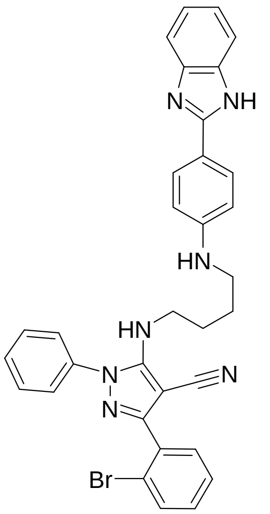

289

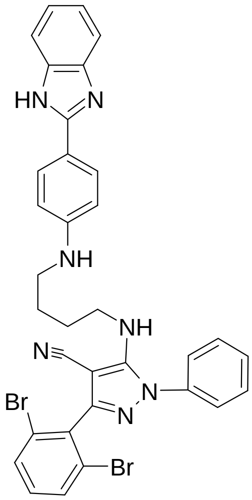

290

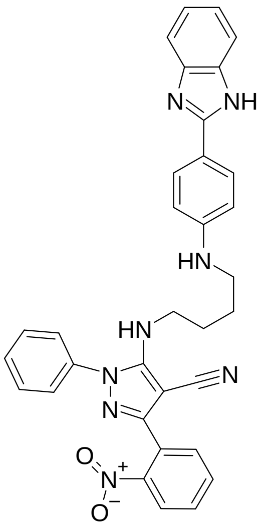

291

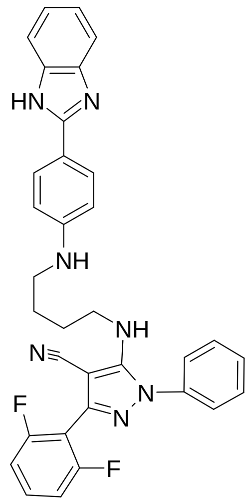

292

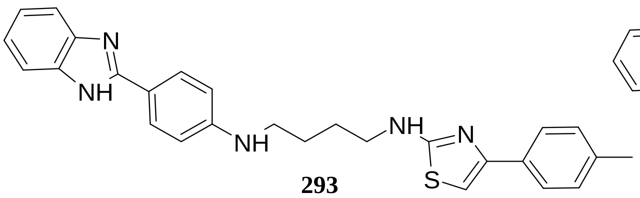

293

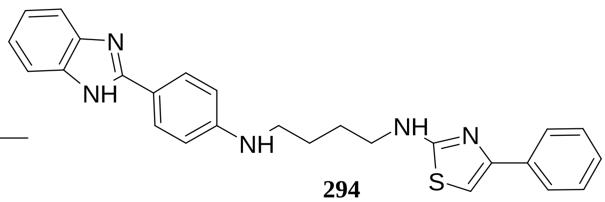

294

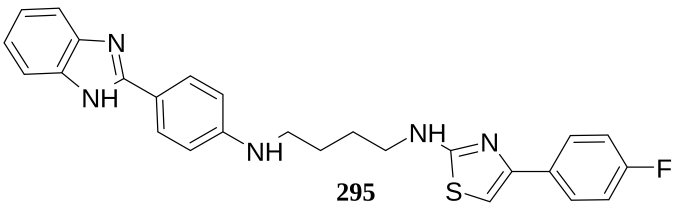

295

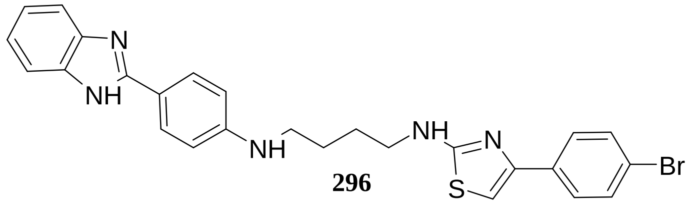

296

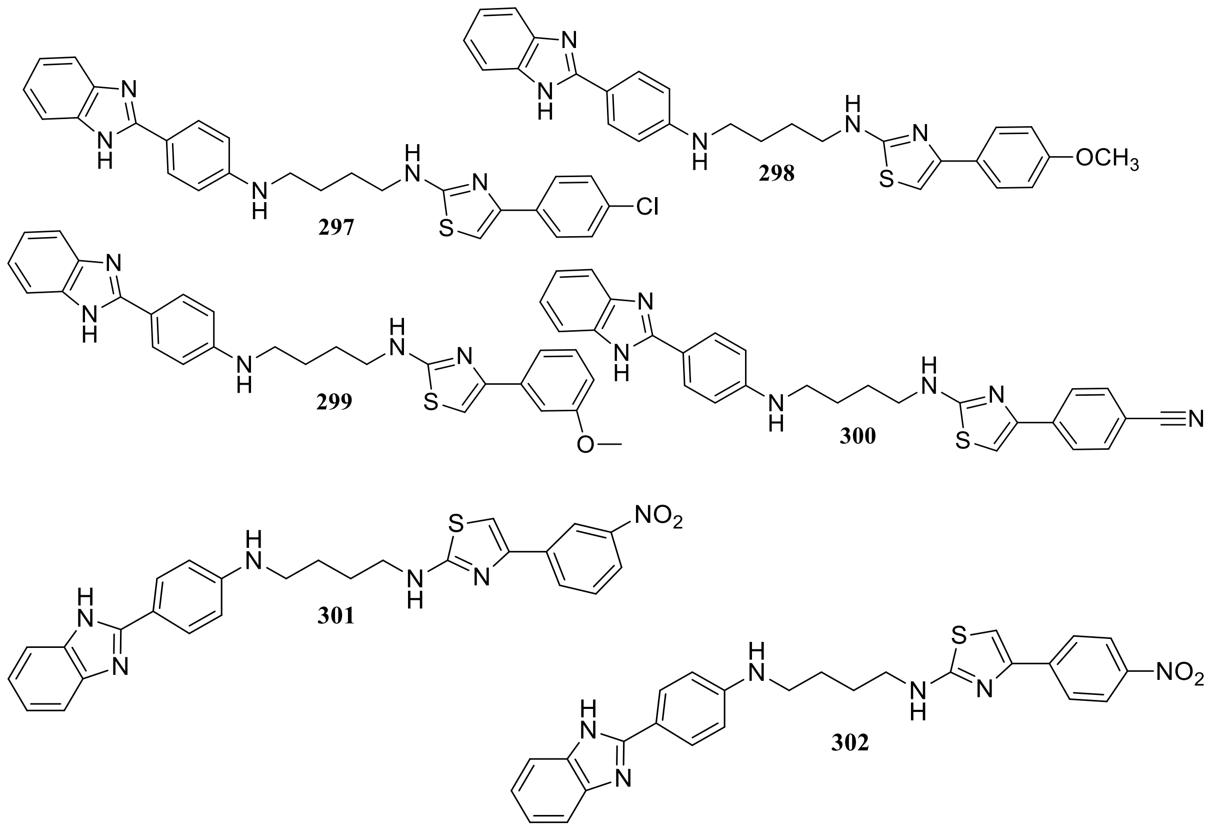

Figure 3.6. Chemical structures of docked thiazole/pyrazole-benzimidazole amine conjugates

Table 3.4. Docking Score, and MMGBSA dG binding energy of thiazole/pyrazole-benzimidazole amide conjugates

S.No.	Comp. No.			S.No.	Comp. No.		
1	**281**			12	**292**		
2	**282**			13	**293**		
3	**283**			14	**294**		
4	**284**			15	**295**		
5	**285**			16	**296**		
6	**286**			17	**297**		
7	**287**			18	**298**		
8	**288**			19	**299**		
9	**289**			20	**300**		
10	**290**			21	**301**		
11	**291**			22	**302**		

Table 3.5 List of compounds selected for synthesis and *in-vitro* analysis

Compound Structure	Compound name
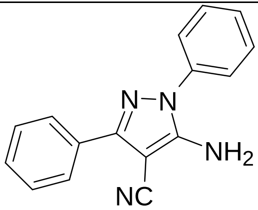	5-Amino-1,3-diphenyl-1H-pyrazole-4-carbonitrile (**4a**) (**P1**)
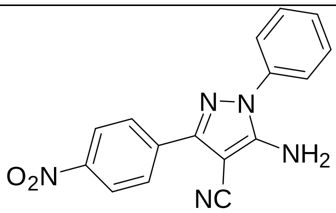	5-Amino-3-(4-nitrophenyl)-1-phenyl-1H-pyrazole-4-carbonitrile (**4b**) (**P2**)
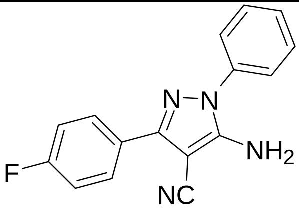	5-Amino-3-(4-fluorophenyl)-1-phenyl-1H-pyrazole-4-carbonitrile (**4f**) (**P3**)
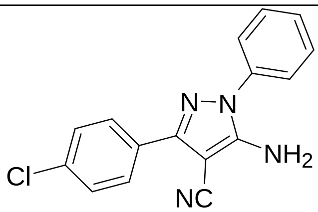	5-Amino-3-(4-chlorophenyl)-1-phenyl-1H-pyrazole-4-carbonitrile (**4h**) (**P4**)
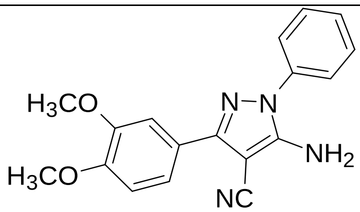	5-Amino-3-(3,4-dimethoxyphenyl)-1-phenyl-1H-pyrazole-4-carbonitrile (**4m**) (**P5**)
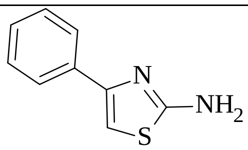	4-Phenylthiazol-2-amine (**7a**) (**P6**)
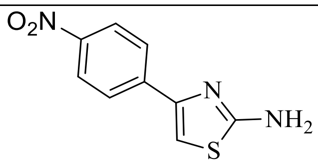	4-Phenylthiazol-2-amine **(7g)**
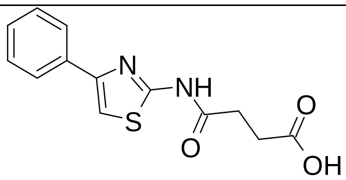	4-Oxo-4-((4-phenylthiazol-2-yl)amino) butanoic acid (**13a**) (**P7**)

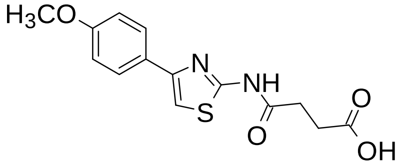	4-((4-(4-Methoxyphenyl)thiazol-2-yl)amino)- 4-oxobutanoic acid (**13b**)(**P8**)
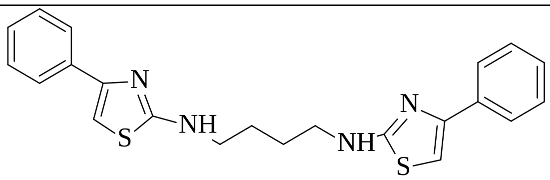	N^1,N^4-Bis(4-phenylthiazol-2-yl)butane-1,4-diamine (**18a**) (**P9**)
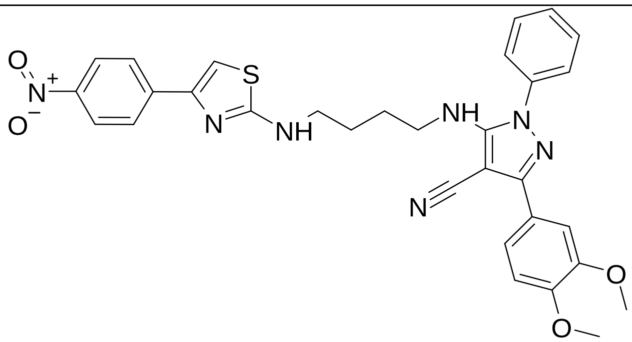	3-(3,4-Dimethoxyphenyl)-5-((4-((4-(4-nitrophenyl)thiazol-2-yl)amino)butyl)amino)-1-phenyl-1H-pyrazole-4-carbonitrile (**19**) (**P10**)
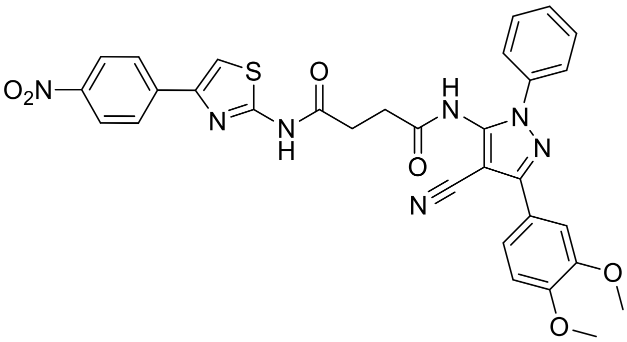	N^1-(4-Cyano-3-(3,4-dimethoxyphenyl)-1-phenyl-1H-pyrazol-5-yl)-N^4-(4-(4-nitrophenyl)thiazol-2-yl)succinimide (**11**) (**P11**)
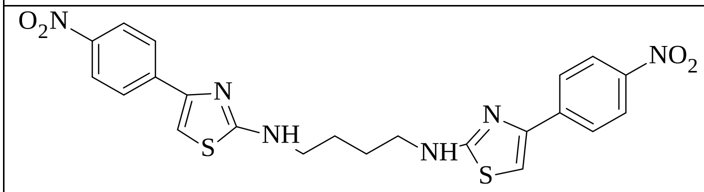	N^1,N^4-Bis(4-(4-nitrophenyl)thiazol-2-yl)butane-1,4-diamine (**18b**) (**P12**)
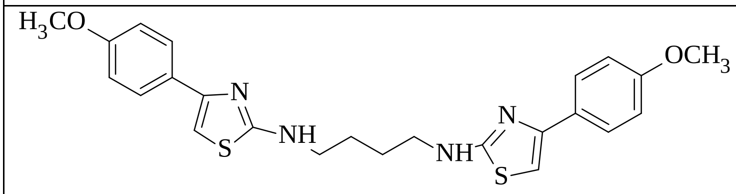	N^1,N^4-Bis(4-(4-methoxyphenyl)thiazol-2-yl)butane-1,4-diamine (**18c**) (**P13**)
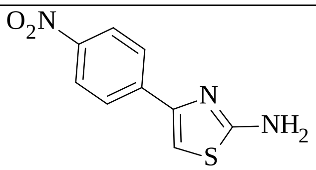	4-(4-nitrophenyl)thiazol-2-amine **(7g) (P14)**

3.2 Synthesis of pyrazole derivatives

The highly functionalized pyrazole derivatives are the potential biologically active scaffolds due to their wide applications in pharmaceuticals (Khan et al., 2016; Lim et al., 2016; Wu et al., 2017; Kiyani and Bamdad, 2018). These scaffolds have been used as analgesics, anti-bacterial (Bekhit and Abdel-Aziem, 2004; Tanitame et al., 2004a; Akbas et al., 2005), anti-convulsant (Özdemir, 2007), anti-pyretic activities (Mantzanidou, 2021), anti-depressant (Naim et al., 2016), anti-fungal (Tanitame et al., 2004b), anti-inflammatory (Badawey and El-Ashmawey, 1998; Tewari & Mishra, 2001), antimalarials (Gilbert et al., 2006), anti-microbials (Foks et al., 2005; Dardari et al., 2006), anti-parasitic (Rathelot et al., 2002; Bernardino et al., 2006), and anti-tumor (Daidone et al., 1998; Taylor and Patel, 1992). Further, these compounds reported to have appreciable anti-hypertensive activity *in-vivo* and, also exhibit properties such as human cannabinoid receptors (hCB1 and hCB2), inhibitors of p38 Kinase and CB1 receptor antagonists.

The most well-known method for the synthesis of the 5-aminopyrazole-4-carbonitriles scaffold is the three-component cyclo-condensation (3-CC) of aldehydes, phenyl hydrazine derivatives, and malononitrile (Srivastava et al., 2013; Chen et al., 2014; Li et al., 2014; Srivastava et al., 2014; Kamal et al., 2015; Maddila et al., 2015; Saha et al., 2015; Kashiwa et al., 2016; Kumari et al., 2016; Ma et al., 2016; Meng et al., 2016; Rakhtshah et al., 2016; Ubale and Shioorkar et al., 2016; Saeed and Channar, 2017; Mishra et al., 2017). A variety of catalysts and reagents like sodium ascorbate (Kiyani and Bamdad, 2018), molecular iodine (Srivastava et al., 2014), ionic liquids (Srivastava et al., 2013), nanoparticles (Rakhtshah et al., 2016; Li et al., 2014), rhodium catalyst with sodium acetate (NaOAc) (Li et al., 2014), piperidine (Saeed and Channar, 2017), piperidinium acetate (Kamal et al., 2015), $Cu(OAc)_2$ (Chen et al., 2014), CuO/ZrO_2 (Maddila et al., 2015), cerium (IV) ammonium nitrate (Meng et al., 2016), graphene oxide-TiO_2 (Kumari et al., 2016), oxone (Kashiwa et al., 2016), palladium and copper (Ma et al., 2016) and alum (Ubale and Shioorkar et al., 2016) have been studied for this reaction.

To our knowledge, metal oxide with inorganic oxide surfaces using multicomponent reactions has not been used as the catalyst in the synthesis of pyrazoles under aqueous conditions. Heterogenous catalysts using inorganic oxide surfaces like zeolites, clays, silica, alumina have received attention due to ease of working process (Pompe et al., 2018; Zhang et al., 2018). Considering the utility of alumina and silica, we synthesized, an efficient, eco-friendly, one-pot, three-component synthesis of 5-amino-1,3-diphenyl-1H-pyrazole-4-

carbonitrile derivatives (**4**) in water using alumina-silica supported MnO_2 as the heterogeneous catalyst (Poonam and Singh, 2019).

3.2.1 Preparation of supported catalysts

The initial studies focussed on the development of heterogeneous catalysts based on inorganic oxides: silica gel (60-120 mesh) and acidic alumina (Pompe et al., 2018). The *in-situ* generation of manganese oxide (MnO_2) was done from manganese acetate tetrahydrate ($Mn(OAc)_2 \cdot 4H_2O$) by the modification of the reported method (Zhong, 2016). A mixture of *n*-propanol, de-ionised water, manganese acetate tetrahydrate and silica and/or alumina was stirred at 80 ^oC for 3 hours. To this, an aqueous solution of $KMnO_4$ was added and the stirring was continued for another 2 hours. The reaction mixture was filtered to get a black solid which was washed with water and dried at 70 ^oC under vacuum for 5 h.

The elemental compositions of manganese acetate tetrahydrate, acidic alumina, silica gel, silica-supported MnO_2, alumina-supported MnO_2, and alumina-silica-supported MnO_2 were established by energy dispersive X-ray (EDX) spectroscopy (Figure 3.7). The SEM images showed the morphology of the prepared catalysts (Figure 3.7). The EDX patterns clearly indicated the expected elemental components with no extra peaks observed for any other impurities. The corresponding analytical data derived from EDX analysis are summarized along with images in Figure 3.7.

The images clearly confirm the presence of silica, alumina and MnO_2 in the catalyst. Moreover, the absence of C shows the conversion of manganese acetate tetrahydrate to manganese oxide.

The X-ray diffraction results for the silica-MnO_2, alumina-MnO_2 and silica-alumina-MnO_2 catalyst are shown in Figure 3.8. The features found in these diffractograms showed the presence of manganese oxide, silica and alumina in the catalyst samples and compared with JCPDS data sheet.

Manganese acetate tetrahydrate

Element	Weight%	Atomic%
C K	2.23	22.21
O K	7.98	59.78
Mn K	8.26	18.01
Totals	18.47	

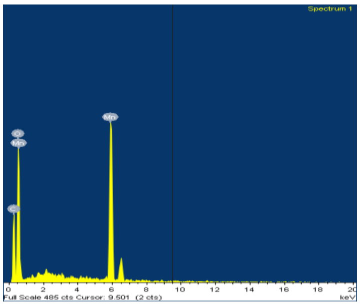

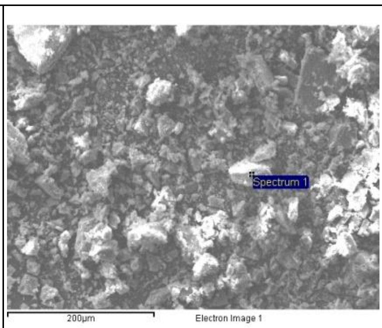

Alumina

Element	Weight %	Atomic%
O K	11.25	72.08
Al K	7.35	27.92
Totals	18.59	

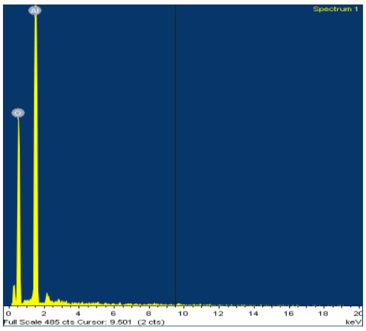

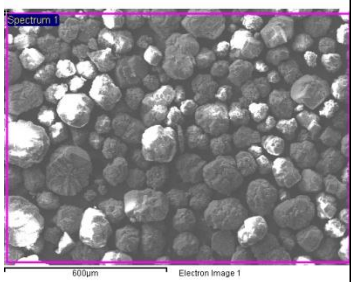

Silica

Element	Weight%	Atomic%
O K	22.91	65.83
Si K	20.88	34.17
Totals	43.79	

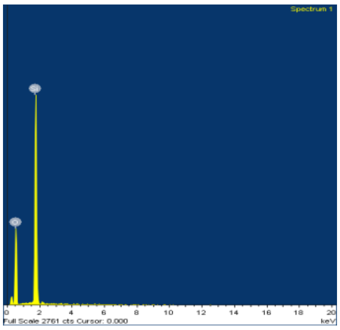

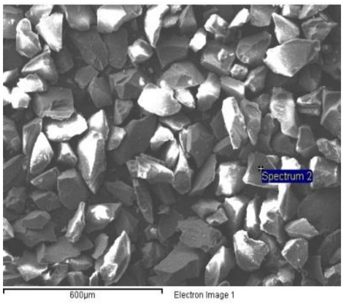

Silica-supported MnO_2

Element	Weight%	Atomic%
O K	25.81	66.18
Si K	22.59	33.00
Mn K	1.09	0.81
Totals	49.48	

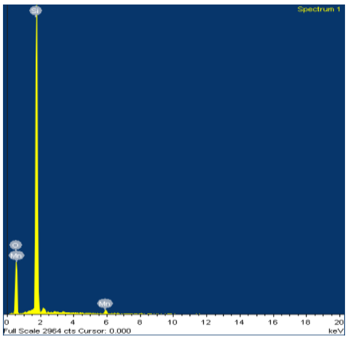

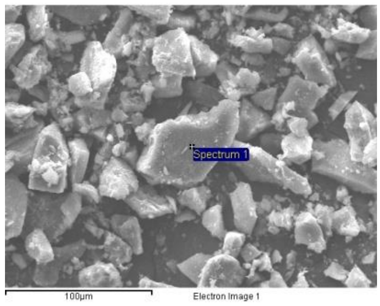

Alumina-supported MnO_2

Element	Weight%	Atomic%
O K	26.73	73.42
Al K	15.65	25.48
Mn K	1.37	1.09
Totals	43.74	

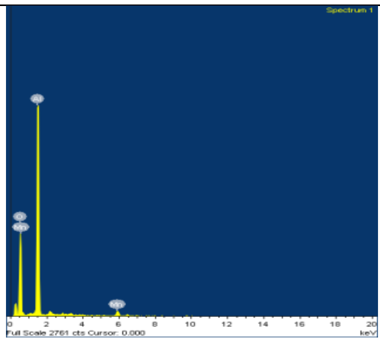

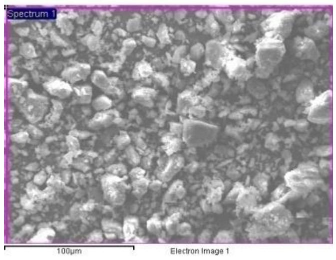

Alumina-silica-supported MnO_2

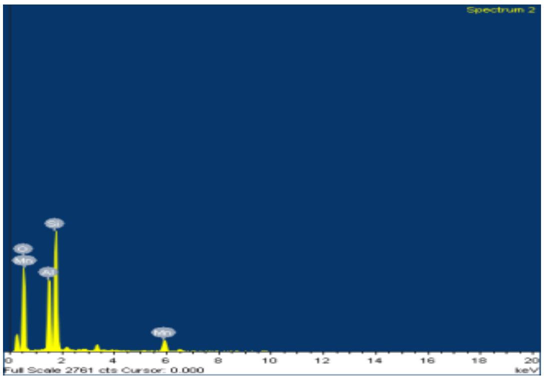

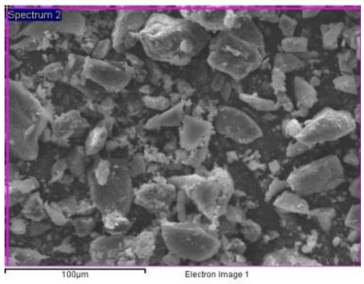

Element	Weight%	Atomic%
O K	25.38	74.39
Al K	4.77	8.30
Si K	8.90	14.86
Mn K	2.87	2.45
Totals	41.92	

Figure 3.7. EDX images, quantitative analytical data and SEM images of catalysts

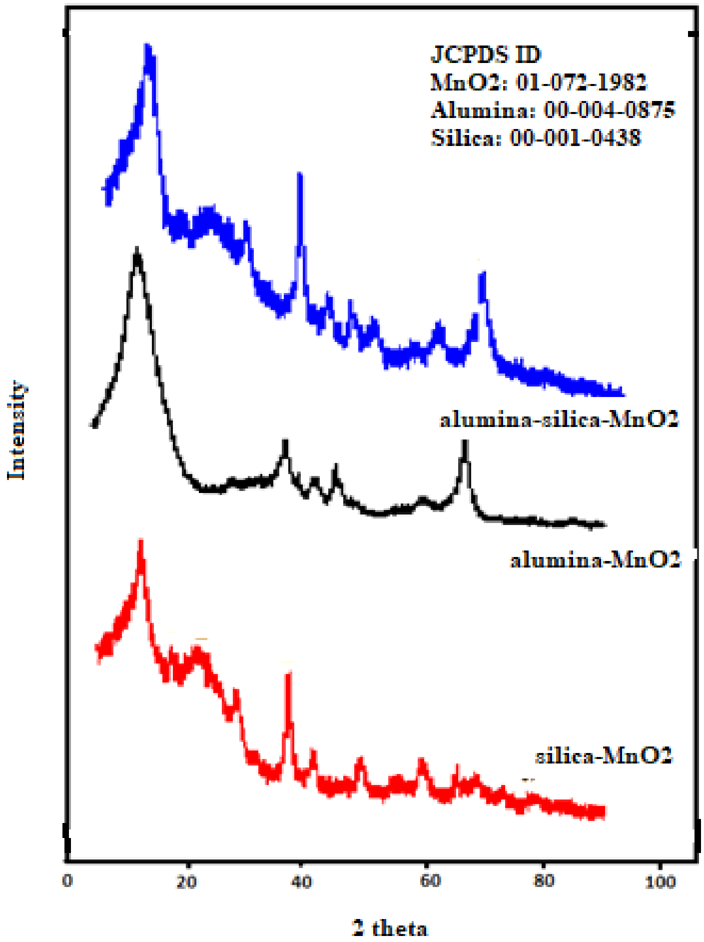

Figure 3.8. XRD results for silica-MnO_2, alumina-MnO_2 and silica-alumina-MnO_2 catalysts

3.2.2 Synthesis of 5-amino-1,3-diphenyl-1H-pyrazole-4-carbonitriles (4)

The use of water as solvents for organic synthesis in order to achieve environmentally friendly methods is in accordance with the principles of green chemistry (Li and Chan 1997; Li, 2005; Mamgain et al., 2009). Our objective was to develop a synthetic method for the synthesis of 5-amino-1,3-diphenyl-1H-pyrazole-4-carbonitriles (**4**) in water at room temperature. A reaction was tried with reactants aldehyde (**1**), malononitrile (**2**), and catalyst (150 mg), all were taken in distilled water (10 mL) into a round-bottomed flask. To the reaction mixture, sodium dodecylbenzene sulphonate (SDBS, 150 mg) was added and stirred at room temperature for 20 min till a white precipitate was obtained. At this point, phenylhydrazine (**3**) (Scheme 2.1, Chapter 2) in water using manganese acetate tetrahydrate, a random selection of metal salt. Even after stirring for 24 hours, we did not get any product (Table 3.6, entry 1). The reaction was repeated in silica gel and alumina with similar outcome. We changed the catalyst and prepared silica-supported MnO_2, alumina-supported MnO_2 and alumina-silica-supported MnO_2 (Zhong, 2016). In a typical case, the product **4a** formation showed the order silica-supported MnO_2 < alumina-supported MnO_2 < alumina-silica-supported MnO_2, though the yield was less than 30% (Table 3.6). We concluded solubility as the major issue. The literature shows the use of surfactant combined catalysts can cater some of these problems (Manabe et al., 2000; Sahu et al., 2014). Hence, we tried the reaction in sodium dodecyl benzenesulfonate (SDBS) in combination with catalysts that gave better results (Table 3.6, entries 8-10). However, the reaction was also tried in SDBS only without the use of metal oxide to ascertain its role. The reaction did not produce any result in 10 minutes as shown by the TLC profile where reactants spots appeared unchanged. On prolonging this reaction for 40 minutes, formation of 10% **4a** was observed.

Table 3.6. Catalyst optimization for the synthesis of 5-amino-1,3-diphenyl-1H-pyrazole-4-carbonitrile (**4a**)

S. No.	Catalyst[#]	Isolated yields (%)	S. No.	Catalyst[#]	Isolated yields (%)
1	$Mn(CH_3COO)_2.4H_2O$	0	6	Alumina-silica-MnO_2	30
2	Alumina (neutral)	0-5	7	SDBS	0
3	Silica gel (100-200 mesh)	0-5	8	Alumina-MnO_2/ SDBS	50
4	Alumina-MnO_2	25	9	Silica-MnO_2/SDBS	40
5	Silica-MnO_2	20	10	Alumina-silica-MnO_2/SDBS	91

[#]reactants 1 mmol; solvent (water) 10 mL; time 10 min; room temperature (35^{o}C); catalyst (1:1, w/w, 500 mg each)

Then, we optimized the reaction conditions for the product **4a** with respect to yield by varying the amount of surfactant and catalyst (Figure 3.9). Since, the catalyst alumina-silica-supported MnO_2 gave better results and so chosen as suitable catalyst for this reaction. The amount of SDBS and catalyst was optimized by changing their amount from 25 to 250 mg of each (Figure 3.9). The reaction that used 150 mg of SDBS and catalyst each gave maximum isolated yield of 91% at room temperature in water.

A broad range of structurally diverse aromatic aldehydes including electron-releasing substituents and electron-withdrawing substituents were used to check the prosperity in the reaction, and gave the corresponding products in high yields in short reaction time without the formation of any major by-products (Table 3.7). The formation of pyrazoles **4** were established on the basis of melting points, FTIR, and ^{1}H NMR and their comparison with the literature (Figures 10-13) (Experimental section, Chapter 2).

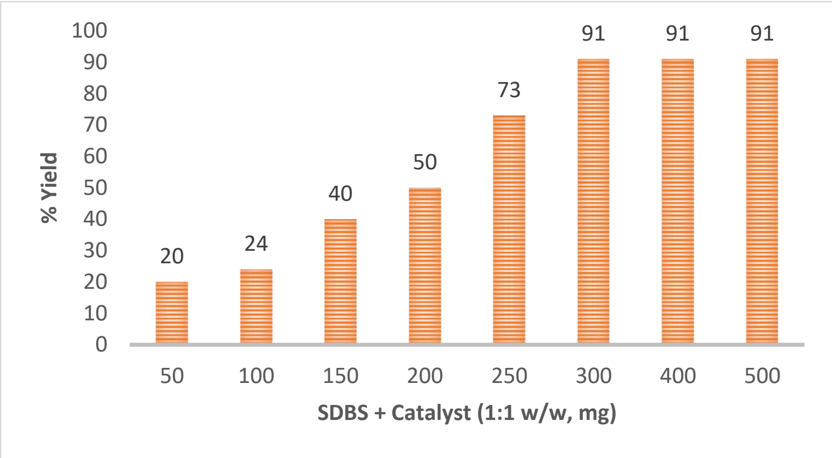

Figure 3.9. Yield optimization with product **4a**, 3 minutes after phenyl hydrazine (**3**) addition

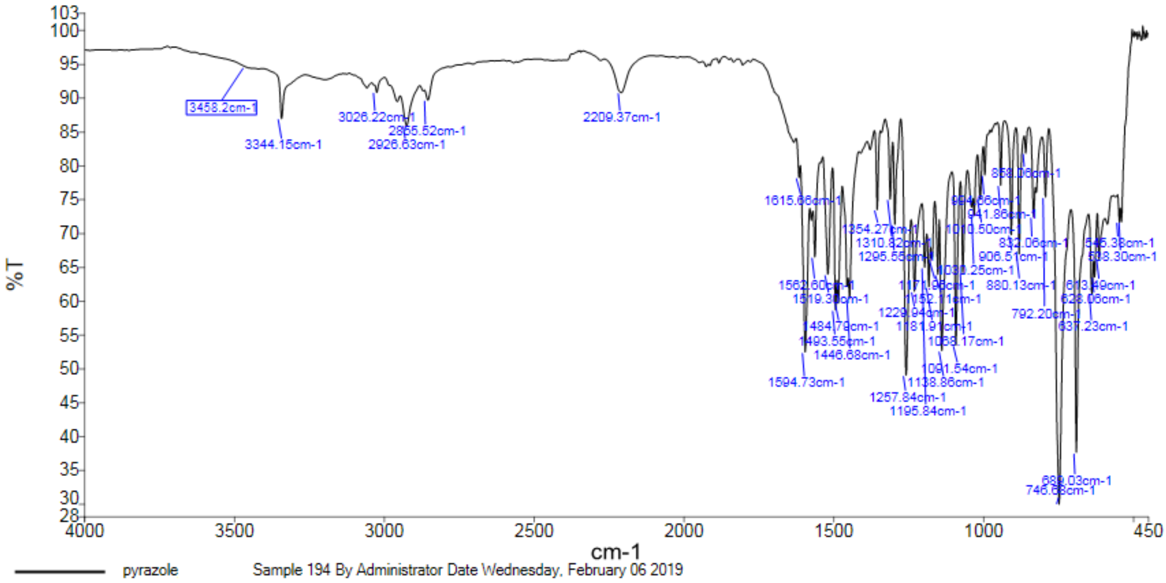

Figure 3.10. FTIR spectrum of 5-amino-1,3-diphenyl-1H-pyrazole-4-carbonitrile (**4a**)

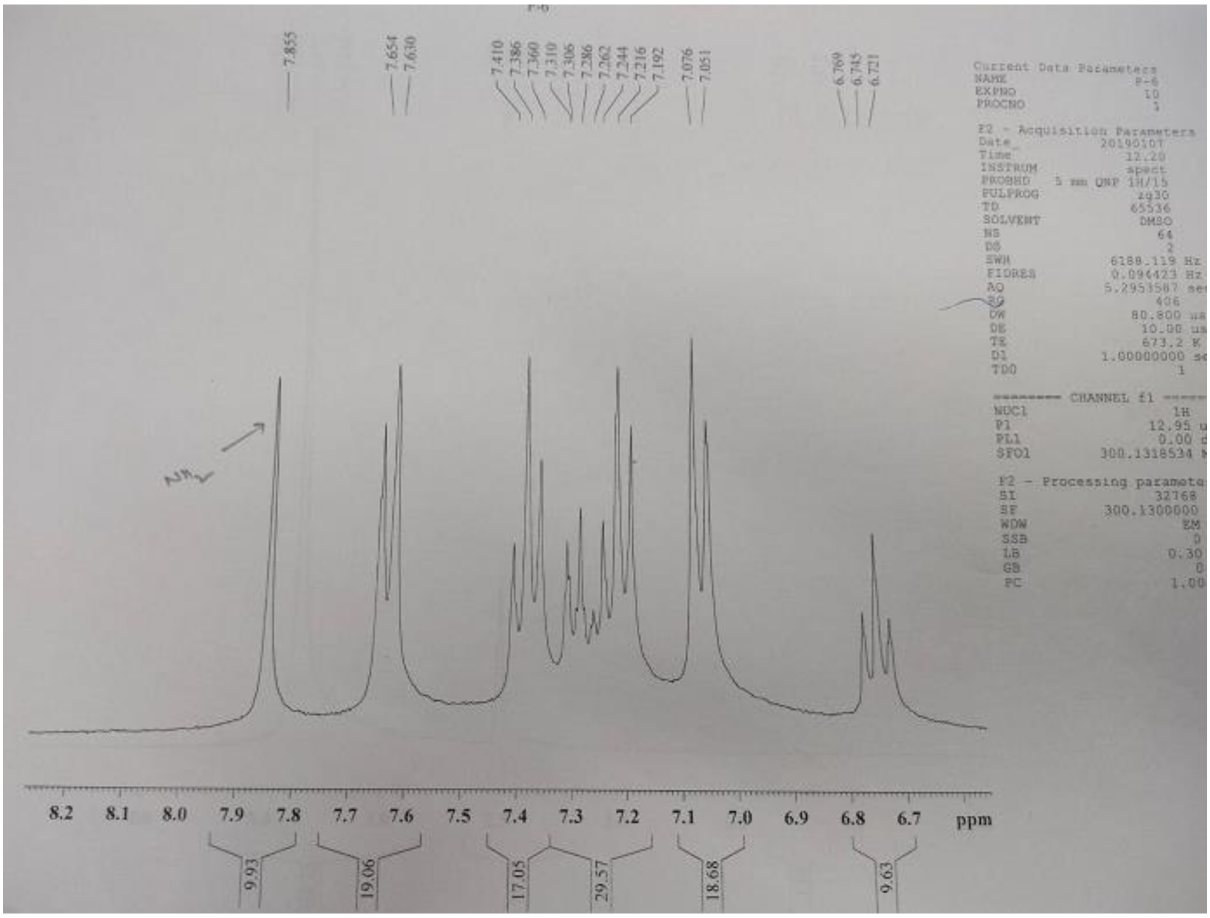

Figure 3.11. ¹H NMR spectrum of 5-amino-1,3-diphenyl-1H-pyrazole-4-carbonitrile (**4a**)

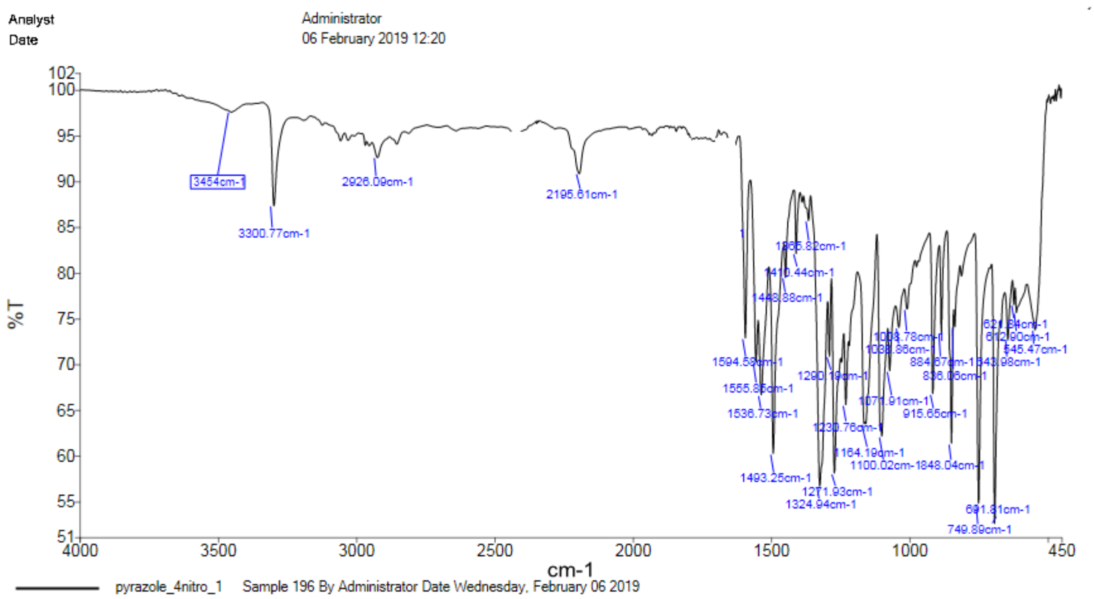

Figure 3.12. FTIR spectrum of 5-amino-3-(4-nitrophenyl)-1-phenyl-1H-pyrazole-4-carbonitrile (**4b**)

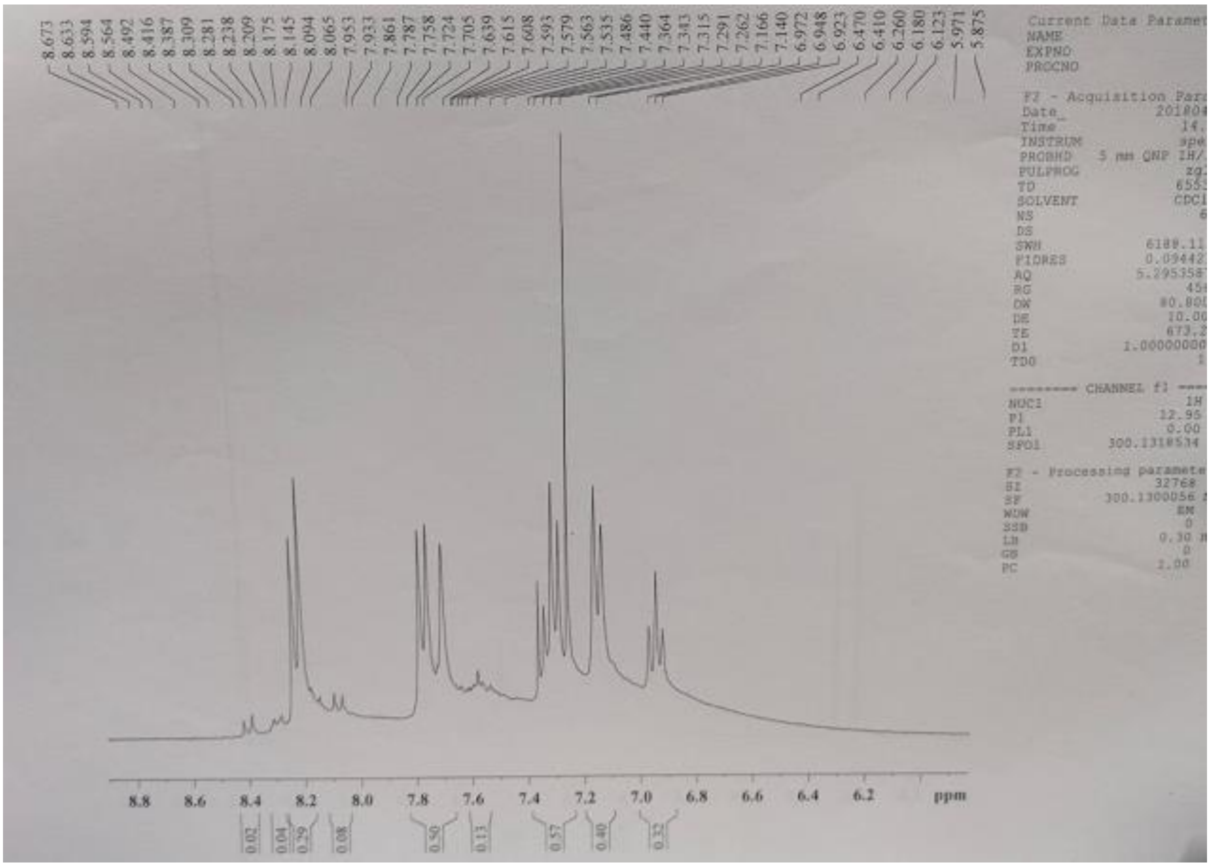

Figure 3.13. ^{1}H NMR spectrum of 5-amino-3-(4-nitrophenyl)-1-phenyl-1H-pyrazole-4-carbonitrile (**4b**)

As per our results and reported literatures (Srivastava et al., 2014; Bamdad and Kiyani, 2017; Badhe et al., 2018; Kiyani and Bamdad, 2018), the product formation takes place through Knoevenagel condensation and Michael addition followed by uncommon hydride transfer and releasing molecular hydrogen (H_2) (Srivastava et al., 2014). A possible reaction mechanism is given in Figure 3.14. The Knoevenagel condensation takes place between the substituted benzaldehyde (**1**) and malononitrile (**2**) which seems to be facilitated through a six-membered ring formation (**303**) using MnO_2. The Michael addition takes place between the Knoevenagel product (**305**) and phenyl hydrazine (**3**). The Michael addition product (**306**) undergoes intermolecular cyclization, and air oxidation to give the final products (**4**). For the prepared heterogeneous solid catalyst, recycling status was also evaluated taking the reactants **1a**, **2** and **3** for the synthesis of **4a** under optimized conditions. The catalyst was recovered by simple filtration and the obtained solid was washed with water (2 × 20 mL). The recovered catalyst was dried for 5 h under vacuum at 70 °C. The performance of the recycled catalyst in reaction up to five successive runs is given in Figure 3.15.

Table 3.7. Synthesized 5-amino-1,3-diphenyl-1H-pyrazole-4-carbonitriles **(4)**

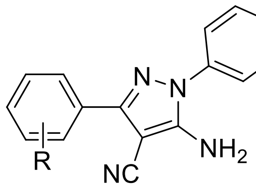

4

Comp. No.	Structure of **4** R =	Time (min)#	Isolated yields (%)
4a	H	3	91
4b	4-NO_2	5	94
4c	2-NO_2	7	90
4d	2-Br	7	86
4e	2-F	7	88
4f	4-F	6	93
4g	4-Br	7	95
4h	4-Cl	6	95
4i	2-Cl	8	90
4j	4-CH_3	10	96
4k	4-OCH_3	6	96
4l	2-OCH_3	12	90
4m	3,4-OCH_3	10	94
4n	3-NO_2	11	93

#time after phenyl hydrazine addition; melting points and literature melting points are given in Experimental section (2.3.2) Chapter 2.

3.3 Synthesis of thiazole derivatives

Thiazole is a five-membered heterocyclic molecule with the chemical formula C_3H_3NS. In 1887, Hantzsch and Waber were the first to describe this biologically active compound (Hantzsch and Weber, 1887). This molecule possesses both an electron accepting (C=N) and an electron donating groups (-S-). The thiazole ring can be found in a variety of natural and synthetic chemicals that have a wide range of biological applications, including antileishmanial (Rios Martinez and Durant-Archibold, 2018), anticonvulsant (Siddiqui and Ahsan, 2011), antiviral (Ghaemmaghami et al., 2010), anti-inflammatory (Giri et al., 2009), anticancer

(Dobbelstein and Moll, 2014), antidiabetic (Chhabria et al., 2016), antimicrobial (Arora et al., 2015), and antihypertensive (Gallardo-Godoy et al., 2011).

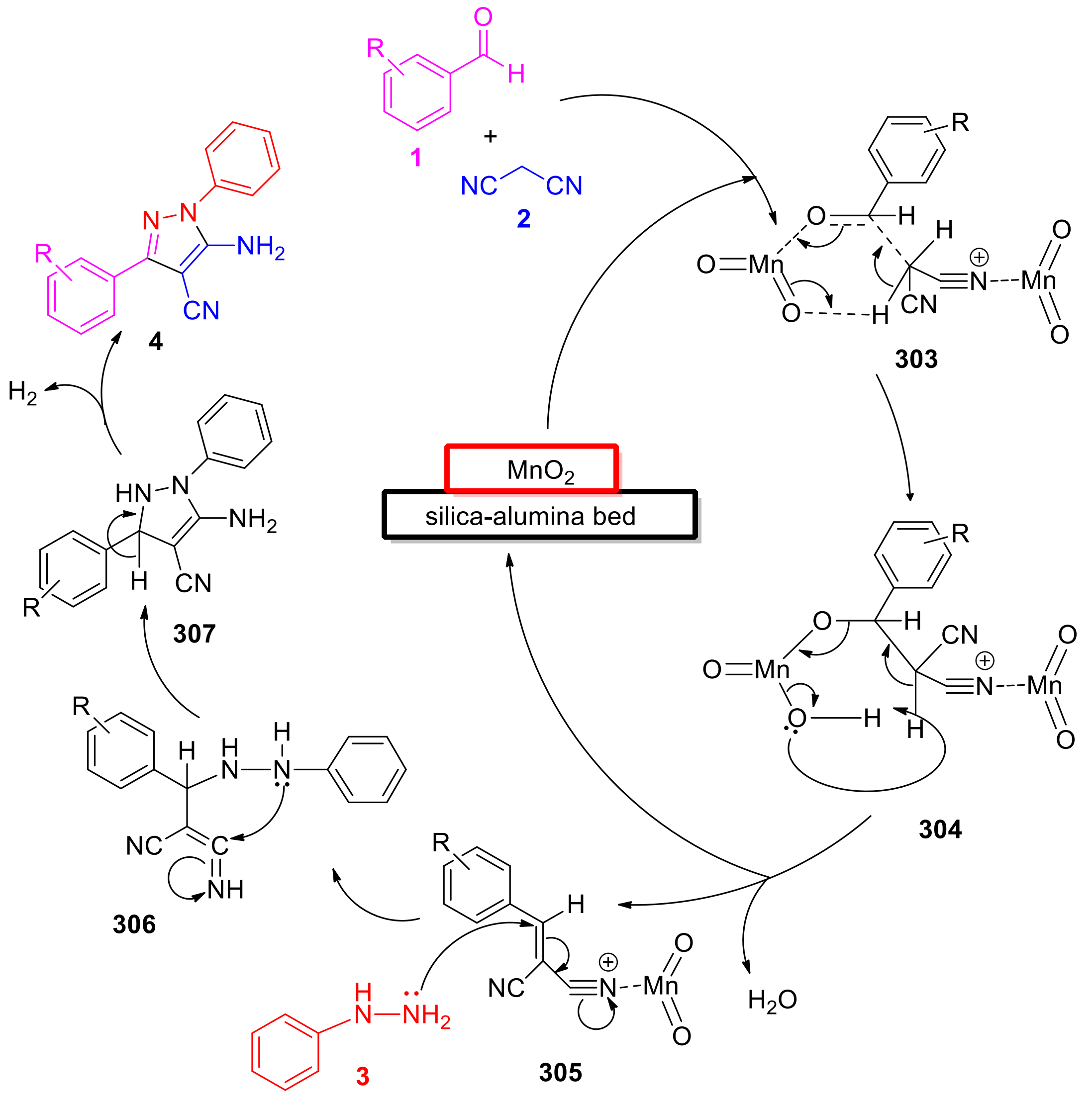

Figure 3.14. A proposed reaction mechanism for the synthesis of pyrazole derivatives (**4**)

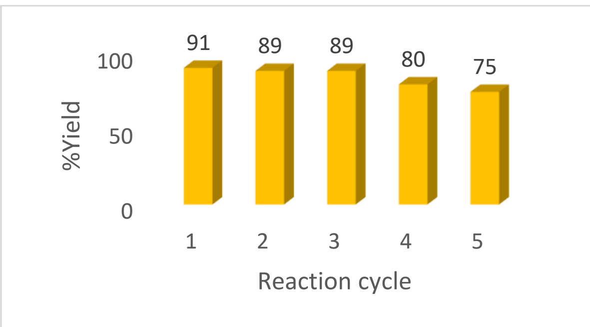

Figure 3.15. Recyclability of the alumina-silica-supported MnO_2 for the product **4a**

The thiazole molecule in vitamin B1 (thiamine) helps neurological system by assisting in the creation of acetylcholine (Hantzsch and Weber, 1887). The medicines bacitracin and penicillin (Bhargava et al., 1983) both have a thiazole motif in their structure. Synthetic drugs belonging to the thiazole family consist of acinitrazole and sulfathiazole antimicrobial agents (Borisenko et al., 2006), pramipexole an antidepressant (Maj et al., 1997), bleomycin and tiazofurin are antineoplastic agents (Milne, 2000), ritonavir - an anti-HIV drug (Souza and Almeida, 2003), cinalukast is antiasthmatic drug (Britschgi et al., 2003), and nizatidine is an antiulcer agent (Evans et al., 1984). The thiazole derivatives have also been successfully used as potential neuroprotective agents (Storch et al., 2000). Tetrahydrobenzothiazole (Harnett et al., 2004), phenolic thiazole (Greig et al., 2004), and benzothiazole (Avila, 2012) are well known for their neuroprotective nature. Benzothiazole derivative is a potent adenosine receptor ($A_{2A}R$) antagonist and is used for the treatment of Parkinson's disease.

Due to the wide utility in medicinal and other fields, different groups designed synthesis of the thiazole moiety possessing $-NH_2$ group at 2-position (Dawane et al., 2009). Many methods for the synthesis of 2-aminothiazole and its derivatives have been published (Mishra et al., 2015). The first and most widely used approach is Hantzsch's synthesis, which involves reacting α-halo carbonyl compounds with thioureas or thioamides in the presence of bromine/iodine (Hantzsch and Weber, 1887), silica chloride (Kesicki et al., 2016), 1,3-di-N-butylimidazolium tetrafluoroborate (Potewar et al., 2007), ammonium 12-molybdophosphate (Das et al., 2006), and cyclodextrin (Elsadek et al., 2021), aqueous $NaICl_2$ (Godse and Telvekar 2015), or combining carbonyl compounds and thiourea (Figure 3.16). Kidwai et al. reported the microwave-assisted preparation of 2-aminothiazoles using substituted thiourea and halo carbonyl compounds (Kidwai et al., 2000). In the present work, quantum dots (QDs) have been used for the synthesis of 2-aminothiazole derivatives in aqueous medium as a catalyst.

MoS_2 is a very popular two-dimensional metal dichalcogenide, which happen to exhibit splendid electronic and optical properties. The MoS_2 QDs possesses the distinct optical properties than its bulk counterparts because of the domination of the quantum confinement and edge effects. The MoS_2 QDs exhibits magnificent blue fluorescence under the influence of near-ultraviolet (UV) region, attributing the K point transitions in the Brillouin zone (Sharma and Mehata, 2020a; Sharma and Mehata, 2020b). The fluorescence properties of the MoS_2 QDs had been exploited to pursue different applications like, cell imaging, chemo-sensing, bio-sensing, QLEDs, etc. (Wang and Ni 2014; Ou et al., 2014; Xu et al., 2015 Dong et al., 2016; Bogale et al., 2016).

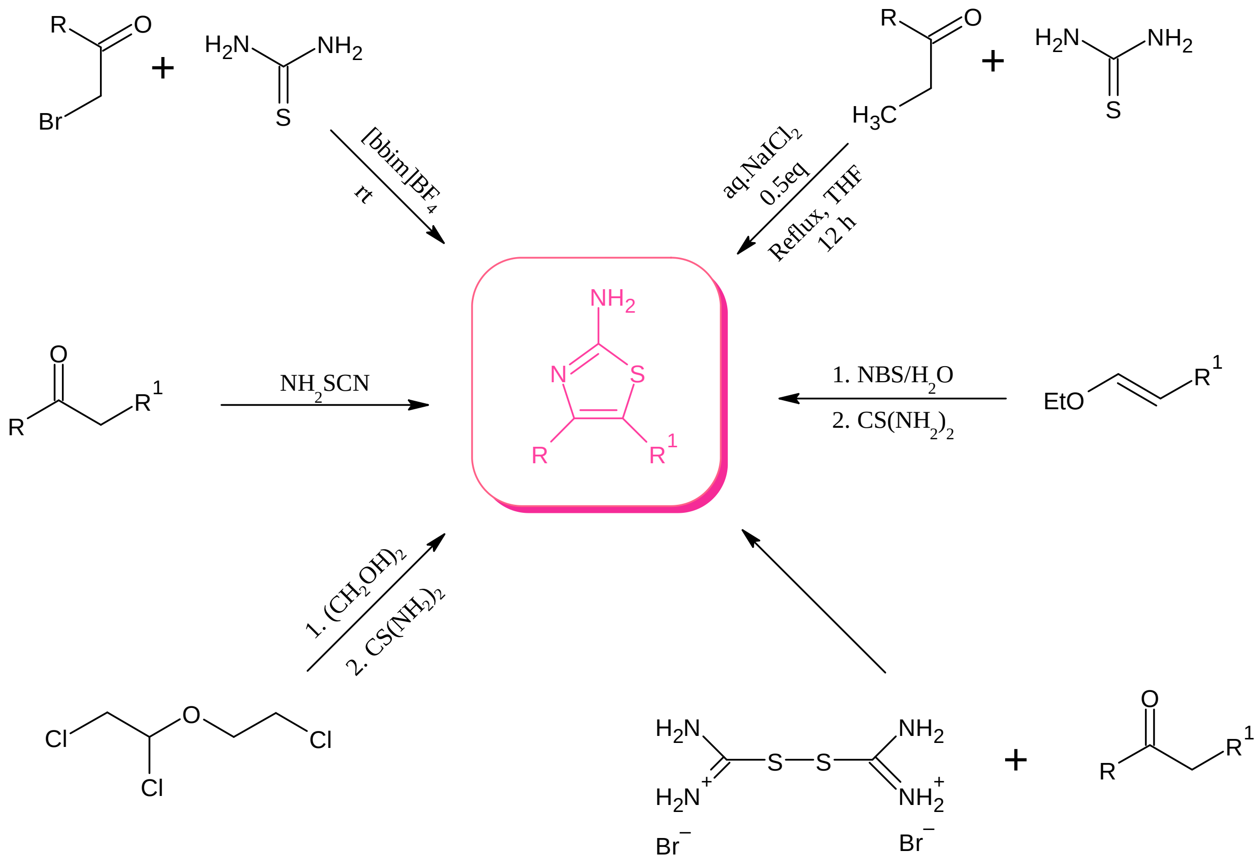

Figure 3.16. Some synthetic routes for 2-aminothiazole derivatives

Here, the bottom-up approach has been applied to synthesize water soluble MoS_2 QDs through facile hydrothermal technique. The blue fluorescent QDs holds high quantum yield (QY) of about 17%, which is very high when compared to other water-soluble quantum dots. The use of MoS_2 QDs in the reaction of thiazole and its derivatives have increased the reaction rate by approximately 30 times.

3.3.1 Synthesis of MoS_2 quantum dots

The MoS_2 QDs were prepared through a hydrothermal route from sodium molybdate and thioacetamide under inert environment (Figure 3.17). Further, 1,4-diamino butane (DAB) was added, stirred for 10 min and transferred to the Teflon lined hydrothermal reactor at 200 ^{o}C for 24 h. The mixture was allowed to cool to the room temperature and then, the surfactant was purified through dialysis process for 48 h. The cellulose membrane of 1 kda was used to eliminate impurities and unreacted reagents. The DI water used for dialysis was changed after every 2 h. The final product obtained is the pale-yellow colloidal solution which exhibit bright blue fluorescence under UV illumination. The purified QDs were then kept at 4 °C until further characterizations.

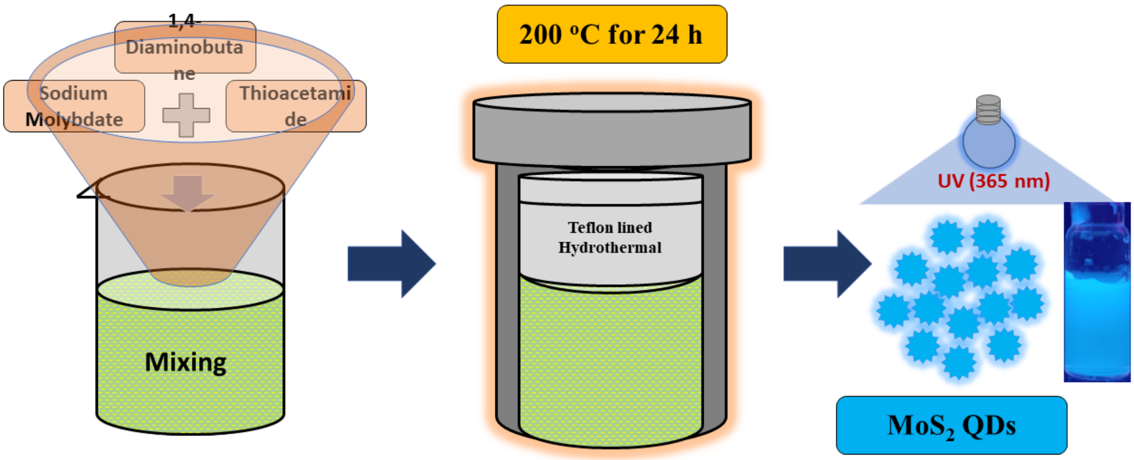

Figure 3.17. Schematic synthesis of functionalized MoS_2 QDs by facile hydrothermal process

The Figures **3.18a-c** demonstrates the high-resolution images of the MoS_2 QDs through HR-TEM. Figure **3.18a** exhibits the occurrence of nano-sphere like formation or usually known as dots like structure. The heterogeneous particle size distribution ranging from 1-4 nm had been recorded in the Figure **3.18b**. The corresponding histogram of the particle size distribution of the QDs describes the average particle size to be ~3 nm (Figure **3.18c**). The UV-visible absorption spectroscopy is a well-recognized diagnostic tool to record the electronic structure of the materials. The absorption spectrum of the MoS_2 QDs was recorded and observed a small hump at 300 nm of wavelength, which is related to the excitonic behaviour of the MoS_2QDs.

3.3.2 Synthesis of 2-aminophenylthiazole derivatives (7)

The synthesis of 2-aminophenylthiazole derivatives have been performed with phenacyl bromide (**5**) and thiourea (**6**) in water dispersed MoS_2 QDs (Scheme 2.2, Chapter 2). The reaction mixture was performed at room temperature. The progress of reaction mixture was monitored by TLC. After completion of reaction, the solid products were filtered and washed with water. The crude products were further recrystallized by using ethanol to get the pure compounds. The performance of the recycled catalyst in reaction up to four successive runs is given in Figure 3.19. The formation of the products **7** gave been confirmed by melting point, IR, and ^{1}H NMR and their comparison with the literature (Experimental section, Section 2.4.2, Chapter 2). In the 1H NMR of 4-phenyl-1,3-thiazol-2-amine (**7a**), the peak at 6.75 ppm has been assigned to the H-thiazole and at 5.12 ppm due to the NH_2 protons. The others peaks have been obtained in the aromatic region (Figure 3.20).

3.4 Synthesis of benzimidazole derivative (9,10)

Due to the versatile applications of benzimidazole molecules, notable efforts have been made by different groups to design efficient methods for synthesis. The benzimidazole ring system is fairly widespread among heterocyclic pharmacophores. Because of their widespread occurrence in bioactive chemicals, these substructures are sometimes referred to as "privileged" (Alaqeel, 2017). The therapeutic potential of benzimidazole nucleus has been recognized since Woolley postulated in 1944 that benzimidazole may operate similarly to purines, activating a variety of biological responses (Woolley, 1944).

Table 3.8 List of 2-aminophenylthiazole derivatives (**7**) synthesized

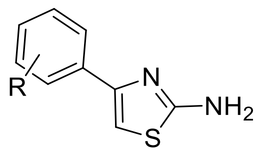

7

Comp. No.	R	Reaction Time (min)	Yield (%)
7a	H	5	92
7b	4-F	12	94
7c	4-Cl	10	95
7d	4-Br	9	95
7e	4-CH_3	5	90
7f	4-OCH_3	4	94
7g	4-NO_2	8	96
7h	4-CN	10	89
7i	3-Br	8	90
7j	3-NO_2	8	91
7k	3-OCH_3	8	94

7l	3,4-dichloro	12	96

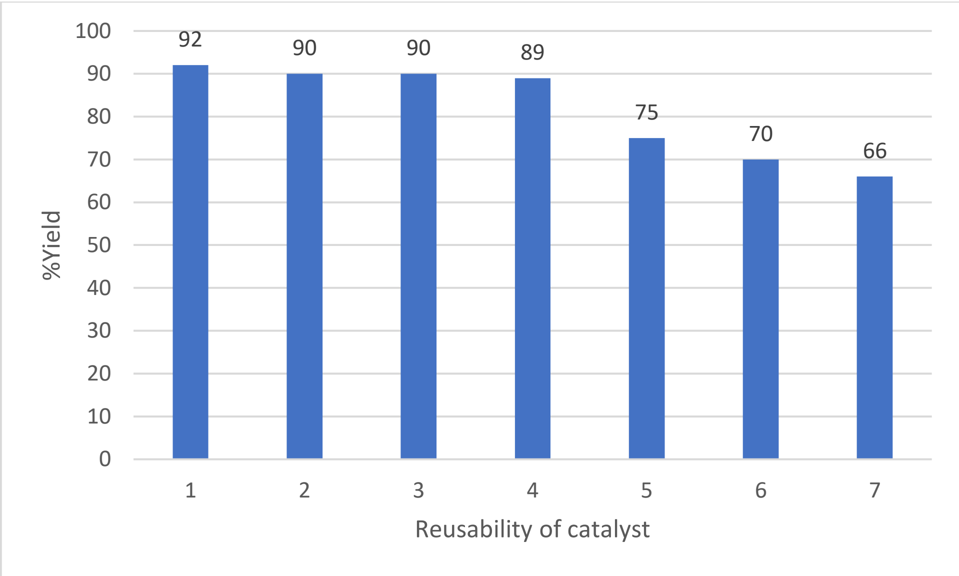

Figure 3.19. Reusability of catalyst MoS_2 QDs for **7a**

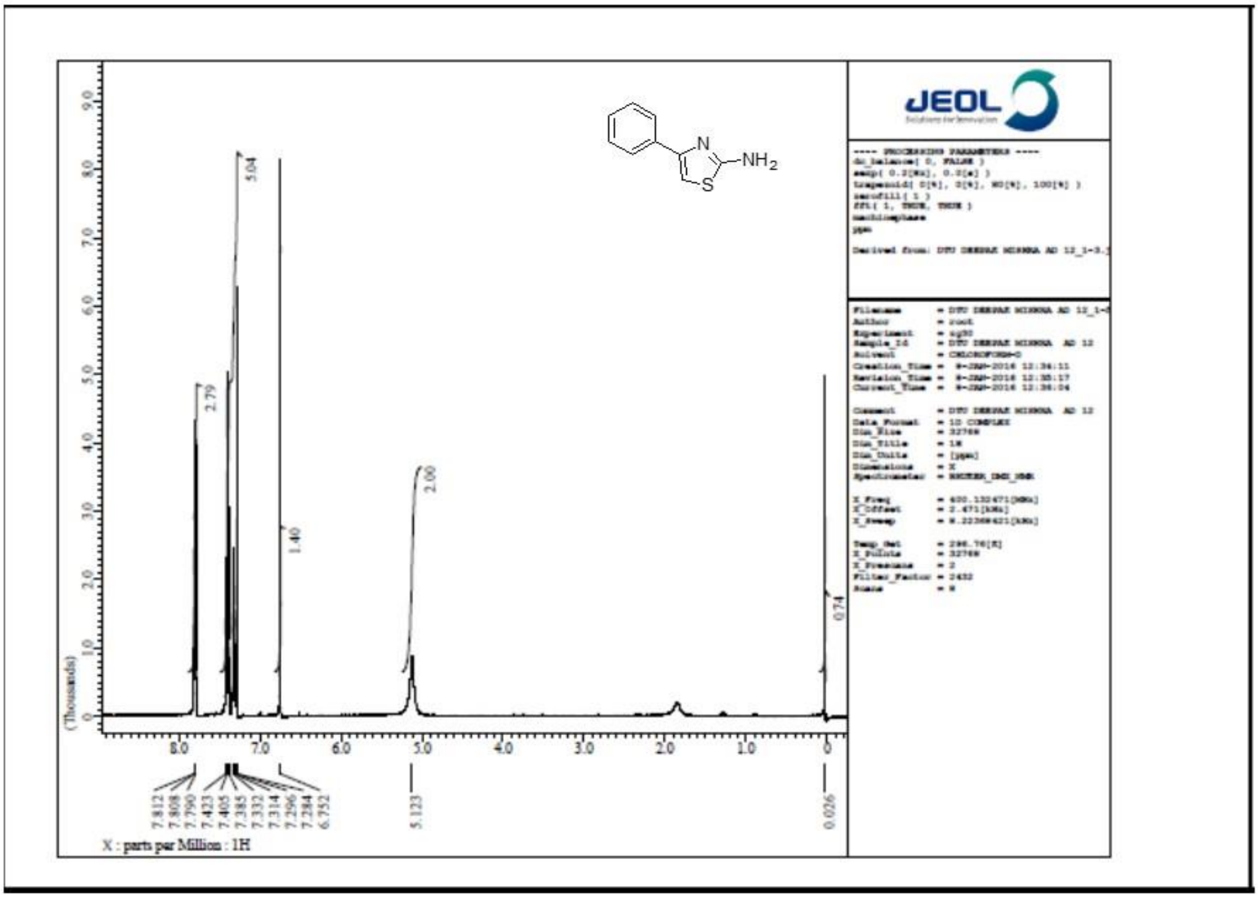

Figure 3.20. ^{1}H NMR spectrum of 4-phenyl-1,3-thiazol-2-amine (**7a**)

Sometime later, Brink discovered that 5,6-dimethylbenzimidazole is a breakdown product of vitamin B12 and that some of its derivatives showed actions that were comparable to those of vitamin B12 (Brink and Folkers 1949; Emerson et al., 1950). When the groups on the core structure of benzimidazole are altered, a broad variety of biological actions are displayed by benzimidazole-based medications (Figure 3.21). The synthesis of benzimidazole has been achieved as given in Schemes 2.3 and 2.4. Benzene-1,2-diamine (**8**) and 4-nitrobenzaldehyde (**1b**) was thoroughly ground with a pestle in a mortar at room temperature until the overall mixture turned into a melt. The melt was then heated at 140 ^{o}C for 2 h. The progress of reaction was monitored by TLC. After completion, the compound was extracted with ethyl acetate and was purified by column chromatography to get compound **9**. The reduction of nitro group was done with H_2/Pd/Charcoal. The compounds **9** and **10** have been characterized with FTIR and H NMR spectroscopy (Experimental section, Sections 2.5 & 2.6; Chapter 2).

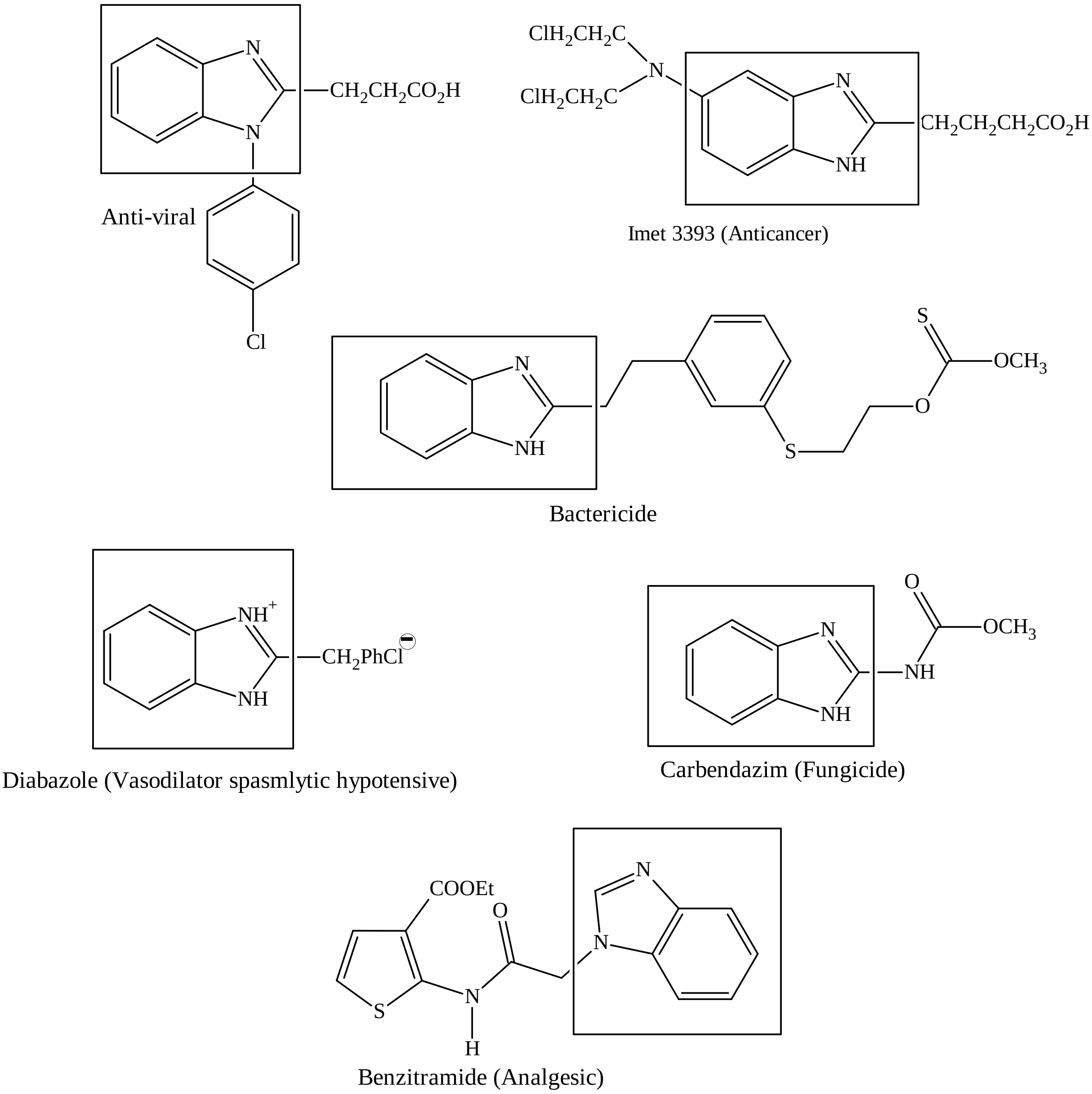

Figure 3.21. Some important drugs having benzimidazole core

3.5 Synthesis of thiazole-pyrazole amide conjugate (11)

The synthesis of amide conjugates was done using two methods. This was done to improve the yield of the product formation. The selected thiazole-pyrazole amide conjugate, N^1-(4-cyano-3-(3,4-dimethoxyphenyl)-1-phenyl-1H-pyrazol-5-yl)-N^4-(4-(4-nitrophenyl) thia -zol-2-yl)succinimide (**11**) was synthesized from 4-(4-nitrophenyl)-1,3-thiazol-2-amine (**7g**) (Scheme 2.5, Chapter 2). The four-carbon source, succinyl dichloride was diluted with DMF and was added dropwise to a solution of **7g** in DMF at room temperature during 25 min. After the addition was completed, the pyrazole **4m** was added dropwise and after addition temperature of the reaction mixture was increased to 60 °C. The content was stirred at room temperature for 24 h and then cold 2% sodium bicarbonate was added to stop the reaction. The product **11** that was separated and filtered, washed thoroughly with water, ethanol, acetone, and finally with hexane to remove the impurities. The final purification was done with column chromatography to get the compound in 36% yield. The formation of the compound was done with spectral data. The appearance of amide peak at 1685 cm^{-1} in FTIR confirmed the formation of amide bond. The absence of >C=O peak above 1700 cm^{-1} further confirmed the non-formation of corresponding acid or acid chloride. In ^1H NMR spectrum, the two methoxy groups appeared at 3.73 ppm and two methyl groups appeared in the aliphatic region 2.50-2.46 ppm. The other peaks were observed in the aromatic region confirmed the conjugate formation. This was further confirmed with ^{13}C NMR and elemental analysis (Experimental section, Chapter 2).

Since the yield of the product was very poor, so we decided to perform the reaction in step-wise manner. First, we prepared the mono derivative having -COOH functional group and amide formation was done by converting -COOH to -COCl. This reaction was performed with the help of succinic anhydride (Tyurina et al., 2021). 2-Aminothiazole derivative (**7**) was dissolved in THF and succinic anhydride (**12**) was added to the reaction mixture. This was kept on stirring for 24 h. The progress of the reaction was monitored by TLC in the solvent system CH_3OH- CH_3Cl (1:9 v/v). After completion of the reaction, the solvent was removed under reduced pressure to obtain the crude products which was recrystallized to get the pure product. In FTIR spectrum, the absence of peak around 1860 and 1780 cm^{-1} confirmed the absence of anhydride and appearance of peak in the region 1670 – 1678 cm^{-1} was for the amide group (Tyurina et al., 2021). In a typical example, the ^1H NMR of 4-oxo-4-((4-phenylthiazol-2-yl)amino)butanoic acid (**13a**), the presence of peak at 12.18 ppm for one proton which disappeared after D_2O exchange confirmed the acid functional group (-COOH) in the molecule. Similarly, the other prepared compounds **13b** & **13c** were characterized (Experimental section, Chapter 2).

3.6 Synthesis of thiazole/pyrazole and benzimidazole amide conjugates

The compound **13a** was further reacted with thionyl chloride to transform the functional group acid (-COOH) to acid chlo ride (-COCl) (4-oxo-4-((4-phenylthiazol-2-yl)amino)butanoyl chloride (**14**). The compound was not separated and further reacted with the

4-(1H-benzo[d]imidazol-2-yl)aniline (**10**) to give the thiazole-benzimidazole amide conjugate, N^1-(4-(1H-benzo[d]imidazol-2-yl)phenyl)-N^4-(4-phenylthiazol-2-yl)succinimide (**15**) in 38% yield. During the process of reaction, thionyl chloride was (**13a**) and the resulting suspension was refluxed for 3 h to give a clear light-yellow solution. The excess of thionyl chloride was removed *in vacuo.* The obtained acid chloride without further characterisation was mixed with dry DMF and cooled to 0 – 4 ^oC. A solution of **10** and triethylamine in dry DMF was added. The resulting mixture was stirred at room temperature for 12 h. The solvent was removed with rotatory evaporator. The solid obtained was washed with aqueous ammonium chloride solution and water, then dried to get the amide conjugates which was recrystallised with ethanol to get the pure compound **15**. Similarly, compound **11** was also prepared and compared with the earlier method. The compound **15** was characterized with spectral data (Experimental section, Chapter 2). The presence of peaks at 3331 and 3259 cm^{-1} in the FTIR accounted for the two amide -NH groups present in the molecule. The peals at 1676, 1672 cm^{-1} was assigned to the carbonyl group of amide linkage. In the ^1H NMR spectrum, the appearance of peaks in the regions 7.84-7.19 ppm was assigned to the aromatic protons. The peaks in the aliphatic region between 2.60-2.55 ppm were accounted for the -CH_2CH_2- group.

3.7 Synthesis of thiazole-thiazole and thiazole-pyrazole amine conjugates

The synthesis of amine conjugates was based on the simple chemistry where amines react with alkyl halides via substitution reactions. This has been observed that in these types of reactions, the products are mixture of amines and hence the yields have been usually poor for a particular compound. The reaction of 4-aryl-1,3-thiazol-2-amine (**7**) with 1,4-diiodobutane (**16**) was carried out in dry DMF in the presence of fused K_2CO_3 (Scheme 2.8, Chapter 2) The reaction was stirred at 80 ^oC for 20 min. After that, halo compound **16** was added dropwise to the reaction mixture and the temperature was raised to 105 ^oC. The heating was continued for 15 h. The progress of the reaction was monitored by TLC (hexane: ethyl acetate 7:3, v/v). After the reaction, the solvent was removed under reduced pressure. The crude product was further purified by column chromatography due to the presence of mixture of amine products. We were able to isolate the mono products, N-(4-iodobutyl)-4-arylthiazol-2-amine (17) in 40-42% yield and the bis-products, N^1,N^4-bis(4-arylthiazol-2-yl)butane-1,4-diamine (**18**) in 38-41% poor yields. The obtained products were characterized with the help of spectroscopic data (Experimental section, Chapter 2).

The characterization of N-(4-iodobutyl)-4-phenylthiazol-2-amine (**17a**) was done with FTIR, ^{1}H NMR, and mass spectra. The change in FTIR spectral profile from primary amine to secondary amine where only a single weak band at 3305 cm^{-1} was obtained, confirmed the alkylation of anime group. All the five aromatic hydrogens appeared in the region 7.79-7.22 ppm. The thiazole proton appeared at 7.05 ppm. The other eight protons obtained in the aliphatic region between 3.35-1.50 ppm. The molecular ion peak at 358 confirmed the formation of mono derivative. The spectral data for other two compounds **17b** and **17c** showed the similar pattern (Experimental section, Chapter 2).

The characterization of the bis product, N^{1},N^{4}-bis(4-phenylthiazol-2-yl)butane-1,4-diamine (**18a**) was done with FTIR, ^{1}H NMR, mass spectra, and elemental analysis. The presence of weak bands at 3305 and 3255 cm^{-1} were assigned to the -NH group of amine bonds. In the ^{1}H NMR spectrum, the appearance of peaks in the aromatic regions between 8.03 and 7.41 ppm for ten protons confirmed the amine conjugate formation. The two thiazole peaks at 7.28 and 6.86 ppm convey that the two protons are not chemically equivalent. The molecular ion pean in mass spectra at 406 further confirmed the formation of compound **18a**. The other amine conjugates **18b** and **18c** were characterized with similar approach (Experimental section, Chapter 2). The 1H NMR spectrum of compounds 18b and 18c are given in Figures 3.22 and 3.23 respectively.

For the synthesis of thiazole-pyrazole amine conjugate, 5-((4-((4-(4-nitrophenyl)thiazol-2-yl)amino)butyl)amino)-1,3-diphenyl-1H-pyrazole-4-carbonitrile (**19**), the reaction of 5-amino-1,3-diphenyl-1H-pyrazole-4-carbonitrile (**4a**) was done with N-(4-iodobutyl)-4-(4-nitrophenyl)thiazol-2-amine (**17b**) in the presence of fused K_2CO_3. The reaction was performed in dry DMF to produce the product in 42% yield. The prepared compound was characterized with the help of FT-IR, NMR spectroscopy, mass spectrometry, and elemental analysis (Experimental section, Chapter 2).

3.8 Biological evaluation of selected synthesized compounds

3.8.1 *In-vitro* studies

The MAO-B inhibition activity of selected synthesized compounds is given in the Table 3.9. The selected compounds belong to pyrazole derivatives, thiazole derivatives, and their amide and amine conjugates (Table 3.5).

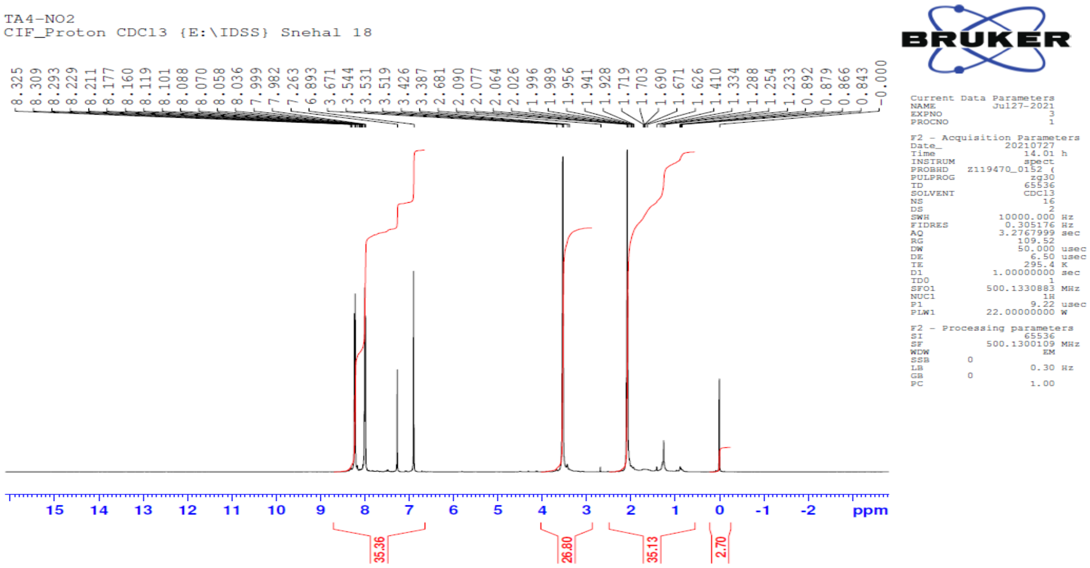

Figure 3.22. ^{1}H NMR N^{1},N^{4}-bis(4-(4-nitrophenyl)thiazol-2-yl)butane-1,4-diamine (**18b**)

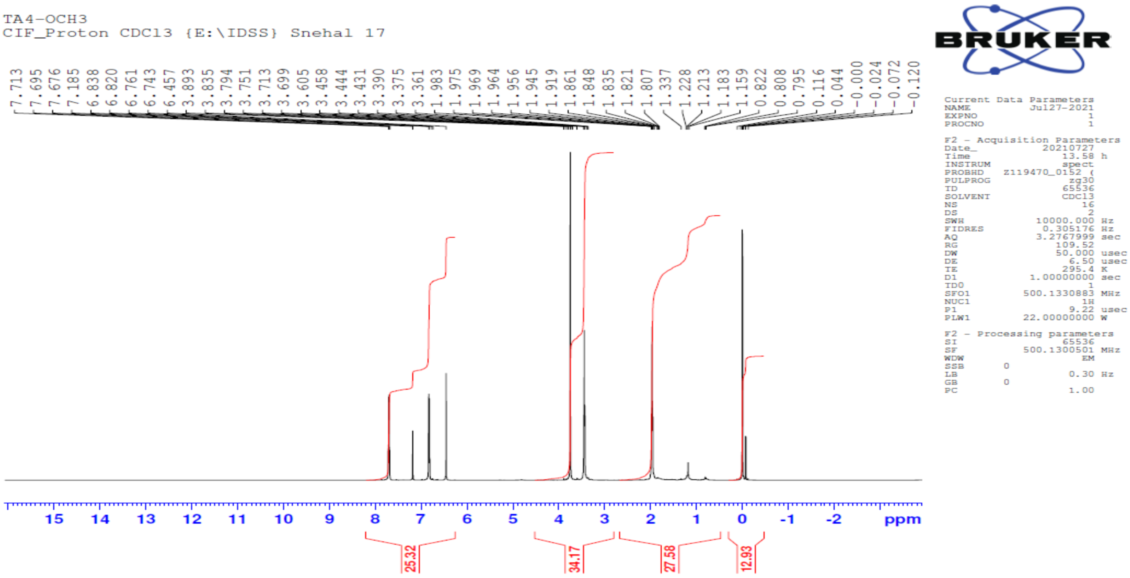

Figure 3.23. ^{1}H NMR N^{1},N^{4}-bis(4-(4-methoxyphenyl)thiazol-2-yl)butane-1,4-diamine (**18b**)

The compound N^{1}-(4-cyano-3-(3,4-dimethoxyphenyl)-1-phenyl-1H-pyrazol-5-yl)-N^{4}-(4-(4-nitrophenyl)thiazol-2-yl)succinimide (**11**) (**P11**) showed the highest activity towards MAO-B inhibition with IC_{50} value of 80.17 ± 0.75 μM followed by the compound 3-(3,4-dimethoxyphenyl)-5-((4-((4-(4-nitrophenyl)thiazol-2-yl)amino)butyl)amino)-1-phenyl-1H-pyrazole-4-carbonitrile (**19**) (**P10**) with IC_{50} value of 86.03 ± 0.26 μM (Table 3.9).

Table 3.9. *In-vitro* studies using Amplex™ Red Monoamine Oxidase Assay Kit

S. No.	**Compd. No.**		
1.	P1 (4a)		
2.	P2 (4b)		
3.	P3 (4f)		
4.	P4 (4h)		
5.	P5 (4m)		
6.	P6 (7a)		
7.	P7 (13a)		
8.	P8 (13b)		
9.	P9 (18a)		
10.	P10 (19)		
11.	P11 (11)		
12.	P12 (18b)		
13.	P13 (18c)		
14.	P14 (7g)		
15.	Safinamide		

The similarity in these two most potent compounds is the functional groups present in them along with their aromatic group which might be occupying the substrate cavity effectively. This can be seen by the π-π interactions of phenyl group of aromatic substrates of **11** with amino acid residue and hydrogen bonding of oxygen of carbonyl of amide functional group. The other hydrophobic interactions, positive charge interactions and polar interactions between the compound **11** and amino acid residues of active core of MAO-B are also responsible for the binding affinity of this compound. This has been observed with the analysis from the two active compounds **11** and **19** that the presence of functional groups to make the conjugates such as amine and amide linkages does not play important role toward activities. The individual compounds present in the conjugates like **4m** (**P5**) and 7g (**P14**) (Table 3.9, entry 5 and 14) do not show appreciable activity or in other words, their IC_{50} values are more than the conjugates. This infers that the conjugates made up of these two moieties are effective and may further be modified to bring the IC_{50} values as per with the drug safinamide (Table 3.9, entry 15). The IC_{50} values for other synthesized compounds were higher and requires further functional group transformation.

3.8.2 Antioxidant (AA) studies

In molecular biology, the development of degenerative processes is linked to the existence of an excess of free radicals, which encourages oxidative reactions that are bad for the organism. Antioxidants have the function of neutralising free radicals in biological cells, which have a detrimental effect on living things (Rodrigo and Rodrigo, 2009; Shahidi and Zhong, 2015; Munteanu and Apetrei, 2021). This has been observed that the oxidative stress has become a popular notion in medical sciences. It actively participates in the physiology of many common disorders, including AD, PD, high blood pressure, preeclampsia, atherosclerosis, and acute renal failure (Prior et al., 2005; Rodrigo and Rodrigo, 2009; Çekiç et al., 2013; Siddeeg et al., 2021).

MAO with amines leads to the production of H_2O_2 (Figure 1.5 Chapter 1), which is sometimes responsible for oxidative stress through the generation of free radicals. Due to the above facts, the synthesized compounds have also been evaluated for AA activities and results are given in Table 3.10. The results show the similarity with *in-vitro* results as both the active compounds also gave better AA. The compound **11** (**P11**) showed 83% AA whereas the compound **19** (**P10**) showed 82% AA. The other evaluated compounds showed AA between 13-79% (Table 3.10).

Table 3.10. Antioxidant activity of synthesized compounds

S.No.	Compound Synthesis	Antioxidant activity (%)
1.	N1-(4-cyano-3-(3,4-dimethoxyphenyl)-1-phenyl-1H-pyrazol-5-yl)-N4-(4-(4-nitrophenyl)thiazol-2-yl)succinamide (**11**) (**P11**)	
2.	3-(3,4-dimethoxyphenyl)-5-((4-((4-(4-nitrophenyl)thiazol-2-yl)amino)butyl)amino)-1-phenyl-1H-pyrazole-4-carbonitrile (**19**) (**P10**)	
3.	5-Amino-1,3-diphenyl-1H-pyrazole-4-carbonitrile (**4a**) (**P1**)	
4.	4-(4-Nitrophenyl)-1,3-thiazol-2-amine (**7g**) (**P14**)	
5.	4-(4-Chlorophenyl)-1,3-thiazol-2-amine (**7c**)	
6.	N^1,N^4-bis(4-(4-nitrophenyl)thiazol-2-yl)butane-1,4-diamine (**18b**)	
7.	5-Amino-3-(3,4-dimethoxyphenyl)-1-phenyl-1H-pyrazole-4-carbonitrile (**4m**) (**P5**)	
8.	4-Oxo-4-((4-phenylthiazol-2-yl)amino)butanoic acid (**13a**) (**P7**)	
9.	4-(4-Methylphenyl)-1,3-thiazol-2-amine (**7e**)	
10.	5-Amino-3-(4-chlorophenyl)-1-phenyl-1H-pyrazole-4-carbonitrile (**4h**) (**P4**)	
11.	N^1,N^4-Bis(4-phenylthiazol-2-yl)butane-1,4-diamine (**18a**) (**P9**)	
12.	4-(4-Bromophenyl)-1,3-thiazol-2-amine (**7d**)	
13.	4-(3-Methoxphenyl)-1,3-thiazol-2-amine (**7k**)	
14.	4-(4-Fluorophenyl)-1,3-thiazol-2-amine (**7b**)	
15.	4-(4-Cyanophenyl)-1,3-thiazol-2-amine (**7h**)	
16.	4-(3-Nitrophenyl)-1,3-thiazol-2-amine (**7j**)	
17.	4-Phenyl-1,3-thiazol-2-amine (**7a**) (**P6**)	
18.	4-(4-Methoxyphenyl)-1,3-thiazol-2-amine (**7f**)	

*****

CHAPTER 4

Conclusion

The present work has been carried out to design and synthesize the MAO-B inhibitors for PD and overcome some of the limitations reported in literature. The work entitled "Synthesis and Evaluation of Heterocycles as Anti-Parkinson Agents" has been divided into four chapters:

Chapter 1 covers the description of Parkinson's disease (PD) and monoamine oxidases (MAOs) and their inhibitors. The literature given in this chapter covers MAO distribution, substrate specificity and kinetics. This chapter also covers MAO-B inhibitors and examples of clinical trial or approved drugs for MAO-B inhibition.

Chapter 2 is the experimental section which explains the procedures for the synthesis of different N-containing heterocyclic molecules. The methods for the synthesis of pyrazole derivatives, thiazole derivatives, 2-(4-nitrophenyl)-1H-benzimidazole, 2-(4-aminophenyl)-1H-benzimidazole, pyrazole-thiazole conjugates through amide bond and amine bond and benzimidazole-pyrazole/thiazole conjugates through amide bond and amine bond have been given in this chapter. Method for in-silico studies, in-vitro studies, and anti-oxidant studies have also been covered in this chapter.

Chapter 3 is the results and discussion which covers detailed explanation about the design of molecules through their *in-silico* studies. The *in-silico* studies have been carried out for individual compounds and their conjugates. A total of more than 300 compounds have been docked, which included pyrazole-thiazole derivatives (amide linkage), benzimidazole-pyrazole/thiazole derivatives (amide linkage), pyrazole-thiazole derivatives (amine linkage), and benzimidazole-pyrazole/thiazole derivatives (amine linkage). To synthesize the conjugates, three N-containing heterocyclic compounds have been synthesized: pyrazole derivatives, thiazole derivatives, and benzimidazole derivatives.

A novel, facile, one-pot, multicomponent protocol for the synthesis of 5-amino-1H-pyrazole-4-carbonitrile derivatives (**4**) has been developed using alumina–silica supported MnO_2 as recyclable catalyst in water and sodium dodecyl benzene sulphonate at room temperature. The cyclo-condensation of substituted benzaldehydes, malononitrile and phenyl hydrazine gave the 5-amino-1,3-diphenyl-1H-pyrazole-4-carbonitriles (**4**) in 86–96% yields (Scheme 2.1).

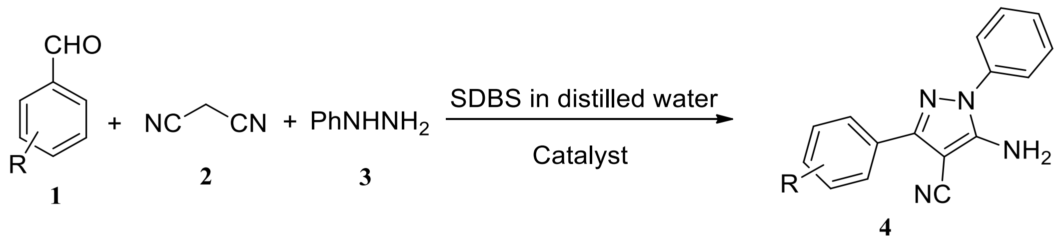

Scheme 2.1. Synthesis of pyrazole derivatives (**4a-n**)

A sustainable, one-pot, multicomponent protocol for the synthesis of 4-phenylthiazole-2-amine derivatives catalyzed by MoS_2 QDs in aqueous medium has been developed. The cyclo-condensation of phenacyl bromide and thiourea gave the thiazole derivatives in 89–96% yields (Scheme 2.2). 2-(4-Nitrophenyl)-1H-benzo[d]imidazole was synthesized using the literature method. In the further step, 2-(4-nitrophenyl)-1H-benzo[d]imidazole was reduced using catalytic hydrogenation to give 4-(1H-benzoimidazol-2-yl)-phenylamine, which underwent a coupling reaction with aromatic acids to give the final product. The synthesized molecules have been reacted with different linkers to form the respective conjugates (Schemes 2.6-2.8).

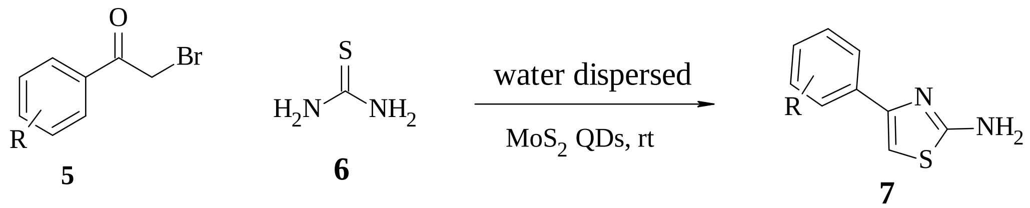

Scheme 2.2. Synthesis of pyrazole derivatives (**7a-l**)

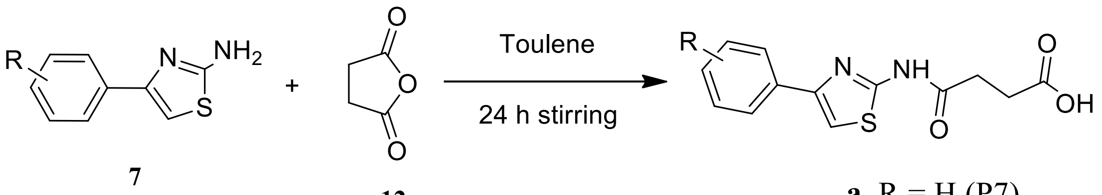

a. R = H (P7)
b. R = 4-OCH_3 (P8)
c. R = 4-NO_2

Scheme 2.6. Synthesis of 4-oxo-4-((4-arylthiazol-2-yl)amino)butanoic acid (**13**)

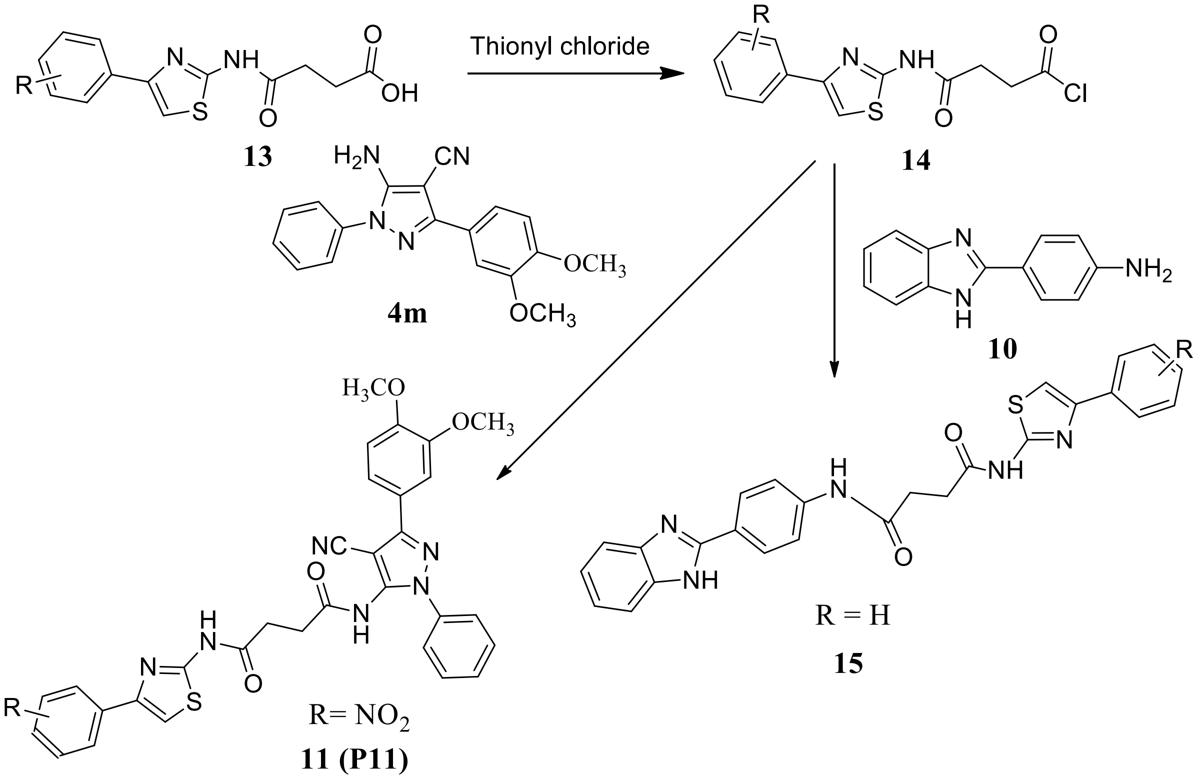

Scheme 2.7. Synthesis of thiazole-pyrazole (**11**) and thiazole-benzimidazole amide (**15**) conjugates

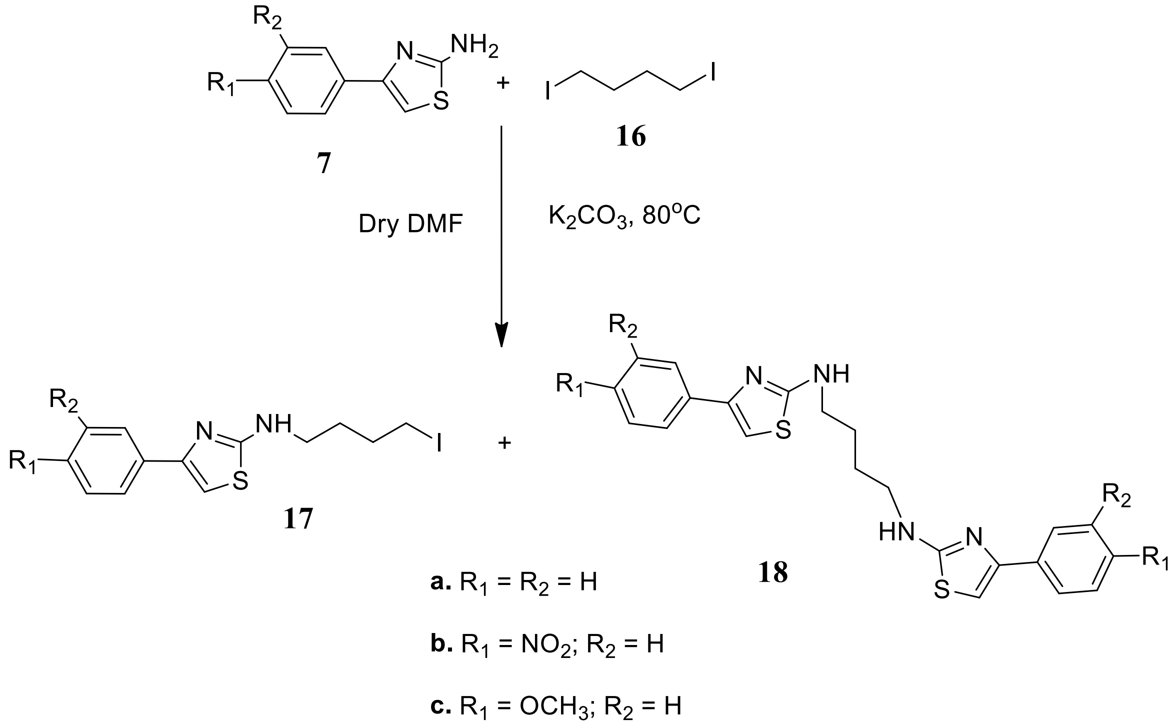

Scheme 2.8. Synthesis of thiazole derivatives (**17** and **18**)

The synthesized derivatives were evaluated for MAO-B inhibition. The *in-vitro* study of seventeen compounds was done using Amplex™ Red Monoamine Oxidase Assay Kit. Over all – two best compounds, N1-(4-cyano-3-(3,4-dimethoxyphenyl)-1-phenyl-1H-pyrazol-5-yl)-N4-(4-(4-nitrophenyl)thiazol-2-yl)succinamide **(P11)** with IC_{50} value of 80.17 μM and 3-(3,4-dimethoxyphenyl)-5-((4-((4-(4-nitrophenyl)thiazol-2-yl) amino)butyl)amino)-1-phenyl-1H-pyrazole-4-carbonitrile **(P10)** with IC_{50} value of 86.03 μM have been obtained. The antioxidant evaluation of the compounds has also been done. The results showed 13 to 83 % antioxidant activities of the compounds. Interestingly, the compounds that shows better in-vitro results also showed good antioxidant activities.

Chapter 4 is the conclusion chapter where all the work carried out has been summarized. This chapter is followed by references and publications.

REFERENCES

Chapter 1

Aliyan, A., Cook, N.P., & Martí, A.A. (2019). Interrogating amyloid aggregates using fluorescent probes. *Chemical reviews*, *119*(23), 11819-11856.

Aradi, S.D., & Hauser, R.A. (2020). Medical management and prevention of motor complications in Parkinson's disease. *Neurotherapeutics*, *17*(4), 1339-1365.

Armstrong, M.J., & Okun, M.S. (2020). Diagnosis and treatment of Parkinson disease: a review. *JAMA*, *323*(6), 548-560.

Ascherio, A., & Schwarzschild, M.A. (2016). The epidemiology of Parkinson's disease: risk factors and prevention. *The Lancet Neurology*, *15*(12), 1257-1272.

Babinski, J., Jarkowski, B., & Plichet, X. (1921). Kinésie paradoxale. Mutisme parkinsonien. *Rev Neurol*, *37*(12), 1266-1270.

Bach, A.W., Lan, N.C., Johnson, D.L., Abell, C.W., Bembenek, M.E., Kwan, S.W., Seeburg, P.H. & Shih, J.C. (1988). cDNA cloning of human liver monoamine oxidase A and B: molecular basis of differences in enzymatic properties. *Proceedings of the National Academy of Sciences*, *85*(13), 4934-4938.

Baldereschi, M., Di Carlo, A., Rocca, W. A., Vanni, P., Maggi, S., Perissinotto, E., Grigoletto, F., Amaducci, L., & Inzitari, D. (2000). Parkinson's disease and parkinsonism in a longitudinal study: two-fold higher incidence in men. *Neurology*, *55*(9), 1358-1363.

Barnham, K.J., & Bush, A.I. (2008). Metals in Alzheimer's and Parkinson's diseases. *Current Opinion in Chemical Biology*, *12*(2), 222-228.

Binda, C., Hubálek, F., Li, M., Herzig, Y., Sterling, J., Edmondson, D. E., & Mattevi, A. (2005). Binding of rasagiline-related inhibitors to human monoamine oxidases: a kinetic and crystallographic analysis. *Journal of Medicinal Chemistry*, *48*(26), 8148-8154.

Blazevic, S., Merkler, M., Persic, D., & Hranilovic, D. (2017). Chronic postnatal monoamine oxidase inhibition affects affiliative behavior in rat pups. *Pharmacology Biochemistry and Behavior*, *153*, 60-68.

Bohnen, N.I., & Albin, R.L. (2011). The cholinergic system and Parkinson disease. *Behavioural Brain Research*, *221*(2), 564-573.

Bologna, M., Truong, D., & Jankovic, J. (2022). The etiopathogenetic and pathophysiological spectrum of parkinsonism. *Journal of the Neurological Sciences*, *433*, 120012.

Borges, M.F.M., Roleira, F.M.F., Milhazes, N.J.S.P., Villare, E.U., & Penin, L.S. (2010). Simple coumarins: Privileged scaffolds in medicinal chemistry. *Frontiers in Medicinal Chemistry*, *4*, 23-85.

Boulaamane, Y., Ibrahim, M.A., Britel, M.R., & Maurady, A. (2022). *In silico* studies of natural product-like caffeine derivatives as potential MAO-B inhibitors/AA2AR antagonists for the treatment of Parkinson's disease. *Journal of Integrative Bioinformatics*, *19*(4), 20210027.

Braak, H., Del, Tredici, K., Bratzke, H., Hamm-Clement, J., Sandmann-Keil, D., & Rüb, U. (2002). Staging of the intracerebral inclusion body pathology associated with idiopathic Parkinson's disease (preclinical and clinical stages). *Journal of Neurology*, *249*, iii1-iii5.

Caccia, C., Maj, R., Calabresi, M., Maestroni, S., Faravelli, L., Curatolo, L., Salvati, P., & Fariello, R.G. (2006). Safinamide: from molecular targets to a new anti-Parkinson drug. *Neurology*, *67*(7), S18-S23.

Carradori, S., D'Ascenzio, M., Chimenti, P., Secci, D., & Bolasco, A. (2014). Selective MAO-B inhibitors: a lesson from natural products. *Molecular Diversity*, *18*, 219-243.

Cash, R., Ruberg, M., Raisman, R., & Agid, Y. (1984). Adrenergic receptors in Parkinson's disease. *Brain Research*, *322*(2), 269-275.

Cerri, S., & Blandini, F. (2020). An update on the use of non-ergot dopamine agonists for the treatment of Parkinson's disease. *Expert Opinion on Pharmacotherapy*, *21*(18), 2279-2291.

Chan, S.L., & Tan, E.K. (2017). Targeting LRRK2 in Parkinson's disease: an update on recent developments. *Expert Opinion on Therapeutic Targets*, *21*(6), 601-610.

Cohen, G., Farooqui, R., & Kesler, N. (1997). Parkinson disease: a new link between monoamine oxidase and mitochondrial electron flow. *Proceedings of the National Academy of Sciences*, *94*(10), 4890-4894.

Cohen, G., Pasik, P., Cohen, B., Leist, A., Mytilineou, C., & Yahr, M.D. (1984). Pargyline and deprenyl prevent the neurotoxicity of 1-methyl-4-phenyl-1,2,3,6-tetrahydropyridine (MPTP) in monkeys. *European Journal of Pharmacology*, *106*(1), 209-210.

Cruces-Sande, A., Rodríguez-Pérez, A.I., Herbello-Hermelo, P., Bermejo-Barrera, P., Méndez-Álvarez, E., Labandeira-García, J.L., & Soto-Otero, R. (2019). Copper increases brain oxidative stress and enhances the ability of 6-hydroxydopamine to cause dopaminergic degeneration in a rat model of Parkinson's disease. *Molecular Neurobiology, 56*, 2845-2854 Database. Landes Bioscience.

De Lau, L.M., & Breteler, M.M. (2006). Epidemiology of Parkinson's disease. *The Lancet Neurology*, *5*(6), 525-535.

Dézsi, L., & Vécsei, L. (2014). Clinical implications of irregular ADMET properties with levodopa and other antiparkinson's drugs. *Expert Opinion on Drug Metabolism & Toxicology*, *10*(3), 409-424.

Dezsi, L., & Vecsei, L. (2017). Monoamine oxidase B inhibitors in Parkinson's disease. *CNS & Neurological Disorders-Drug Targets*, *16*(4), 425-439.

Dorsey, E.R., Elbaz, A., Nichols, E., Abbasi, N., Abd-Allah, F., Abdelalim, A., Adsuar, J.C., Ansha, M.G., Brayne, C., Choi, J.Y.J., & Murray, C.J. (2018). Global, regional, and national burden of Parkinson's disease, 1990–2016: A systematic analysis for the Global Burden of Disease Study 2016. *The Lancet Neurology*, *17*(11), 939-953.

Duvoisin, R.C. (1967). Cholinergic-anticholinergic antagonism in parkinsonism. *Archives of Neurology*, *17*(2), 124-136.

Edmondson, D.E., Binda, C., Wang, J., Upadhyay, A.K., & Mattevi, A. (2009). Molecular and mechanistic properties of the membrane-bound mitochondrial monoamine oxidases. *Biochemistry*, *48*(20), 4220-4230.

Eeden V.D., S.K.V.D., Tanner, C. M., Bernstein, A.L., Fross, R.D., Leimpeter, A., Bloch, D. A., & Nelson, L. M. (2003). Incidence of Parkinson's disease: variation by age, gender, and race/ethnicity. *American Journal of Epidemiology*, *157*(11), 1015-1022.

Ellis, J.M., & Fell, M.J. (2017). Current approaches to the treatment of Parkinson's Disease. *Bioorganic & Medicinal Chemistry Letters*, *27*(18), 4247-4255.

Fahn, S. (2018). The 200-year journey of Parkinson disease: Reflecting on the past and looking towards the future. *Parkinsonism & Related Disorders*, *46*, S1-S5.

Finberg, J.P., & Rabey, J.M. (2016). Inhibitors of MAO-A and MAO-B in psychiatry and neurology. *Frontiers in Pharmacology*, *7*, 340.

Fox, S.H., Katzenschlager, R., Lim, S.Y., Ravina, B., Seppi, K., Coelho, M., Poewe, W., Rascol, O., Goetz, C.G., & Sampaio, C. (2011). The Movement Disorder Society evidence-based medicine review update: treatments for the motor symptoms of Parkinson's disease. *Movement Disorders*, *26*(S3), S2-S41.

Gardoni, F., Morari, M., Kulisevsky, J., Brugnoli, A., Novello, S., Pisano, C. A., Caccia, C., Mellone, M., Melloni, E., Padoani, G., Sosti, V., & Keywood, C. (2018). Safinamide modulates striatal glutamatergic signaling in a rat model of levodopa-induced dyskinesia. *Journal of Pharmacology and Experimental Therapeutics*, *367*(3), 442-451.

Gharibkandi, N.A., & Hosseinimehr, S.J. (2019). Radiotracers for imaging of Parkinson's disease. *European Journal of Medicinal Chemistry*, *166*, 75-89.

Golbe, L.I., Lazzarini, A.M., Duvoisin, R.C., Iorio, G.D., Sanges, G., Bonavita, V., & la Sala, S. (1996). Clinical genetic analysis of Parkinson's disease in the Contursi kindred. *Annals of Neurology 40*(5), 767-775.

Haaxma, C.A., Bloem, B.R., Borm, G.F., Oyen, W.J., Leenders, K.L., Eshuis, S., & Horstink, M.W. (2007). Gender differences in Parkinson’s disease. *Journal of Neurology, Neurosurgery & Psychiatry, 78*(8), 819-824.

Halliday, G.M., Blumbergs, P.C., Cotton, R.G.H., Blessing, W. W., & Geffen, L.B. (1990). Loss of brainstem serotonin-and substance P-containing neurons in Parkinson's disease. *Brain Research, 510*(1), 104-107.

Hauser, D.N., & Hastings, T.G. (2013). Mitochondrial dysfunction and oxidative stress in Parkinson's disease and monogenic parkinsonism. *Neurobiology of Disease, 51*, 35-42.

He, X.J., & Nakayama, H. (2009). Neurogenesis in Neurotoxin-induced Animal Models for Parkinson's Disease-A Review of the Current Status. *Journal of Toxicologic Pathology*, *22*(2), 101-108.

Hely, M. A., Reid, W. G., Adena, M. A., Halliday, G. M., & Morris, J. G. (2008). The Sydney multicenter study of Parkinson's disease: the inevitability of dementia at 20 years. *Movement disorders*, *23*(6), 837-844.

Hoehn, M.M., & Yahr, M.D. (1998). Parkinsonism: onset, progression, and mortality. *Neurology*, *50*(2), 318-318.

Horrocks, M.H., Tosatto, L., Dear, A.J., Garcia, G.A., Iljina, M., Cremades, N., Serra M.D., Knowles, T.P.J., Dobson, C.M., & Klenerman, D. (2015). Fast flow microfluidics and single-molecule fluorescence for the rapid characterization of α-synuclein oligomers. *Analytical Chemistry*, *87*(17), 8818-8826.

Ilie, I. M., & Caflisch, A. (2019). Simulation studies of amyloidogenic polypeptides and their aggregates. *Chemical Reviews*, *119*(12), 6956-6993.

Inskip, M., Mavros, Y., Sachdev, P.S., & Fiatarone Singh, M.A. (2016). Exercise for individuals with Lewy body dementia: a systematic review. *Public Library of Sciences One*, *11*(6), e0156520.

Jankovic, J. (2008). Parkinson’s disease: clinical features and diagnosis. *Journal of Neurology, Neurosurgery & Psychiatry*, *79*(4), 368-376.

Jankovic, J., & Tan, E.K. (2020). Parkinson’s disease: Etiopathogenesis and treatment. *Journal of Neurology, Neurosurgery & Psychiatry*, *91*(8), 795-808.

Kalia, L.V., & Lang, A. E. (2015). Parkinson's disease. *The Lancet*, *386*(9996), 896-912.

Kasper, D., Fauci, A., Hauser, S., Longo, D., Jameson, J., & Loscalzo, J. (2015). *Harrison's Principles of Internal Medicine, 19e* (Vol. 1, No. 2). New York, NY, USA: Mcgraw-hill.

Katzenschlager, R., Sampaio, C., Costa, J., Lees, A., & Cochrane Movement Disorders Group. (1996). Anticholinergics for symptomatic management of Parkinson s disease. *Cochrane Database of Systematic Reviews*, *2010*(1).

Kawabata, K., & Katsuno, M. (2021). Trihexyphenidyl, Biperiden, and Other Anticholinergics in the Treatment of Parkinson's Disease. In *Neuro Psychopharmaco therapy* (pp. 1-8). Cham: Springer International Publishing.

Kersten, H., & Wyller, T.B. (2014). Anticholinergic drug burden in older people's brain–how well is it measured? *Basic & Clinical Pharmacology & Toxicology*, *114*(2), 151-159.

Knoll, J., Ecsery, Z., Magyar, K., & Sátory, É. (1978). Novel (−) deprenyl-derived selective inhibitors of B-type monoamine oxidase. The relation of structure to their action. *Biochemical Pharmacology*, *27*(13), 1739-1747.

Kordower, J. H., Olanow, C.W., Dodiya, H. B., Chu, Y., Beach, T.G., Adler, C.H., Halliday, G.M. & Bartus, R.T. (2013). Disease duration and the integrity of the nigrostriatal system in Parkinson's disease. *Brain*, *136*(8), 2419-2431.

Kotagal, V., Albin, R.L., Müller, M.L.T.M., Koeppe, R.A., Frey, K.A., & Bohnen, N.I. (2013). Gender differences in cholinergic and dopaminergic deficits in Parkinson disease. *Journal of Neural Transmission*, *120*, 1421-1424.

Lampropoulos, I.C., Malli, F., Sinani, O., Gourgoulianis, K.I., & Xiromerisiou, G. (2022). Worldwide trends in mortality related to Parkinson's disease in the period of 1994–2019: Analysis of vital registration data from the WHO Mortality Database. *Frontiers in Neurology*, *13*.

Lang, A.E., & Lozano, A.M. (1998). Parkinson's disease. *New England Journal of Medicine*, *339*(16), 1130-1143.

Langston, J.W., Ballard, P., Tetrud, J.W., & Irwin, I. (1983). Chronic Parkinsonism in humans due to a product of meperidine-analog synthesis. *Science*, *219*(4587), 979-980.

Latt, M.D., Lewis, S., Zekry, O., & Fung, V.S.C. (2019). Factors to consider in the selection of dopamine agonists for older persons with Parkinson's disease. *Drugs & Aging*, *36(3)*, 189-202.

Li, G., Ma, J., Cui, S., He, Y., Xiao, Q., Liu, J., & Chen, S. (2019). Parkinson's disease in China: a forty-year growing track of bedside work. *Translational Neurodegeneration*, *8*, 22.

Li, L., Zhang, C.W., Chen, G.Y.J., Zhu, B., Chai, C., Xu, Q.H., Tan, E.K., Zhu, Q., Lim, K.L. & Yao, S.Q. (2014). A sensitive two-photon probe to selectively detect monoamine oxidase B activity in Parkinson's disease models. *Nature Communications*, *5*(1), 3276.

Li, Z., Wang, P., Yu, Z., Cong, Y., Sun, H., Zhang, J., Zhang, J., Sun, C., Zhang, Y., & Ju, X. (2015). The effect of creatine and coenzyme Q10 combination therapy on mild cognitive impairment in Parkinson's disease. *European Neurology*, *73*(3-4), 205-211.

Lin, C.Y., Lin, Y.C., Huang, C.Y., Wu, S.R., Chen, C.M., & Liu, H.L. (2020). Ultrasound-responsive neurotrophic factor-loaded microbubble-liposome complex: Preclinical investigation for Parkinson's disease treatment. *Journal of Controlled Release*, *321*, 519-528.

Lu, F.M., & Yuan, Z. (2015). PET/SPECT molecular imaging in clinical neuroscience: recent advances in the investigation of CNS diseases. *Quantitative Imaging in Medicine and Surgery*, *5*(3), 433-447.

Mahul-Mellier, A.L., Burtscher, J., Maharjan, N., Weerens, L., Croisier, M., Kuttler, F., Leleu, M., Knott, G.W. & Lashuel, H.A. (2020). The process of Lewy body formation, rather than simply α-synuclein fibrillization, is one of the major drivers of neurodegeneration. *Proceedings of the National Academy of Sciences*, *117*(9), 4971-4982.

Manyam, B.V. (1990). Paralysis agitans and levodopa in "Ayurveda": ancient Indian medical treatise. *Movement Disorders*, *5*(1), 47-48.

Marti, J.S., Kettler, R., Da Prada, M., & Richards, J.G. (1990). Molecular neuroanatomy of MAO-A and MAO-B. In *Amine Oxidases and Their Impact on Neurobiology* (pp. 49-53). Springer Vienna.

Matos, M.J., Vilar, S., García-Morales, V., Tatonetti, N.P., Uriarte, E., Santana, L., & Viña, D. (2014). Insight into the Functional and Structural Properties of 3-Arylcoumarin as an Interesting Scaffold in Monoamine Oxidase B Inhibition. *ChemMedChem*, *9*(7), 1488-1500.

Mehra, S., Sahay, S., & Maji, S.K. (2019). α-Synuclein misfolding and aggregation: Implications in Parkinson's disease pathogenesis. *Biochimica et Biophysica Acta (BBA)-Proteins and Proteomics*, *1867*(10), 890-908.

Morari, M., Brugnoli, A., Pisanò, C.A., Novello, S., Caccia, C., Melloni, E., Padoani, G., Vailati, S., & Sardina, M. (2018). Safinamide differentially modulates in vivo glutamate and GABA release in the rat hippocampus and basal ganglia. *Journal of Pharmacology and Experimental Therapeutics*, *364*(2), 198-206.

Moustafa, A.A., Chakravarthy, S., Phillips, J.R., Gupta, A., Keri, S., Polner, B., Frank, M.J., & Jahanshahi, M. (2016). Motor symptoms in Parkinson's disease: A unified framework. *Neuroscience & Biobehavioral Reviews*, *68*, 727-740.

Natale, G., Pignataro, A., Marino, G., Campanelli, F., Calabrese, V., Cardinale, A., Pelucchi, S., Marcello, E., Gardoni, F., Viscomi, M.T., Picconi, B., Ammassari-Teule, M., Calabresi, P., & Ghiglieri, V. (2021). Transcranial magnetic stimulation exerts "rejuvenation" effects on corticostriatal synapses after partial dopamine depletion. *Movement Disorders*, *36*(10), 2254-2263.

Niciu, M.J., Kelmendi, B., & Sanacora, G. (2012). Overview of glutamatergic neurotransmission in the nervous system. *Pharmacology Biochemistry and Behavior*, *100*(4), 656-664.

Nutt, J.G., Obeso, J.A., & Stocchi, F. (2000). Continuous dopamine-receptor stimulation in advanced Parkinson's disease. *Trends in Neurosciences*, *23*, S109-S115.

Onyango, I.G. (2008). Mitochondrial dysfunction and oxidative stress in Parkinson's disease. *Neurochemical Research*, *33*, 589-597.

Perez, X.A., Bordia, T., & Quik, M. (2018). The striatal cholinergic system in L-dopa-induced dyskinesias. *Journal of Neural Transmission*, *125*, 1251-1262.

Pisanò, C.A., Brugnoli, A., Novello, S., Caccia, C., Keywood, C., Melloni, E., Vailati, S., Padoani, G., & Morari, M. (2020). Safinamide inhibits in vivo glutamate release in a rat model of Parkinson's disease. *Neuropharmacology*, *167*, 108006.

Poewe, W., Seppi, K., Tanner, C.M., Halliday, G.M., Brundin, P., Volkmann, J., Schrag, A. E., & Lang, A.E. (2017). Parkinson disease. *Nature Reviews Disease Primers*, *3*, 17013.

Politis, M., & Niccolini, F. (2015). Serotonin in Parkinson's disease. *Behavioural Brain Research*, *277*, 136-145.

Polymeropoulos, M.H., Lavedan, C., Leroy, E., Ide, S.E., Dehejia, A., Dutra, A., Pike, B., Root, H., Rubenstein, J., Boyer, R., Stenroos, E.S., Chandrasekharappa, S., Athanassiadou, A., Papapetropoulos, T., Johnson, W.G., Lazzarini, A.M., Duvoisin, R.C., Iorio, G.D., Golbe, L.I., & Nussbaum, R.L. (1997). Mutation in the α-synuclein gene identified in families with Parkinson's disease. *Science*, *276*(5321), 2045-2047.

Pretorius, J., Malan, S.F., Castagnoli Jr, N., Bergh, J.J., & Petzer, J.P. (2008). Dual inhibition of monoamine oxidase B and antagonism of the adenosine A_{2A} receptor by (E, E)-8-(4-phenylbutadien-1-yl) caffeine analogues. *Bioorganic & Medicinal Chemistry*, *16*(18), 8676-8684.

Qu, Y., Li, J., Qin, Q., Wang, D., Zhao, J., An, K., Mao, Z., Min, Z., Xiong, Y., Li, J., & Xue, Z. (2023). A systematic review and meta-analysis of inflammatory biomarkers in Parkinson's disease. *NPJ Parkinson's Disease*, *9*, 18.

Reiner, A., & Levitz, J. (2018). Glutamatergic signalling in the central nervous system: ionotropic and metabotropic receptors in concert. *Neuron*, *98*(6), 1080-1098.

Rizek, P., Kumar, N., & Jog, M.S. (2016). An update on the diagnosis and treatment of Parkinson disease. *CMAJ*, *188*(16), 1157-1165.

Robertson, R.G., Clarke, C.A., Boyce, S., Sambrook, M.A., & Crossman, A.R. (1990). The role of striatopallidal neurones utilizing gamma-aminobutyric acid in the pathophysiology of MPTP-induced parkinsonism in the primate: evidence from [3H]flunitrazepam autoradiography. *Brain Research*, *531*(1-2), 95-104.

Rodriguez-Enriquez, F., Costas-Lago, M.C., Besada, P., Alonso-Pena, M., Torres-Terán, I., Viña, D., Fontenla, J.Á., Sturlese, M., Moro, S., Quezada, E., & Terán, C. (2020). Novel coumarin-pyridazine hybrids as selective MAO-B inhibitors for the Parkinson's disease therapy. *Bioorganic Chemistry*, *104*, 104203.

Sahay, S., Ghosh, D., Singh, P.K., & Maji, S.K. (2017). Alteration of structure and aggregation of α-synuclein by familial Parkinson's disease associated mutations. *Current Protein and Peptide Science*, *18*(7), 656-676.

Scatton, B., Javoy-Agid, F., Rouquier, L., Dubois, B., & Agid, Y. (1983). Reduction of cortical dopamine, noradrenaline, serotonin and their metabolites in Parkinson's disease. *Brain Research*, *275*(2), 321-328.

Schrag, A., & Schott, J.M. (2006). Epidemiological, clinical, and genetic characteristics of early-onset parkinsonism. *The Lancet Neurology*, *5*(4), 355-363.

Simon, D.K., Tanner, C.M., & Brundin, P. (2020). Parkinson disease epidemiology, pathology, genetics, and pathophysiology. *Clinics in Geriatric Medicine*, *36*(1), 1-12.

Stefanis, L. (2012). α-Synuclein in Parkinson's disease. Cold Spring Harbor Perspectives in Medicine, *2*(2), a009399.

Stocchi, F. (2011). Continuous dopaminergic stimulation and novel formulations of dopamine agonists. *Journal of Neurology*, *258*(Suppl 2), 316-322.

Sun, C., & Armstrong, M.J. (2021). Treatment of Parkinson's disease with cognitive impairment: current approaches and future directions. *Behavioral Sciences*, *11*(4), 54.

Tipton, K.F. (2018). 90 years of monoamine oxidase: some progress and some confusion. *Journal of Neural Transmission*, *125*, 1519-1551.

Tozzi, A., de Iure, A., Bagetta, V., Tantucci, M., Durante, V., Quiroga-Varela, A., Costa, C., Di Filippo, M., Ghiglieri, V., Latagliata, E.C., Wegrzynowicz, M., & Calabresi, P. (2016). Alpha-synuclein produces early behavioral alterations via striatal cholinergic synaptic dysfunction by interacting with GluN2D N-methyl-D-aspartate receptor subunit. *Biological Psychiatry*, *79*(5), 402-414.

Tozzi, A., Sciaccaluga, M., Loffredo, V., Megaro, A., Ledonne, A., Cardinale, A., Federici, M., Bellingacci, L., Paciotti, S., Ferrari, E., Rocca, A.L., Martini, A., Mercuri, N.B., Gardoni, F., Picconi, B., Ghiglieri, V., De Leonibus, E., Calabresi, P. (2021). Dopamine-dependent early synaptic and motor dysfunctions induced by α-synuclein in the nigrostriatal circuit. Brain, *144*(11), 3477-3491.

Triarhou, L.C. (2013). Dopamine and Parkinson's disease. In Madame Curie Bioscience

Tyler, K.L. (1992). A history of Parkinson's disease. *Handbook of Parkinson's disease*, 1-34.

Vindis, C., Séguélas, M.H., Lanier, S., Parini, A., & Cambon, C. (2001). Dopamine induces ERK activation in renal epithelial cells through H_2O_2 produced by monoamine oxidase. *Kidney International*, *59*(1), 76-86.

Vos, T., Allen, C., Arora, M., Barber, R.M., Bhutta, Z.A., Brown, A., Carter, A., Casey, D.C., Charlson, F.J., Chen, A.Z. Coggeshall, M., & Boufous, S. (2016). Global, regional, and national incidence, prevalence, and years lived with disability for 310 diseases and injuries, 1990–2015: a systematic analysis for the Global Burden of Disease Study 2015. *The Lancet*, *388*(10053), 1545-1602.

Vos, T., Allen, C., Arora, M., Barber, R.M., Bhutta, Z.A., Brown, A., Carter, A., Casey, D.C., Charlson, F.J., Chen, A.Z. & Coggeshall, M., (2016). Global, regional, and national incidence, prevalence, and years lived with disability for 310 diseases and injuries, 1990–2015: a systematic analysis for the Global Burden of Disease Study 2015. *The Lancet*, *388*(10053), 1545-1602.

Wawruch, M., Macugova, A., Kostkova, L., Luha, J., Dukat, A., Murin, J., Drobna V., Wilton L. & Kuzelova, M. (2012). The use of medications with anticholinergic properties and risk factors for their use in hospitalised elderly patients. *Pharmacoepidemiology and Drug Safety*, *21*(2), 170-176.

Wegrzynowicz, M., Bar-On, D., Calo, L., Anichtchik, O., Iovino, M., Xia, J., Ryazanov, S., Leonov, A., Giese, A., Dalley, J.W., Griesinger, C., & Spillantini, M.G. (2019). Depopulation of dense α-synuclein aggregates is associated with rescue of dopamine neuron dysfunction and death in a new Parkinson's disease model. *Acta Neuropathologica*, *138*, 575-595.

William, L.J. (2017). The MPTP story. *Journal of Parkinsons Disease* 7: S11–S19.

Youdim, M.B., & Bakhle, Y.S. (2006a). Monoamine oxidase: isoforms and inhibitors in Parkinson's disease and depressive illness. *British Journal of Pharmacology*, *147*(S1), S287-S296.

Youdim, M.B., Edmondson, D., & Tipton, K.F. (2006b). The therapeutic potential of monoamine oxidase inhibitors. *Nature Reviews Neuroscience*, *7*(4), 295-309.

Chapter 2

Banothu, J., Vaarla, K., Bavantula, R., & Crooks, P. A. (2014). Sodium fluoride as an efficient catalyst for the synthesis of 2,4-disubstituted-1, 3-thiazoles and selenazoles at ambient temperature. *Chinese Chemical Letters*, *25*(1), 172-175.

Binda, C., Hubálek, F., Li, M., Herzig, Y., Sterling, J., Edmondson, D. E., & Mattevi, A. (2005). Binding of rasagiline-related inhibitors to human monoamine oxidases: a kinetic and crystallographic analysis. *Journal of Medicinal Chemistry*, *48*(26), 8148-8154.

Can, O.D., Osmaniye, D., Özkay, U.D., Sağlık, B.N., Levent, S., Ilgın, S., Baysal, M., Özkay, Y., & Kaplancıklı, Z.A. (2017). MAO enzymes inhibitory activity of new benzimidazole derivatives including hydrazone and propargyl side chains, *European Journal of Medicinal Chemistry*, *131*, 92-106.

Khan, A.T., Parvin, T., & Choudhury, L.H. (2009). A simple and convenient one-pot synthesis of benzimidazole derivatives using cobalt (II) chloride hexahydrate as catalyst. *Synthetic Communications*, *39*(13), 2339-2346.

King, L.C., & Miller, F.M. (1949). The reaction of diazoketones with thioamide derivatives. *Journal of the American Chemical Society*, *71*(1), 367-368.

Kiyani, H., & Bamdad, M. (2018). Sodium ascorbate as an expedient catalyst for green synthesis of polysubstituted 5-aminopyrazole-4-carbonitriles and 6-amino-1, 4-dihydropyrano [2, 3-c] pyrazole-5-carbonitriles. *Research on Chemical Intermediates*, *44*, 2761-2778.

Lim, S.S., Yang, W., Krishnarjuna, B., Sivaraman, K.K., Chandrashekaran, I. R., Kass, I. & Scammells, P. (2013). Crystal Structure of FVO PfAMA1. Ligands for the Malaria Apical Membrane Antigen 1 as Inhibitors of Parasite Invasion of Host Erythrocytes: Screening, Structure and Dynamics.

Mahapatra, G. N. (1956). Bromination of 2-amino thiazoles and their use as possible fungicides and bactericides. *Journal of Indian Chemical Society*, *33*, 527-531.

Mishra, A., Verma, C., Chauhan, S., Quraishi, M.A., Ebenso, E.E., & Srivastava, V. (2018). Synthesis, characterization, and corrosion inhibition performance of 5-aminopyrazole carbonitriles towards mild steel acidic corrosion. *Journal of Bio-and Tribo-Corrosion*, *4*, 1-15.

Mishra, D., Fatima, A., Rout, C., & Sing, R. (2015). An efficient one-pot synthesis of 2-aminothiazole derivatives. *Der Chemica Sinica*, *6*, 14-18.

Mishra, D., Singh, R., & Rout, C. (2017). Synthesis of highly functionalized pyrazoles using $AlCl_3$ as catalyst. *Journal of Chemical and Pharmaceutical Research*, *9*(6), 16-19.

Patil, S.V., Patil, S.S., & Bobade, V. D. (2016). A simple and efficient approach to the synthesis of 2-substituted benzimidazole via sp3 C–H functionalization. *Arabian Journal of Chemistry*, *9*, S515-S521.

Poonam, & Singh, R. (2019). Facile one-pot synthesis of highly functionalized pyrazoles using Alumina-Silica-supported MnO2 as recyclable catalyst in water. *Research on Chemical Intermediates*, *45*(9), 4531-4542.

Potewar, T.M., Ingale, S.A., & Srinivasan, K.V. (2008). Catalyst-free efficient synthesis of 2-aminothiazoles in water at ambient temperature. *Tetrahedron*, *64*(22), 5019-5022.

Srivastava, M., Rai, P., Singh, J., & Singh, J. (2014). Efficient iodine-catalyzed one pot synthesis of highly functionalised pyrazoles in water. *New Journal of Chemistry*, *38*(1), 302-307.

Vijayakumar, S., Manogar, P., Prabhu, S., & Singh, R.A.S. (2018). Novel ligand-based docking; molecular dynamic simulations; and absorption, distribution, metabolism, and excretion approach to analyzing potential acetylcholinesterase inhibitors for Alzheimer's disease. *Journal of Pharmaceutical Analysis*, *8*(6), 413-420.

Zhu, D., Chen, J., Xiao, H., Liu, M., Ding, J., & Wu, H. (2009). Efficient and expeditious synthesis of di-and trisubstituted thiazoles in PEG under catalyst-free conditions. *Synthetic Communications*, *39*(16), 2895-2906.

Chapter 3

Akbas, E., Berber, I., Sener, A., & Hasanov, B. (2005). Synthesis and antibacterial activity of 4-benzoyl-1-methyl-5-phenyl-1H-pyrazole-3-carboxylic acid and derivatives. *Il Farmaco*, *60*(1), 23-26.

Alaqeel, S.I. (2017). Synthetic approaches to benzimidazoles from *o*-phenylenediamine: A literature review. *Journal of Saudi Chemical Society*, *21*(2), 229-237.

Arora, P., Narang, R., Bhatia, S., Nayak, S.K., Singh, S.K., & Narasimhan, B. (2015). Synthesis, molecular docking and QSAR studies of 2,4-disubstituted thiazoles as antimicrobial agents. *Journal of Applied Pharmaceutical Science*, *5*(2), 028-042.

Avila, B., Roth, A., Streets, H., Dwyer, D.S., & Kurth, M.J. (2012). Triazolbenzo [d] thiazoles: Efficient synthesis and biological evaluation as neuroprotective agents. *Bioorganic & Medicinal Chemistry Letters*, *22*(18), 5976-5978.

Badawey, E.S.A., & El-Ashmawey, I.M. (1998). Nonsteroidal antiinflammatory agents-Part 1: Antiinflammatory, analgesic and antipyretic activity of some new 1-(pyrimidin-2-yl)-3-pyrazolin-5-ones and 2-(pyrimidin-2-yl)-1,2,4,5,6,7-hexahydro-3H-indazol-3-ones. *European Journal of Medicinal Chemistry*, *33*(5), 349-361.

Badhe, K., Dabholkar, V., & Kurade, S. (2018). One-pot synthesis of 5-amino-1H-pyrazole-4-carbonitrile using calcined Mg-Fe hydrotalcite catalyst. *Current Organocatalysis*, *5*(1), 3-12.

Bamdad, M., & Kiyani, H. (2017). One-pot and efficient synthesis of 5-aminopyrazole-4-carbonitriles catalyzed by potassium phthalimide. *Heterocycles*, *94*(2), 276-285.

Bekhit, A.A., & Abdel-Aziem, T. (2004). Design, synthesis and biological evaluation of some pyrazole derivatives as anti-inflammatory-antimicrobial agents. *Bioorganic & medicinal chemistry*, *12*(8), 1935-1945.

Bernardino, A.M., Gomes, A.O., Charret, K.S., Freitas, A.C., Machado, G.M., Canto-Cavalheiro, M.M., Leon, L.L. & Amaral, V.F. (2006). Synthesis and leishmanicidal activities of 1-(4-X-phenyl)-N′-[(4-Y-phenyl)methylene]-1H-pyrazole-4-carbohydrazides. *European Journal of Medicinal Chemistry*, *41*(1), 80-87.

Bhagavan, N.V., & Ha, C.E. (2015). Three-dimensional structure of proteins and disorders of protein misfolding. *Essentials of Medical Biochemistry*, *2*, 31-51.

Bhargava, P., Lakhan, R., & Tripathi, R. (1983). Local anesthetics. part II. Synthesis of 2-(N, N-disubstituted aminoacetamido)-4-p-fluorophenyl and m-methoxyphenyl thiazoles. *Chemischer Informationsdienst*, *14*(1).

Borisenko, V.E., Koll, A., Kolmakov, E.E., & Rjasnyi, A.G. (2006). Hydrogen bonds of 2-aminothiazoles in intermolecular complexes (1:1 and 1:2) with proton acceptors in solutions. *Journal of Molecular Structure*, *783*(1-3), 101-115.

Brink, N.G., & Folkers, K. (1949). Vitamin B12. VI. 5, 6-Dimethylbenzimidazole, a degradation product of vitamin B12. *Journal of the American Chemical Society*, *71*(8), 2951-2951.

Britschgi, M., Greyerz, S., Burkhart, C., & Pichler, W.J. (2003). Molecular aspects of drug recognition by specific T cells. *Current Drug Targets*, *4*(1), 1-11.

Çekiç, S.D., Çetinkaya, A., Avan, A.N., & Apak, R. (2013). Correlation of total antioxidant capacity with reactive oxygen species (ROS) consumption measured by oxidative conversion. *Journal of Agricultural and Food Chemistry*, *61*(22), 5260-5270.

Chen, B., Zhu, C., Tang, Y., & Ma, S. (2014). Copper-mediated pyrazole synthesis from 2,3-allenoates or 2-alkynoates, amines and nitriles. *Chemical Communications*, *50*(57), 7677-7679.

Chhabria, M.T., Patel, S., Modi, P, Brahmkshatriya, P.S. (2016). Thiazole: A review on chemistry, synthesis and therapeutic importance of its derivatives. *Current Topics in Medicinal Chemistry*, *16*(26), 2841-2862.

Choudhari, S. (2014). Additional bioinformatic analyses involving protein sequences, *Bioinformatics for Beginners*, 183-207.

Daidone, G., Maggio, B., Plescia, S., Raffa, D., Musiu, C., Milia, C., Perra, G. & Marongiu, M.E. (1998). Antimicrobial and antineoplastic activities of new 4-diazopyrazole derivatives. *European Journal of Medicinal Chemistry*, *33*(5), 375-382.

Dardari, Z., Lemrani, M., Sebban, A., Bahloul, A., Hassar, M., Kitane, S., Berrada, M. & Boudouma, M. (2006). Antileishmanial and Antibacterial Activity of a New Pyrazole Derivative Designated 4-[2-(1-(Ethylamino)-2-methyl-propyl)phenyl]-3-(4-methyphenyl)-1-phenylpyrazole. *Arch Pharm (Weinheim)*, *339*(6), 291-298.

Das, B., Reddy, V. S., & Ramu, R. (2006). A rapid and high-yielding synthesis of thiazoles and aminothiazoles using ammonium-12-molybdophosphate. *Journal of Molecular Catalysis A: Chemical*, *252*(1-2), 235-237.

Dawane, B.S., Konda, S.G., Kamble, V.T., Chavan, S.A., & Bhosale, R.B. (2009). Multicomponent one-pot synthesis of substituted Hantzsch thiazole derivatives under solvent free conditions. *E-Journal of Chemistry*, *6*(S1), S358-S362.

Dobbelstein, M., & Moll, U. (2014). Targeting tumour-supportive cellular machineries in anticancer drug development. *Nature Reviews Drug Discovery*, *13*(3), 179-196.

Dong, H., Tang, S., Hao, Y., Yu, H., Dai, W., Zhao, G., Cao, Y., Lu, H., Zhang, X. and Ju, H. (2016). Fluorescent MoS_2 quantum dots: ultrasonic preparation, up-conversion and down-conversion bioimaging, and photodynamic therapy. *ACS Applied Materials & Interfaces*, *8*(5), 3107-3114.

Elsadek, M.F., Mohamed Ahmed, B., & Farahat, M.F. (2021). An overview on synthetic 2-aminothiazole-based compounds associated with four biological activities. *Molecules*, *26*(5), 1449.

Emerson, G., Brink, N.G., Holly, F.W., Koniuszy, F., Heyl, D., & Folkers, K. (1950). Vitamin B12. VIII. Vitamin B12-like activity of 5,6-dimethylbenzimidazole and tests on related compounds. *Journal of the American Chemical Society*, *72*(7), 3084-3085.

Evans, D.C., Ruffolo, R.R., Warrick, M.W., & Lin, T.M. (1984) Specific histamine (H_2-receptor) antagonist actions of nizatidine. *Federation Proceedings*, *43*, 1074– 1074.

Foks, H., Pancechowska-Ksepko, D., Kędzia, A., Zwolska, Z., Janowiec, M., & Augustynowicz-Kopeć, E. (2005). Synthesis and antibacterial activity of 1H-pyrazolo[3, 4-b] pyrazine and -pyridine derivatives. *Farmaco*, *60*(6-7), 513-517.

Gallardo-Godoy, A., Gever, J., Fife, K.L., Silber, B.M., Prusiner, S.B., & Renslo, A.R. (2011). 2-Aminothiazoles as therapeutic leads for prion diseases. *Journal of Medicinal Chemistry*, *54*(4), 1010-1021.

Ghaemmaghami, S., May, B.C., Renslo, A.R., & Prusiner, S.B. (2010). Discovery of 2-aminothiazoles as potent antiprion compounds. *Journal of Virology*, *84*(7), 3408-3412.5.

Ghodse, S.M., & Telvekar, V.N. (2015). Synthesis of 2-aminothiazole derivatives from easily available thiourea and alkyl/aryl ketones using aqueous $NaICl_2$. *Tetrahedron Letters*, *56*(2), 472-474.

Gilbert, A.M., Failli, A., Shumsky, J., Yang, Y., Severin, A., Singh, G., Hu, W., Keeney, D., Petersen, P.J. & Katz, A.H. (2006). Pyrazolidine-3,5-diones and 5-hydroxy-1H-pyrazol-3(2 H)-ones, inhibitors of UDP-N-acetylenolpyruvyl glucosamine reductase. *Journal of Medicinal Chemistry*, *49*(20), 6027-6036.

Giri, R.S., Thaker, H.M., Giordano, T., Williams, J., Rogers, D., Sudersanam, V., & Vasu, K. K. (2009). Design, synthesis and characterization of novel 2-(2,4-disubstituted-thiazole-5-yl)-3-aryl-3H-quinazoline-4-one derivatives as inhibitors of NF-κB and AP-1 mediated transcription activation and as potential anti-inflammatory agents. *European Journal of Medicinal Chemistry*, *44*(5), 2184-2189.

Greig, N., Mattson, M., Zhu, X., Yu, Q.S., & Holloway, H. (2004). *U.S. Patent Application No. 10/332,115*.

Hantzsch, A., & Weber, J.H. (1887). Hantzsch Thiazole Synthesis. *Chemische Berichte*, *20*, 3118.

Harnett, J.J., Roubert, V., Dolo, C., Charnet, C., Spinnewyn, B., Cornet, S., ... & Chabrier, P. E. (2004). Phenolic thiazoles as novel orally-active neuroprotective agents. *Bioorganic & Medicinal Chemistry Letters*, *14*(1), 157-160.

Kamal, A., Sastry, K.V., Chandrasekhar, D., Mani, G.S., Adiyala, P.R., Nanubolu, J.B., Singarapu, K.K. & Maurya, R.A. (2015). One-pot, three-component approach to the synthesis of 3,4,5-trisubstituted pyrazoles. *The Journal of Organic Chemistry*, *80*(9), 4325-4335.

Kashiwa, M., Kuwata, Y., Sonoda, M., & Tanimori, S. (2016). Oxone-mediated facile access to substituted pyrazoles. *Tetrahedron*, *72*(2), 304-311.

Kesicki, E.A., Bailey, M.A., Ovechkina, Y., Early, J.V., Alling, T., Bowman, J., Zuniga, E.S., Dalai, S., Kumar, N., Masquelin, T., Hipskind, P.A. & Parish, T. (2016). Synthesis and evaluation of the 2-aminothiazoles as anti-tubercular agents. *Public Library of Science One*, *11*(5), e0155209.

Khan, M.F., Alam, M.M., Verma, G., Akhtar, W., Akhter, M., & Shaquiquzzaman, M. (2016). The therapeutic voyage of pyrazole and its analogs: a review. *European Journal of Medicinal Chemistry, 120*, 170-201.

Kidwai, M., Dave, B., & Bhushan, K.R. (2000). Alumina-supported synthesis of aminoazoles using microwaves. *Chemical Papers-Slovak Academy of Sciences*, *54*(4), 231-234.

Kiyani, H., & Bamdad, M. (2018). Sodium ascorbate as an expedient catalyst for green synthesis of polysubstituted 5-aminopyrazole-4-carbonitriles and 6-amino-1, 4-dihydropyrano [2, 3-c] pyrazole-5-carbonitriles. *Research on Chemical Intermediates, 44*, 2761-2778.

Kumari, S., Shekhar, A., & Pathak, D.D. (2016). Graphene oxide–TiO_2 composite: an efficient heterogeneous catalyst for the green synthesis of pyrazoles and pyridines. *New Journal of Chemistry, 40*(6), 5053-5060.

Li, C.J. (2005). Organic reactions in aqueous media with a focus on carbon-carbon bond formations: a decade update. *Chemical Reviews, 105*(8), 3095-3166.

Li, C.J., & Chan, T.H. (1997). *Organic reactions in aqueous media*. Wiley.

Li, D.Y., Mao, X.F., Chen, H.J., Chen, G.R., & Liu, P.N. (2014). Rhodium-catalyzed addition–cyclization of hydrazines with alkynes: Pyrazole synthesis via unexpected C–N bond cleavage. *Organic Letters*, *16*(13), 3476-3479.

Lim, F.P.L., Luna, G., & Dolzhenko, A.V. (2016). A New, One-Pot, Multicomponent synthesis of bioactive N-pyrazolylformamidines under Microwave Irradiation. *Synthesis*, *48*(15), 2423-2428.

Ma, C., Wen, P., Li, J., Han, X., Wu, Z., & Huang, G. (2016). Palladium and copper cocatalyzed intermolecular cyclization reaction: Synthesis of 5-aminopyrazole derivatives. *Advanced Synthesis & Catalysis, 358*(7), 1073-1077.

Maddila, S., Rana, S., Pagadala, R., Kankala, S., Maddila, S., & Jonnalagadda, S.B. (2015). Synthesis of pyrazole-4-carbonitrile derivatives in aqueous media with CuO/ZrO_2 as recyclable catalyst. *Catalysis Communications, 61*, 26-30.

Maj, J., Rogóż, Z., Skuza, G., & Kołodziejczyk, K. (1997). Antidepressant effects of pramipexole, a novel dopamine receptor agonist. *Journal of Neural Transmission, 104,* 525-533.

Mamgain, R., Singh, R., & Rawat, D.S. (2009). DBU-catalyzed three-component one-pot synthesis of highly functionalized pyridines in aqueous ethanol. *Journal of Heterocyclic Chemistry, 46*(1), 69-73.

Manabe, K., Mori, Y., Wakabayashi, T., Nagayama, S., & Kobayashi, S. (2000). Organic synthesis inside particles in water: lewis acid− surfactant-combined catalysts for organic reactions in water using colloidal dispersions as reaction media. *Journal of the American Chemical Society*, *122*(30), 7202-7207.

Mantzanidou, M, Pontiki, E, & Hadjipavlou-Litina, D. (2021). Pyrazoles and pyrazolines as anti-inflammatory agents. *Molecules*, *26*(11), 3439.

Meng, F.J., Sun, T., Dong, W.Z., Li, M.H., & Tuo, Z.Z. (2016). Discovery of novel pyrazole derivatives as potent neuraminidase inhibitors against influenza H1N1 virus. *Arch Pharm (Weinheim)*, *349*(3), 168-174.

Milne, G.W. (2000). Handbook of Antineoplastic Agents, Gower. *London, UK*, 20.

Mishra, C.B., Kumari, S., & Tiwari, M. (2015). Thiazole: A promising heterocycle for the development of potent CNS active agents. *European Journal of Medicinal Chemistry*, *92*, 1-34.

Mishra, D., Singh, R., & Rout, C. (2017). Synthesis of highly functionalized pyrazoles using $AlCl_3$ as catalyst. *Journal of Chemical and Pharmaceutical Research*, *9(*6), 16-19.

Munteanu, I.G., & Apetrei, C. (2021). Analytical methods used in determining antioxidant activity: A review. *International Journal of Molecular Sciences*, *22*(7), 3380.

Naim, M.J., Alam, O., Nawaz, F., Alam, M.J., & Alam, P. (2016). Current status of pyrazole and its biological activities. *Journal of Pharmacy & Bioallied Sciences*, *8*(1), 2-17.

Özdemir, Z., Kandilci, H.B., Gümüşel, B., Çalış, Ü., & Bilgin, A.A. (2007). Synthesis and studies on antidepressant and anticonvulsant activities of some 3-(2-furyl)-pyrazoline derivatives. *European Journal of Medicinal Chemistry*, *42*(3), 373-379.

Pompe, C.E., Slagter, M., de Jongh, P.E., & de Jong, K.P. (2018). Impact of heterogeneities in silica-supported copper catalysts on their stability for methanol synthesis. *Journal of Catalysis*, *365*, 1-9.

Poonam & Singh, R. (2019). Facile one-pot synthesis of 5-amino-1 H-pyrazole-4-carbonitriles using alumina–silica-supported MnO2 as recyclable catalyst in water. *Research on Chemical Intermediates*, *45*(9), 4531-4542.

Potewar, T.M., Ingale, S.A., & Srinivasan, K.V. (2007). Efficient synthesis of 2, 4-disubstituted thiazoles using ionic liquid under ambient conditions: a practical approach towards the synthesis of Fanetizole. *Tetrahedron*, *63*(45), 11066-11069.

Prior, R.L., Wu, X., & Schaich, K. (2005). Standardized methods for the determination of antioxidant capacity and phenolics in foods and dietary supplements. *Journal of Agricultural and Food Chemistry*, *53*(10), 4290-4302.

Rakhtshah, J., Salehzadeh, S., Gowdini, E., Maleki, F., Baghery, S., & Zolfigol, M.A. (2016). Synthesis of pyrazole derivatives in the presence of a dioxomolybdenum complex supported on silica-coated magnetite nanoparticles as an efficient and easily recyclable catalyst. *Royal Society of Chemistry Advances*, *6*(106), 104875-104885.

Rathelot, P., Azas, N., El-Kashef, H., Delmas, F., Di Giorgio, C., Timon-David, P., Maldonado, J. & Vanelle, P. (2002). 1,3-Diphenylpyrazoles: Synthesis and antiparasitic activities of azomethine derivatives. *European Journal of Medicinal Chemistry*, *37*(8), 671-679.

Rios Martinez, C.H., & Durant-Archibold, A.A. (2018). Latest Research on synthetics compounds with antileishmanial activity. *Mini-Reviews in Organic Chemistry*, *15*(4), 330-342.

Rodrigo, R., & Rodrigo, R. (2009). Oxidative stress and antioxidants: their role in human disease (Vol. 358). New York: Nova Biomedical Books.

Saeed, A., & Channar, P.A. (2017). A green mechanochemical synthesis of new 3,5-dimethyl-4-(arylsulfanyl)pyrazoles. *Journal of Heterocyclic Chemistry*, *54*(1), 780-783.

Saha, A., Payra, S., & Banerjee, S. (2015). One-pot multicomponent synthesis of highly functionalized bio-active pyrano[2,3-c]pyrazole and benzylpyrazolyl coumarin derivatives using ZrO_2 nanoparticles as a reusable catalyst. *Green Chemistry*, *17*(5), 2859-2866.

Sahu, P.K., Sahu, P.K., & Agarwal, D.D. (2014). Role of surfactant and micelle-promoted mild, efficient, sustainable synthesis of 2-aminobenzothiazolomethyl naphthols and 5-(2-aminobenzothiazolomethyl)-6-hydroxyquinolines in water at room temperature. *Royal Society of Chemistry Advances*, *4*(76), 40414-40420.

Shahidi, F., & Zhong, Y. (2015). Measurement of antioxidant activity. *Journal of Functional Foods*, *18*, 757-781.

Sharma, P., & Mehata, M.S. (2020a). Colloidal MoS_2 quantum dots based optical sensor for detection of 2, 4, 6-TNP explosive in an aqueous medium. *Optical Materials*, *100*, 109646.

Sharma, P., & Mehata, M.S. (2020b). Rapid sensing of lead metal ions in an aqueous medium by MoS2 quantum dots fluorescence turn-off. *Materials Research Bulletin*, *131*, 110978.

Siddeeg, A., AlKehayez, N.M., Abu-Hiamed, H.A., Al-Sanea, E.A., & Al-Farga, A.M. (2021). Mode of action and determination of antioxidant activity in the dietary sources: An overview. *Saudi Journal of Biological Sciences*, *28*(3), 1633-1644.

Siddiqui, N., & Ahsan, W. (2011). Synthesis, anticonvulsant and toxicity screening of thiazolyl–thiadiazole derivatives. *Medicinal Chemistry Research*, *20*, 261-268.

Souza, M.V.N.D., & Almeida, M.V.D. (2003). Drugs anti-HIV: past, present and future perspectives. *Quimica Nova*, *26*, 366-372.

Srivastava, M., Rai, P., Singh, J., & Singh, J. (2013). An environmentally friendlier approach—ionic liquid catalysed, water promoted and grinding induced synthesis of highly functionalised pyrazole derivatives. *RSC Advances*, *3*(38), 16994-16998.

Srivastava, M., Rai, P., Singh, J., & Singh, J. (2014). Efficient iodine-catalyzed one pot synthesis of highly functionalised pyrazoles in water. *New Journal of Chemistry*, *38*(1), 302-307.

Storch, A., Burkhardt, K., Ludolph, A.C., & Schwarz, J. (2000). Protective effects of riluzole on dopamine neurons: involvement of oxidative stress and cellular energy metabolism. *Journal of Neurochemistry*, *75*(6), 2259-2269.

Subramaniyana, V., Palania, M., Srinivasana, P., & Singh, S.K. (2018). Novel ligand-based docking; molecular dynamic simulations; and absorption, distribution, metabolism, and excretion approach to analyzing potential acetylcholinesterase inhibitors for Alzheimer's disease. *Journal of Pharmaceutical Analysis, 8*, 413-420.

Tanitame, A., Oyamada, Y., Ofuji, K., Fujimoto, M., Iwai, N., Hiyama, Y., Suzuki, K., Ito, H., Terauchi, H., Kawasaki, M., Nagai, K. & Yamagishi, J.I. (2004a). Synthesis and antibacterial activity of a novel series of potent DNA gyrase inhibitors. Pyrazole derivatives. *Journal of Medicinal Chemistry*, *47*(14), 3693-3696.

Tanitame, A., Oyamada, Y., Ofuji, K., Kyoya, Y., Suzuki, K., Ito, H., Kawasaki, M., Nagai, K., Wachi, M. & Yamagishi, J.I. (2004b). Design, synthesis and structure–activity relationship studies of novel indazole analogues as DNA gyrase inhibitors with Gram-positive antibacterial Srivastava activity. *Bioorganic & medicinal chemistry letters*, *14*(11), 2857-2862.

Taylor, E.C., & Patel, H.H. (1992). Synthesis of pyrazolo 3,4-dpyrimidine analogues of the potent agent N-{4-[2-(2-amino-4(3H)-oxo-7H-pyrrolo[2,3-d]pyrimidin-5-yl)ethylbenzoyl}-L-glutamic acid (LY231514). *Tetrahedron*, *48*(37), 8089-8100.

Tewari, A.K., & Mishra, A. (2001). Synthesis and anti-inflammatory activities of N^4, N^5-disubstituted-3-methyl-1H-pyrazolo[3,4-c]pyridazines. *Bioorganic & Medicinal Chemistry, 9*(3), 715-718.

Tyurina, T.G., Kryuk, T.V., Kudryavtseva, T.A., Semenova, R.G., Romanenko, N.A., & Volkova, G.K. (2021). Study of succinic anhydride amidation by 2-aminothiazol. *Journal of Physics: Conference Series, 2052*, 012047.

Ubale, M., & Shioorkar, M. (2016). potassium aluminum sulfate: green catalyst for synthesis of 1, 3, 5-substituted pyrazole. *Heterocyclic Letters, 6*(2), 217-221.

Wang, Y., & Ni, Y. (2014). Molybdenum disulfide quantum dots as a photoluminescence sensing platform for 2, 4, 6-trinitrophenol detection. *Analytical Chemistry*, *86*(15), 7463-7470.

Woolley, D.W. (1944). Some biological effects produced by benzimidazole and their reversal by purines. *Journal of Biological Chemistry*, *152*(2), 225-232.

Wu, Z., Wu, S., Ye, Y., Zhou, X., Wang, P., Xue, W., & Hu, D. (2017). Synthesis and bioactivities of novel 1-(3-chloropyridin-2-yl)-N-substituted-5-(trifluoromethyl)-pyrazole carboxamide derivatives. *Journal of Heterocyclic Chemistry, 54*(1), 325-330.

Zhang, W., Chen, J., Xu, S., Chu, Y., Wei, Y., Zhi, Y., Huang, J., Zheng, A., Wu, X., Meng, X., Xiao, F.& Liu, Z. (2018). Methanol to olefins reaction over cavity-type zeolite: Cavity controls the critical intermediates and product selectivity. *ACS Catalysis*, *8*(12), 10950-10963.

Zhong, N. (2016). Facile synthesis of MnO_2 nanoparticles well dispersed on graphene for the enhanced electrochemical performance. *International Journal of Electrochemical Science*, *11*, 2525-2533.

Publications

Publications in peer-reviewed journals: 04

1. Geetanjali, **Poonam**, Babita Veer and Ram Singh; Alcohol abuse and related Health issues; *International Research Journal of Medical Sciences*, 4(8), 18-23, **2016**. (UGC-CARE)
2. **Poonam** and Ram Singh; Facile one-pot synthesis of highly functionalized pyrazoles using Alumina-Silica-supported MnO_2 as recyclable catalyst in water, *Research on Chemical Intermediates*; 45(9), 4531-4542, **2019**. [IF = **3.134** (2021)]. (Science Citation Index)
3. **Poonam** and Ram Singh; Use of bimetallic nanoparticles in the synthesis of heterocyclic molecules; *Current Organic Chemistry*; 25(3), 351-360, **2021**. [IF = **2.226** (2021)]. (Science Citation Index Expanded)
4. **Poonam**, Geetika Bhasin, Richa Srivastava, and Ram Singh; Oxadiazoles: Moiety to Synthesis and Utilize; *Journal of the Iranian Chemical Society*, 19, 665-677, **2022**. [IF = **2.271** (2021)], (Science Citation Index Expanded)

Submitted – 02

1. Poonam and Ram Singh; Ionic liquids: Potential Energetic Materials; *Journal of Iranian Chemical Society*; ***Submitted***.
2. Poonam, Prateek Sharma, M.S. Mehata, Ram Singh; Sustainable synthesis of 4-phenylthiazole-2-amine derivatives catalyzed by MoS2 QDs in aqueous medium; *Green Chemistry*; ***Submitted***.

Book Chapter – 02

1. Ram Singh, **Poonam** and Geetanjali; Chemotaxonomic significance of alkaloids in plants; Chemotaxonomic Significance of Alkaloids in Plants. In: Ramawat K. (eds) Biodiversity and Chemotaxonomy (Sustainable Development and Biodiversity), vol 24; pp 121-136 (Chapter 6); Springer, Cham; Print ISBN 978-3-030-30745-5; Online ISBN 978-3-030-30746-2; 11 November 2019
2. **Poonam**, Geetanjali, and Ram Singh; Chapter 3: Applications of Ionic Liquids in Organic Synthesis (pp 41-62); Series Title: Nanotechnology in the Life Sciences; Book Title: Applications of Nanotechnology for Green Synthesis; Inamuddin and Abdullah M. Asiri (Eds), 2020, Springer Nature

Number of Conferences: 09

1. D. Mishra, **Poonam**, C. Rout and Ram Singh; Synthesis of chromen-2-one derivatives as potential anti-alzheimeric agents; 1st National Conference on Emerging Trends and Future Challenges in Chemical Sciences; organized by Department of Chemistry, Kirori Mal College; University of Delhi, February 3-4, 2016(O1)
2. G. Bhasin, **Poonam**, R. Srivastava, Geetanjali and Ram Singh; Synthesis and Studies of β-Aminocarbonyl compounds as Anti-cancer agents; 6th International Symposium on "Current Trends in Drug Discovery & Research", organized by CSIR-CDRI, Lucknow; 25-28 February, 2016 (p. 133)
3. **Poonam** and Ram Singh; Green Chemistry and its Role for Sustainability; Oral presentation at National Seminar on "Role of Analytical Sciences in Sustainable Development" (RASSD-2016) organized by Department of Chemistry, Hansraj college, University of Delhi on 4th-5th March 2016. (*Best Oral Award*; OL-62)
4. G. Bhasin, **Poonam**, R. Srivastava, Ram Singh; Design and synthesis of ionic liquids as energetic materials; Oral presentation at National Conference on "Global Challenges – Role of Science & Technology in Imparting their Solutions (GCRSTS-2016)" organized by The Technological Institute of Textile & Sciences & ISAS-DC on Apr 23-24, 2016. (CAE-123; ISBN: 978-81-909307-3-4)
5. Babita Veer, **Poonam**, Geetanjali and Ram Singh; Remediation of halogenated aromatic compounds with flavins: An environmental friendly approach; National Conference on Advances in Multidisciplinary Aspects of Science & Engineering (AMASE–2016) organized by Deenbandhu Chhotu Ram University of Science & Technology, Murthal, Sonepat (Haryana); November 23, 2016.
6. **Poonam**, G. Bhasin, Richa Srivastava and Ram Singh; Green and sustainable synthesis of nanoparticles; The 104th *Indian Science Congress* 2017; S.V. University, Tirupati, 3-7 January **2017** (pp: 189)
7. **Poonam** and Ram Singh; Eco-friendly, one-pot, three-component synthesis of polysubstituted amino pyrazoles; International Conference on Advances in Analytical Sciences (ICAAS-2018) organized by Indian Society of Analytical Scientists (ISAS)-Delhi Chapter & CSIR-Indian Institute of Petroleum Dehradun, March 15-17, **2018** (A194).
8. **Poonam** and Ram Singh; One-pot, three-component synthesis of substituted dihydropyrimidines using Cd quantum dots; 26th World Congress on Chemistry, UK

during October 30-31, **2019**. Journal of Chemistry & Applied Chemical Engineering; 3, 39, 2019 (ISSN: 2576-3954)

9. **Poonam**; and Ram Singh; Environmentally benign synthesis and studies of mixed bimetallic nanoparticles; 3 days International conference "Indian Analytical Congress (IAC)" on 12-14 Dec, **2019**, organized by ISASDC and FICCI at Amity University, Noida, NCR, India.

*****